NASA CR-134660

R74AEG327

QUIET ENGINE PROGRAM
FLIGHT ENGINE DESIGN STUDY

by

J.F. Klapproth
R.E. Neitzel
C.T. Seeley

GENERAL ELECTRIC COMPANY

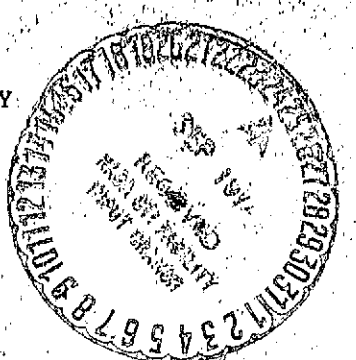

Prepared For

National Aeronautics and Space Administration

NASA Lewis Research Center
Contract NAS3-12430

1. Report No.	2. Government Accession No.	3. Recipient's Catalog No.
NASA CR-134660		

4. Title and Subtitle	5. Report Date
QUIET ENGINE PROGRAM FLIGHT ENGINE DESIGN STUDY	July 1974
	6. Performing Organization Code

7. Author(s)	8. Performing Organization Report No.
J.F. Klapproth, R.E. Neitzel, and C.T. Seeley	R74AEG327
	10. Work Unit No.

9. Performing Organization Name and Address	11. Contract or Grant No.
General Electric Company Aircraft Engine Group Cincinnati, Ohio 45215	NAS3-12430
	13. Type of Report and Period Covered
12. Sponsoring Agency Name and Address	Contractor Report
National Aeronautics and Space Administration Washington, D.C. 20546	14. Sponsoring Agency Code

15. Supplementary Notes

Project Manager, E.W. Conrad
V/STOL and Noise Division
NASA - Lewis Research Center, Cleveland, Ohio

16. Abstract

This report presents the results of a Preliminary Flight Engine Design Study based on the Quiet Engine Program high-bypass, low-noise turbofan engines. This study considered engine configurations, weight, noise characteristics, and performance over a range of flight conditions typical of a subsonic transport aircraft. The study included high and low tip speed engines in various acoustically treated nacelle configurations.

17. Key Words (Suggested by Author(s))	18. Distribution Statement
Acoustics, Turbofan Engine, Noise Reduction	Unclassified - Unlimited

19. Security Classif. (of this report)	20. Security Classif. (of this page)	21. No. of Pages	22. Price*
Unclassified	Unclassified	121	$3.00

*For sale by the National Technical Information Service, Springfield, Virginia 22151

TABLE OF CONTENTS

TABLE OF CONTENTS (Concluded)

LIST OF ILLUSTRATIONS

LIST OF ILLUSTRATIONS (Continued)

LIST OF ILLUSTRATIONS (Concluded)

LIST OF TABLES

LIST OF TABLES (Concluded)

1.0 SUMMARY

Preliminary flight engine designs were defined incorporating the basic noise reduction and aerodynamic features of the Quiet Engine Program fans and a modern core sized to produce 22,000 lb (97,900 N) SLS thrust. The preliminary flight engines were designed in both a low tip speed version (Quiet Engine Program Fan A derivative) and a high tip speed version (Fan C derivative). The basic size, weight, cost, noise, and performance characteristics for each of the above two engines in a variety of nacelle suppression configuration variations were defined. These characteristics were then evaluated in conjunction with typical CTOL transport aircraft characteristics to determine the economic impact of engines designed with high or low speed fans and with varying amounts of noise suppression in terms of the effect on direct operating cost.

Using the acoustic technology from the Quiet Engine Program in these preliminary flight engine designs and the acoustically treated nacelles defined in this study in a typical CTOL tri-jet transport results in projected noise levels well below FAR 36 requirements. The acoustic results of the study described in this report are summarized in Table I.

TABLE I. Predicted EPNL Relative to FAR 36 for Tri-Jet CTOL Transport.

(FAR 36 Takeoff and Approach Certification Conditions).

Nacelle Configuration	Key to Figure 1	High Speed Engine		Low Speed Engine	
		Takeoff	Approach	Takeoff	Approach
Hardwall	A	103.1	106.9	97.0	99.0
Treated Wall	B	97.8	99.6	93.5	94.5
Treated Wall + 1 Inlet Splitter + 1 Aft Splitter	C	95.2	96.0		
Treated Wall + 1 Aft Splitter	D			92.5	93.0
Treated Wall + 3 Inlet Splitters + 2 Aft Splitters	E	91.4	91.0	89.0	87.5
FAR 36		100	105	100	105

As can be seen in Table I, both high speed and low speed engines meet the FAR 36 requirements in a treated-wall nacelle configuration, and are significantly below the FAR 36 requirements in the fully suppressed nacelle.

The economic penalty associated with the maximum feasible noise reduction (fully suppressed nacelles) is significant. Using the low speed engine in a treated-wall nacelle as the base (present technology), the differential effects on the DOC of a typical tri-jet CTOL transport were estimated for the various engine/nacelle configurations. (Table II).

TABLE II. DOC Comparison,
Tri-Jet CTOL Transport [200,500 lb (91,200 kg) TOGW].

	High Speed Engine	Low Speed Engine
Hardwall	-3.0%	-0.6%
Treated Wall	-2.4%	Base
Treated Wall +1 Inlet Splitter + 1 Aft Splitter	-0.6%	
Treated Wall +1 Aft Splitter		+0.7%
Treated Wall +3 Inlet Splitters +2 Aft Splitters	+3.5%	+7.2%

The EPNL/DOC relationship determined in the preliminary flight engine design study is discussed in Section 8.0. Considering both noise and DOC effects, at full power takeoff noise levels between FAR 36 and FAR 36 minus 5 EPNdB, with a typical tri-jet transport, a high speed engine in a treated wall nacelle appears to be the most economically attractive. The high speed engine yields a greater noise reduction for similar noise reduction features. For significant noise reductions below about FAR 36 minus 5 EPNdB, the cost increases for both low and high speed engines. For noise levels below approximately FAR 36 minus 5 EPNdB to FAR 36 minus 7 EPNdB, the lower source noise of the low speed engine begins to dominate, and on a DOC basis appears more economically attractive. Technology developed since the conduct of the preliminary flight engine design study documented in this report indicates that the range of economic attractiveness of high speed fan engines may extend to lower noise levels.

2.0 INTRODUCTION

One of the phases of the Quiet Engine Program is the assessment of the economic impact of utilizing the technology developed in the above effort in a modern flight-type engine on CTOL-type aircraft. The elements of this study include:

1. A preliminary flight engine design incorporating the basic features of the QEP fans developed above with a modern core - matched to the engine thrust requirement of 22,000 lb (97,900 N) SLS. The study is to include both a low tip speed (Fan A derivative) and high tip speed (Fan C derivative) engine.

2. For each engine, identify the basic characteristics including size, weight, cost, noise, and performance in a reference untreated (i.e. hardwall) nacelle.

3. Establish the installed characteristics in a nacelle with varying degrees of noise suppression evaluating the effect on performance, weight, cost, and noise.

4. Evaluate the impact of the various suppressed engine configurations on the aircraft economics of new tri-jet aircraft.

5. Evaluate the impact of the various suppressed engine configurations on the economics of a DC-8-type aircraft (Appendix C).

6. Compare the effect of noise suppression (ΔEPNdB) on high and low speed fan engines on the aircraft operating costs (ΔDOC) for each engine.

This report describes the work performed in carrying out elements 1 to 5 to obtain the DOC/EBNdB Trade Study.

The NASA/GE Experimental Quiet Engine Program which served as the basis for the DOC Trade Study was directed toward the overall objective of achieving a noise reduction equivalent to 15-20 EPNdB relative to the large jet aircraft then in service (e.g. 707, DC-8 aircraft). The major elements incorporated in the program to obtain this overall system reduction were:

1. Use of a high bypass ratio engine to reduce jet noise.

2. Development of fan components which minimized the fan source noise concurrent with good aero performance.

3. Installation of the basic engine in nacelles utilizing acoustic materials to reduce the amount of internal noise radiated to the farfield.

The desired jet noise reduction is achieved by use of engines with bypass ratios of about 6. The associated fan pressure ratios of 1.5 to 1.6 and the resultant jet velocities then generate significantly less noise than other major engine noise sources such as the fan.

To address the problem of fan source noise reduction, the Quiet Engine Program included the design and development of three full-size fan components. Features incorporated in these fans to reduce source noise included:

1. Two rotor chord spacing between the fan rotor trailing edge and the stator (or OGV) leading edge.

2. A stator vane to rotor blade ratio of slightly over 2.

3. Acoustically treated panels in the engine frame and casings.

The primary program elements are illustrated in Figure 1. Two low speed fans [U_T = 1160 ft/sec (354 m/sec) at alt cruise] and one high speed fan [U_T = 1550 ft/sec (473 m/sec) at alt cruise] were designed and fabricated. These two configurations were chosen to evaluate the impact on an engine system of high (low tip speed) and low (high tip speed) aerodynamic loading fans when significant noise reduction is required. Complete aerodynamic and aeromechanical performance including tolerance to inflow distortions was established by aero component tests at the General Electric Full-Scale Fan Test Facility at Lynn, Massachusetts. Acoustic performance was obtained by testing each fan component in the Fan Noise Test Facility at the NASA Lewis Research Center. For each fan, the acoustic performance included the baseline fan (i.e. with hardwall inlet and discharge ducts), with various combinations of acoustic treatment in the duct walls and with acoustically treated splitters both in the fan inlet and fan exhaust ducts. The aero performance of these fans are described in Reference 1, 2, and 3.

Engine tests were carried out using the 40-bladed, tip-shrouded Fan A for the low speed fan (since its efficiency and acoustic characteristics were slightly better than the low speed 26-blade Fan B) and using the high speed fan (Fan C). The proven CF6 core was used (operated at a derated rpm and turbine inlet temperature) with each fan. For the low speed fan engine, the fan was driven by a four-stage low pressure turbine derived directly from the CF6 fan turbine by removing the CF6 fifth stage. The high speed Fan C engine used a new, more highly loaded two-stage, low pressure turbine. Both engines were tested for performance and noise levels over the full thrust range from approach power settings to the takeoff power of 22,000 lb (97,900 N).

Engine acoustic tests were carried out for the basic engine (i.e. hardwall inlet and exhaust ducts) as well as for a number of acoustically treated configurations using acoustic panels in the duct surfaces and treated splitters in the inlet and exhaust. Acoustic treatment in the core nozzle for turbine noise suppression was also evaluated in each engine.

The overall objective of 15-20 EPNdB reduction was achieved if the observed static noise characteristics of the suppressed engine are utilized in a flyover noise prediction accounting for the aircraft position, altitude, and

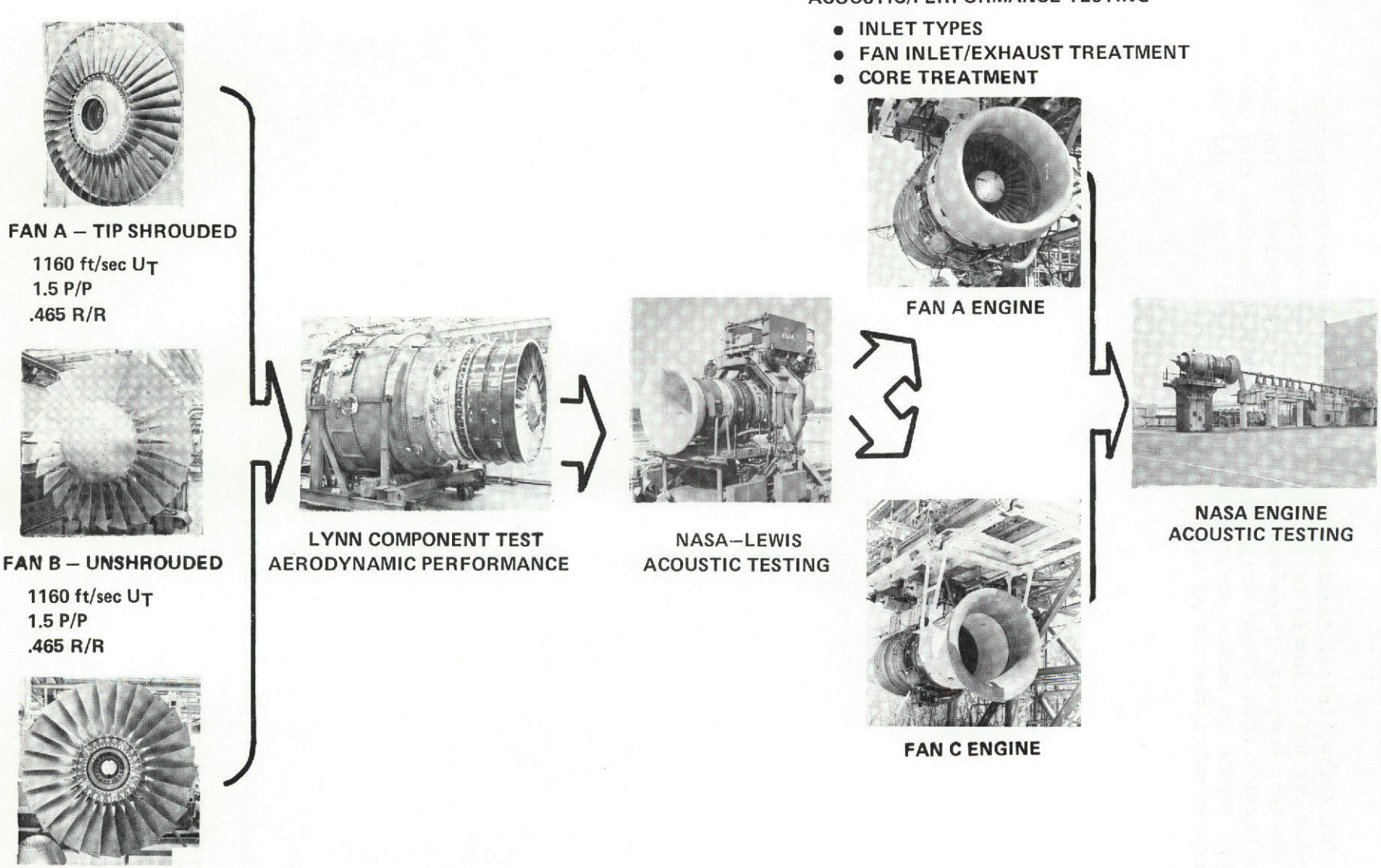

Figure 1. NASA-GE Quiet Engine Program Elements.

velocity. The technological feasibility of the Quiet Engine Program was demonstrated. The noise levels of the Quiet Engines are representative of a new engine design; however, these engines are not flight weight. The Quiet Engines are heavier than flight weight engines primarily because they used an existing core engine to reduce program costs. (This same core in the CF6 engine produces twice the thrust of the Quiet Engine.)

3.0 LOW SPEED ENGINE CHARACTERISTICS

3.1 BASIC ENGINE

The low speed engine, representing current levels of technology, was derived from the Quiet Engine Program Fan A, adapted to a modern core and sized for a SLS takeoff thrust of 22,000 lb (97,900 N) with nominal installation losses. The primary cycle characteristics are tabulated in Table III. An engine cycle representative of CTOL applications, has been selected to provide for a mixed core and fan stream ahead of the nozzle. The jet velocity shown in Table III represents the velocity after mixing. Inlet recoveries, duct losses, mixing losses, and nozzle thrust coefficients used in the cycle are shown in Table IV. The engine flowpath configuration is shown in Figure 2. A short tabulation of the major component characteristics is contained in Table V.

The low speed engine fan applies the measured performance characteristics of Fan A in the bypass flow. The cycle pressure ratio was set so as to assure a clean stall margin of 17% which was considered appropriate to provide stall-free operation in the most severe operational environment anticipated for this engine. The fan radius ratio was reduced from the Fan A value of 0.465 to 0.4 in the low speed engine. Booster stages were used to provide the desired core supercharging pressure ratio of 2.5. Five booster stages were selected to meet the requirement of boost pressure ratio plus an adequate stall margin, and this selection was based on aerodynamic loadings consistent with the CF6-50 engine booster stages.

The five-stage, low pressure turbine was selected to provide a moderately highly loaded turbine consistent with the design efficiency objective.

The overall nominal (hardwall) engine takeoff performance is shown in Figure 3 and altitude cruise performance is shown in Figure 4.

3.2 NACELLE CONFIGURATIONS

Overall arrangement: The engine is installed in a long duct nacelle illustrated in Figure 5. The major features are:

1. Mixed core and fan flows. This arrangement provides a thermodynamic advantage with an improved SFC and mixes out the higher velocity core jet to reduce the exhaust jet noise.

2. Fan thrust reverser upstream of the mixing plane. Actuation of the fan thrust reverser (closing off the duct upstream of the mixing plane) effectively provides a large increase in the core nozzle area, resulting in a spoiling of core thrust and eliminating need for a separate core thrust reverser.

Table III. QEP Trade Study, Low Speed Fan Cycle.

	M = 0, SL T/O 86° F (30° C) Day	M = 0.85, 35K Max Cruise Std. + 10° C Day
Thrust - lb (N)	22,000 (97,900)	4950 (22,000)
$W\sqrt{\theta}/\delta$ - lb/sec (kg/sec)	830 (377)	933 (424)
Fan Pressure Ratio	1.43	1.49
Bypass Ratio	6.8	6.8
Turbine Rotor (Cycle) Temperature, ° F (° C)	2330 (1277)	2140 (1172)
Core Supercharging Pressure Ratio	2.2	2.5
Core Corrected Flow - lb/sec (kg/sec)	56 (25.4)	58 (26.4)
Overall Pressure Ratio	24	28
Jet Velocity - ft/sec (m/sec)	900 (274)	---

Table IV. Nominal Installation Allowances, Low Speed Engine.

	M = 0, SL T/O 86° F (30° C) Day	M = 0.85, 35K Max Cruise Std. + 10° C Day
Inlet Recovery, P/P_o	0.9982	0.9974
Duct Loss, $\Delta P/P$ % (includes mixer friction loss)	1.08	1.34
Mixing Loss, $\Delta P/P$ %	0.34	0.96
Nozzle Thrust Coefficient, Cv	0.996	0.996

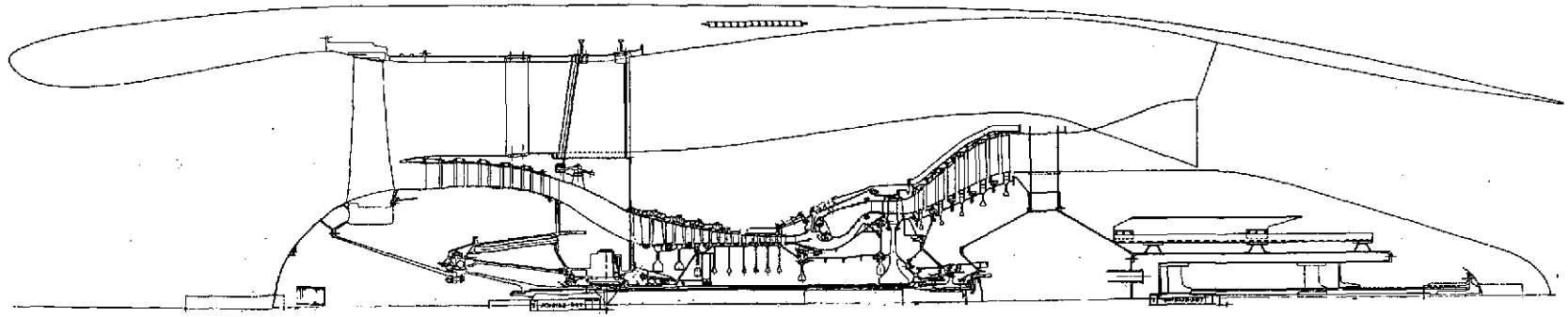

Figure 2. Engine with Low Speed Fan.

Table V. QEP Trade Study, Design Summary - Low Speed Fan.

Fan Aero (Cruise)	
Diameter, inches (meters)	68.7 (1.74)
Corrected Flow, lb/sec (kg/sec)	933 (424)
Pressure Ratio	1.49
Corrected Tip Speed, Cruise/Takeoff, ft/sec (N/sec)	1160/1060 (354/323)
Corrected Flow/Annulus Area, lb/sec-ft^2 (kg/sec-m^2)	42.3 (207)
Fan Blade	
Material	Solid TI
Shroud Location	Tip
Tip Chord, inches (meters)	7.8 (0.20)
Blade - Vane Spacing	2 Chords
N_B	40
Bypass OGV	
N_V	90
Booster	
Core Supercharging Pressure Ratio	2.5
Number of Booster Stages	5
Booster Corrected Flow, lb/sec (kg/sec)	124 (56.4)
Low Pressure Turbine	
Number of Stages	5
Average Pitch Line Loading	1.20
Last Stage Tip Diameter, inches (meters)	44 (1.12)
Core Design	
Core Corrected Flow, lb/sec (kg/sec)	58 (26.4)
Number of Compressor Stages	9
Core Compressor Ratio	12
Number of Turbine Stages	1

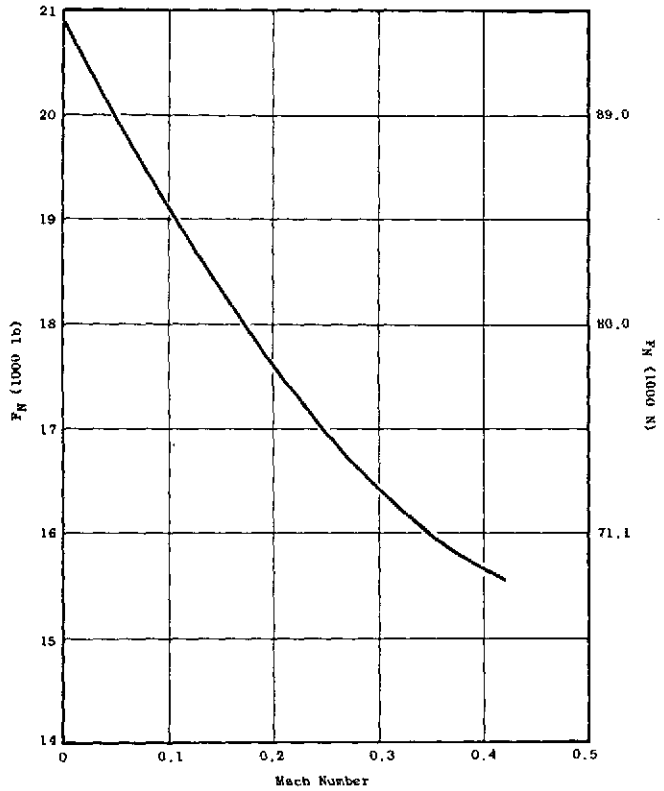

Figure 3. Hardwall Engine Takeoff Performance, Low Speed Engine.

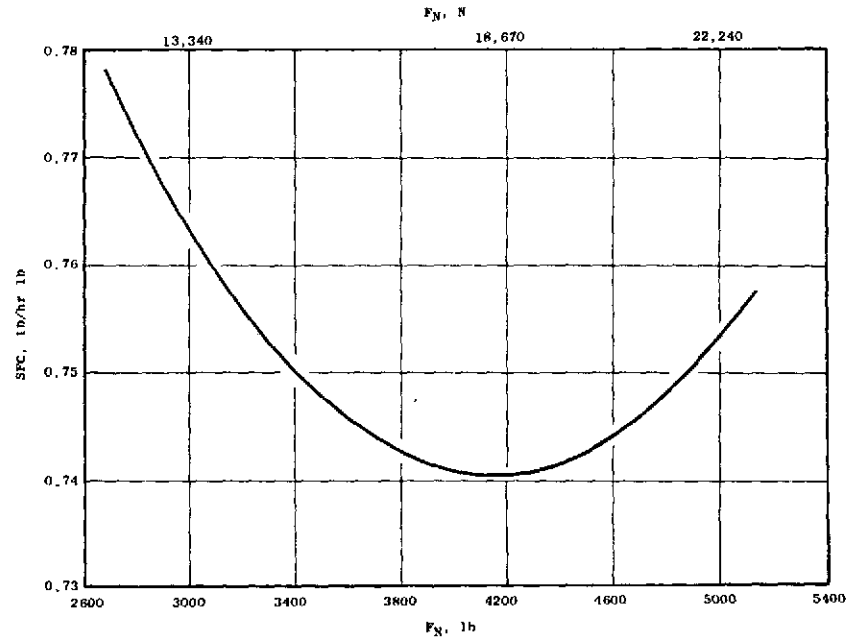

Figure 4. Hardwall Engine Cruise Performance, Low Speed Engine.

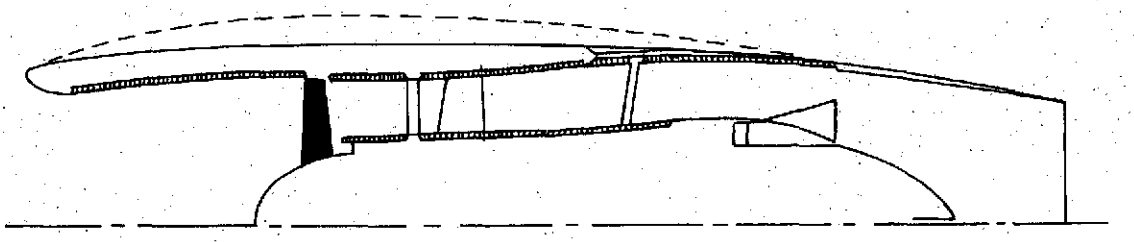

a. Wall Treatment

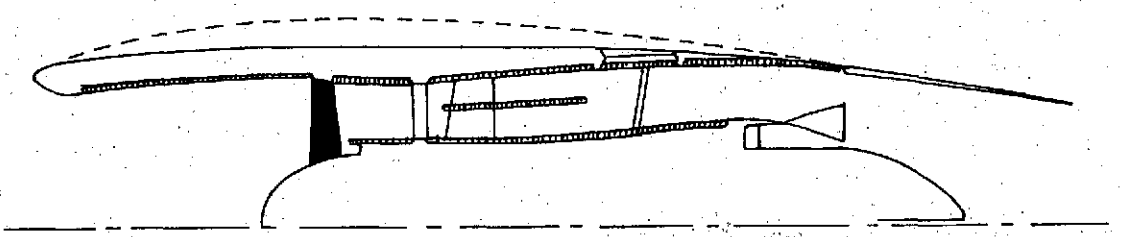

b. Wall Treatment Plus One Aft Splitter

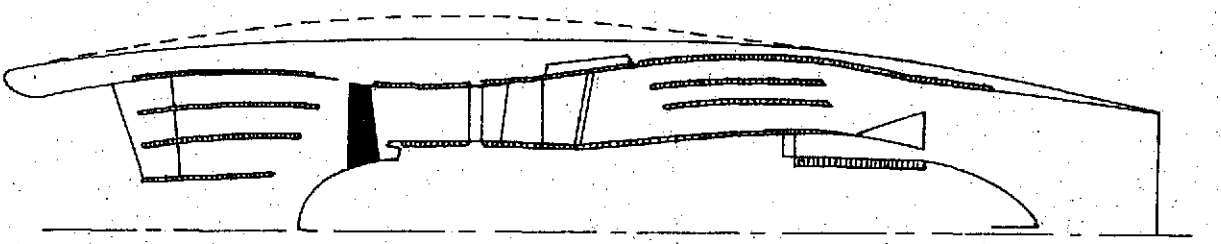

c. Wall Treatment Plus Three Inlet Splitters and Two Aft Splitters Plus Core Treatment

Figure 5. QEP Low Speed Engine.

The impact of incorporating various degrees of acoustical treatment was investigated by comparing the following configurations:

1. Basic nacelle without treatment

2. With wall treatment only

3. With wall treatment and single aft splitter

4. With wall treatment

   + 3 inlet splitters

   + 2 aft splitters

Schematics of these installations are shown in Figure 5. Configuration 5(b) (with single aft splitter) was selected since the low speed engine with wall treatment is dominated by aft fan noise, and the major impact on flyover EPNdB will be realized by reducing the aft noise constituent. Configuration 5(c) incorporates massive suppression in both fan inlet and exhaust ducts and also requires turbine and core noise suppression. This arrangement represents the minimum noise level that could be reasonably achieved with this engine and entails significant compromise in the nacelle.

The only type of acoustic liner considered in this study is the single-layer lining formed with a perforated plate bonded to a honeycomb cellular structure which is, in turn, bonded to an impervious backing sheet. The perforated plate is the resistive impedance element, while reactive impedance is due to both the perforated plate and the air volume in the honeycomb cells. By using combinations of different lining constructions, it is possible to broaden the effective bandwidth of the single-layer type. The acoustic suppression realized by this treatment is discussed in Section 4.0.

The external aerodynamic characteristics and pertinent internal characteristics are summarized in Table VI. The nacelle weights and engineering cost estimates are tabulated in Table VII.

3.3 INSTALLED PERFORMANCE

The internal installation losses are summarized in Table VIII for the takeoff thrust and in Table IX for altitude cruise SFC. The installed takeoff thrusts and cruise SFC characteristics are compared in Figures 6 and 7.

The effects of the various installed performance, weights, and costs on aircraft operating costs (DOC) are evaluated in Section 7.0.

Table VI. Low Speed Engine Nacelle Description.

Nacelle Configuration	Hardwall	Treated Walls	Treated Walls + 1 Aft Splitter	Treated Walls + 3 Inlet Splitters + 2 Aft Splitters
External Characteristics				
Nacelle Length, in. (m)	226 (5.75)	226 (5.75)	226 (5.75	262 (6.67)
Maximum Dia, in. (m)	85.8 (2.18)	85.8 (2.18)	85.8 (2.18)	89.6 (2.28)
Accessory Bulge, in. (m)	5.9 (0.15)	5.9 (0.15)	5.9 (0.15)	2.1 (0.05)
Highlight Dia, in. (m)	71 (1.8)	71 (1.8)	71 (1.8)	71 (1.8)
Fan Cowl Afterbody Angle	6°/13°	6°/13°	6°/13°	6°/13°
Internal Characteristics				
Inlet Length (Highlight to Fan), in. (m)	62 (1.58)	62 (1.58)	62 (1.58)	84 (2.14)
Wall Treated Area, ft^2 (m^2)	---	69 (6.41)	69 (6.41)	56 (5.20)
Splitter Treated Area, ft^2 (m^2)	---	---	---	164 (15.2/20.45) (net)
Fan Exhaust				
Length (OGV - Mixer), in. (m)	95 (2.41)	95 (2.41)	95 (2.41)	106 (2.69)
Wall Treated Area, ft^2 (m^2)	---	179 (16.65)	179 (16.65)	148 (13.75)
Splitter Treated Area,	---	---	56 (5.20)	169 (15.7/29.5) (net)
Core Exhaust				
Length (Frame - Mixer), in. (m)	20 (0.51)	20 (0.51)	20 (0.51)	31 (0.78)
Nozzle				
Length (Mixer - Exit), in. (m)	52 (1.32)	52 (1.32)	52 (1.32)	55 (1.40)
Treated Area, ft^2 (m^2)	---	---	---	31 (2.88)

Table VII. Low Speed Engine Nacelle Weights and Price.

Nacelle Configuration	Hardwall Weight, lb(kg)	Hardwall Price ($1000)	Treated Walls Weight, lb(kg)	Treated Walls Price ($1000)	Treated Walls +1 Aft Splitter Weight, lb(kg)	Treated Walls +1 Aft Splitter Price ($1000)	Treated Walls +3 Inlet Splitters +2 Aft Splitters Weight, lb(kg)	Treated Walls +3 Inlet Splitters +2 Aft Splitters Price ($1000)
Inlet								
Cowl + Treatment	302(137)	37	392(178)	38	392(178)	38	528(240)	77
Splitter(s)	---	---	---	---	---	---	431(196)	22
Nose Cone	17(7.7)	1	17(7.71)	1	17(7.7)	1	17(7.7)	1
Fan Cowl	151(68.5)	20	155(70.4	20	155(70.4)	20	164(74.5)	21
Fan Exhaust Duct								
Walls	233(107)	25	259(118)	27	259(118)	27	313(142)	33
Splitter(s)					69(31.4)	4	234(106)	14
Thrust Reverser								
Cascade - Blocker	640(291)	136	640(291)	136	640(291)	136	640(291)	136
Tanslating Cowl	398(181)	36	427(194)	39	427(194)	39	452(206)	42
Mixer	173(78.5)	17	173(78.5)	17	173(78.5)	17	173(78.5)	17
Core Plug	49(22.2)	2	49(22.2)	2	49(22.2)	2	59(26.8)	3
Engine Mount	85(38.6)	---	85(38.6)	---	85(38.5)	---	85(38.6)	---
Nacelle Equipment	694(316)	---	694(316)	---	694(316)	---	694(316)	---
Total	2742(1247)	274	2891(1313)	280	2960(1346)	284	3790(1722)	366

Table VIII. Low Speed Engine Installation Loss Comparisons.

Takeoff, Vp (1) = 100 Kts., Sea Level, 86° F (30° C) Day

Configuration	Hardwall		Treated Duct Walls		Treated Wall + Aft Splitter		Treated Wall + 3 Inlet Splitters + 2 Aft Splitters	
	$\Delta P/P\%$	$\Delta\%\ F_N/F_N$	$\Delta P/P\%$	$\Delta\%\ F_N/F_N$	$\Delta P/P\%$	$\Delta\%\ F_N/F_N$	$\Delta P/P\%$	$\Delta\%\ F_N/F_N$
Inlet Loss (2)	0	0	0.068	-0.18	0.068	-0.18	0.768	-2.04
Fan Duct Loss (2)	0	0	0.052	-0.07	0.355	-0.48	0.807	-1.09
Total Thrust Loss, $\Delta F_N/F_N$		0		-0.25		-0.66		-3.13
Installed F_N, lb (N)		18,443(82,000)		18,397(81,700)		18,321(81,500)		17,723(78,900)

(1) Vp = Aircraft flight velocity.

(2) Losses in addition to those incorporated in nominal (hardwall) engine
Nozzle CV = 0.996 for all cases (including uninstalled).

Table IX. Low Speed Engine Installation Loss Comparisons
M = 0.8, 30,000 ft (9.144 m), Standard Day

Configuration	Hardwall (1)		Treated Duct Walls (1)		Treated Wall + Aft Splitter (1)		Treated Wall + 3 Inlet Splitters +2 Aft Splitters (2)	
	ΔP/P%	Δ%SFC/SFC	ΔP/P%	Δ%SFC/SFC	ΔP/P%	Δ%SFC/SFC	ΔP/P%	Δ%SFC/SFC
Inlet Loss	0	0	0.103	+0.17	0.103	+0.17	1.153	+1.86
Fan Duct Loss	0	0	0.063	+0.08	0.428	+0.57	0.983	+1.31
Aircondition, Bleed 1 PPS Horsepower Extraction 50 HP		+4.30		+4.30		+4.30		+4.30
Total Installed Δ%SFC/SFC SFC Increase		+4.3		+4.55		+5.04		+7.47
Installed SFC Mx Cruise		0.6578		0.6595		0.6626		0.6789

(1) Nacelle and Pylon drag = 412 lb (1830 N)

(2) Nacelle and Pylon Drag = 472 lb (2100 N)

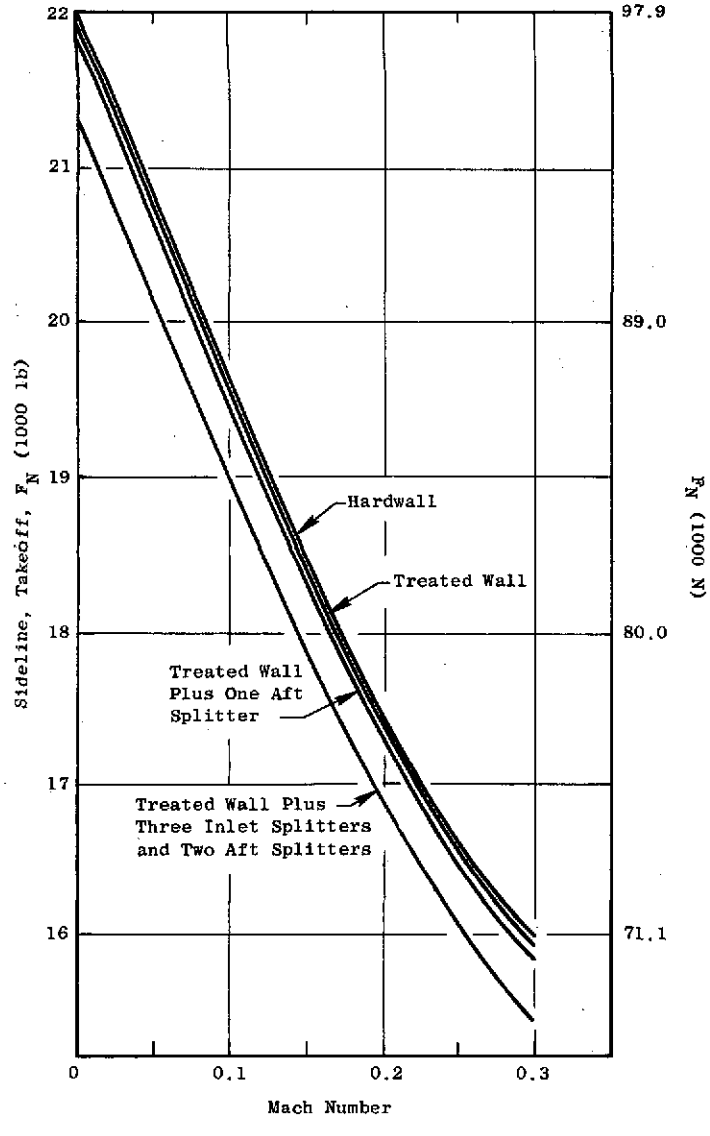

Figure 6. Installed Takeoff Performance Comparison, Low Speed Engine.

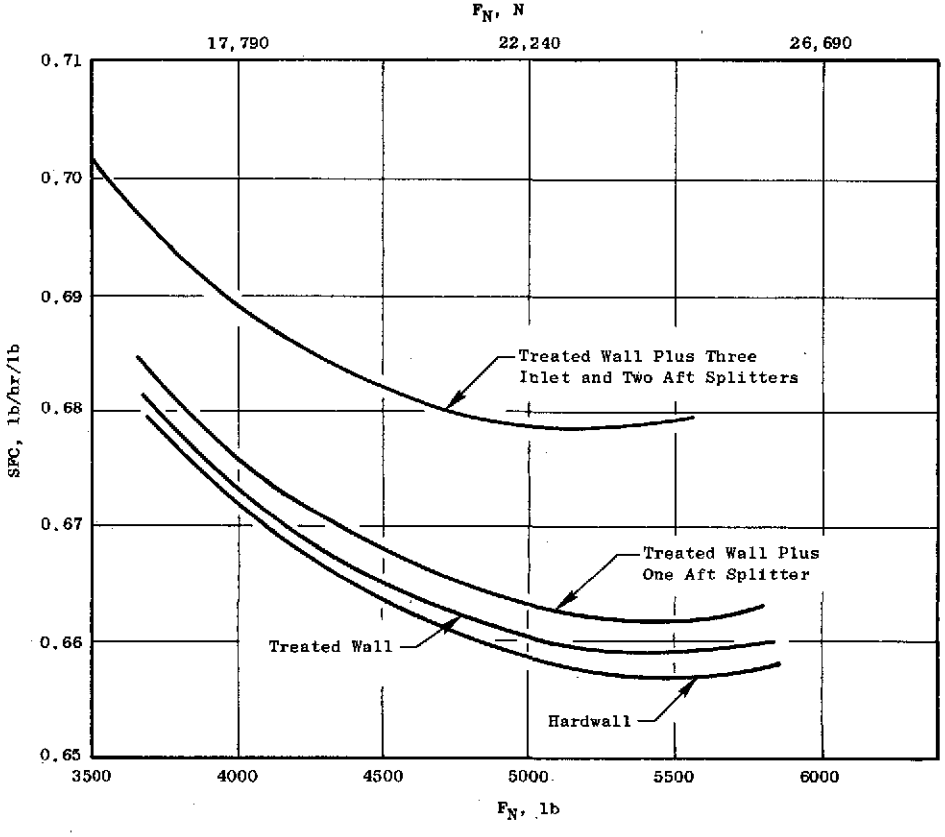

Figure 7. Installed Cruise Performance Comparison, Low Speed Engine.

4.0 LOW SPEED ENGINE STATIC NOISE CHARACTERISTICS

4.1 ENGINE STATIC SIDELINE CHARACTERISTICS

4.1.1 Unsuppressed Engine Characteristics

The 200-ft (60.96 m) sideline static characteristics are obtained by summing the individual contributions of the four primary component noise sources. At each angle the 1/3 octave band spectral distribution is described for each component. The parameters used in the turbine noise estimates are listed in Table X. Figure 8 shows spectral distributions of the four noise sources at approach power for the angle corresponding to the maximum forward noise (at 50°) and for the maximum aft noise (at 120°). Figure 9 shows the corresponding 1/3 octave band spectral distribution at takeoff power. Corresponding distributions are used at every 10° increment from 20° to 160°.

The noise sources expressed in PNdB at the 200-ft (60.96 m) sideline at the approach power setting (fan rpm = 60% of altitude cruise design point) are shown in Figure 10 for sideline angles from 20° to 150°. These sources are summed to obtain the total shown in Figure 10. For the unsuppressed engine, the fan is clearly the dominant noise source at takeoff. The corresponding directivity plot for the takeoff condition (fan rpm = 90% of altitude cruise design point) is shown in Figure 10. Here again, the fan component is the dominant point noise source. The overall 200-ft (60.96 m) sideline perceived noise levels as a function of the acoustic angle are summarized in Figure 11 for takeoff and approach power settings.

4.1.2 Noise Suppression

The initial step in suppression is the use of acoustic material in the fan duct. Treatments selected for the low speed fan duct were tuned to suppress the dominant frequencies which controlled PNdB level at takeoff. The predicted effectiveness of this treatment was based on both static duct test as well as measurements obtained from Quiet Engine A. The suppression characteristics at various 1/3 octave band frequencies are shown in Figure 12. Corresponding suppression was incorporated at other angles, again based on measured results from Quiet Engine A. This effectiveness at the other angles expressed as a fraction of that obtained at the angle of maximum suppression is shown in Figure 13.

The suppression obtained from the treatment in the aft fan duct is shown in Figure 14 for approach and takeoff power settings. Again the suppression at other angles was related to that at the maximum angle as shown in Figure 13.

Acoustic insertion losses based on acoustic probe data also were estimated using a three-ring splitter in addition to the wall treatment at the inlet, with the overall suppression also shown in Figure 12. The two cases where splitters are inserted in the aft duct are shown in Figure 14. The single splitter was limited in effectiveness since it was inserted into the initial fan duct with the constraints of no increase in the nacelle diameter and was made compatible with the original thrust reverser. The two-ring splitter was

Table X. Low Speed Engine Parameters.

Turbine

4th Stage Blade Number	191
5th Stage Blade Number	175

Takeoff

Speed, rpm	3550
Weight Flow, lb/sec	111 (50.5 Kg/sec)
Fourth Stage Blade Passing Frequency	10,000 Hz
Fifth Stage Blade Passing Frequency	10,000 Hz

Approach

Speed, rpm	2470
Weight Flow, lb/sec	69 (31.4 Kg/sec)
Fourth Stage Blade Passing Frequency	8,000 Hz
Fifth Stage Blade Passing Frequency	8,000 Hz

Combustor

Takeoff

Corrected rpm	3170
Combustor Inlet Temperature T_3, ° R	1480 (549° C)
Turbine Inlet Temperature T_4, ° R	2788 (1277° C)
Compressor Discharge Pressure P_3, $16/in^2$	353.6 (24.9 Kg/cm^2)
Compressor Discharge Weight Flow W_3, lb/sec	104.1 (49.4 Kg/sec)

Approach

Corrected rpm	2470
Combustor Inlet Temperature T_3, ° R	1211 (405° C)
Turbine Inlet Temperature T_4, ° R	2123 (907° C)
Compressor Discharge Pressure P_3, lb/in^2	193.4 (13.62 Kg/cm^2)
Compressor Discharge Weight Flow W_3, lb/sec	65.5 (29.8 Kg/sec)

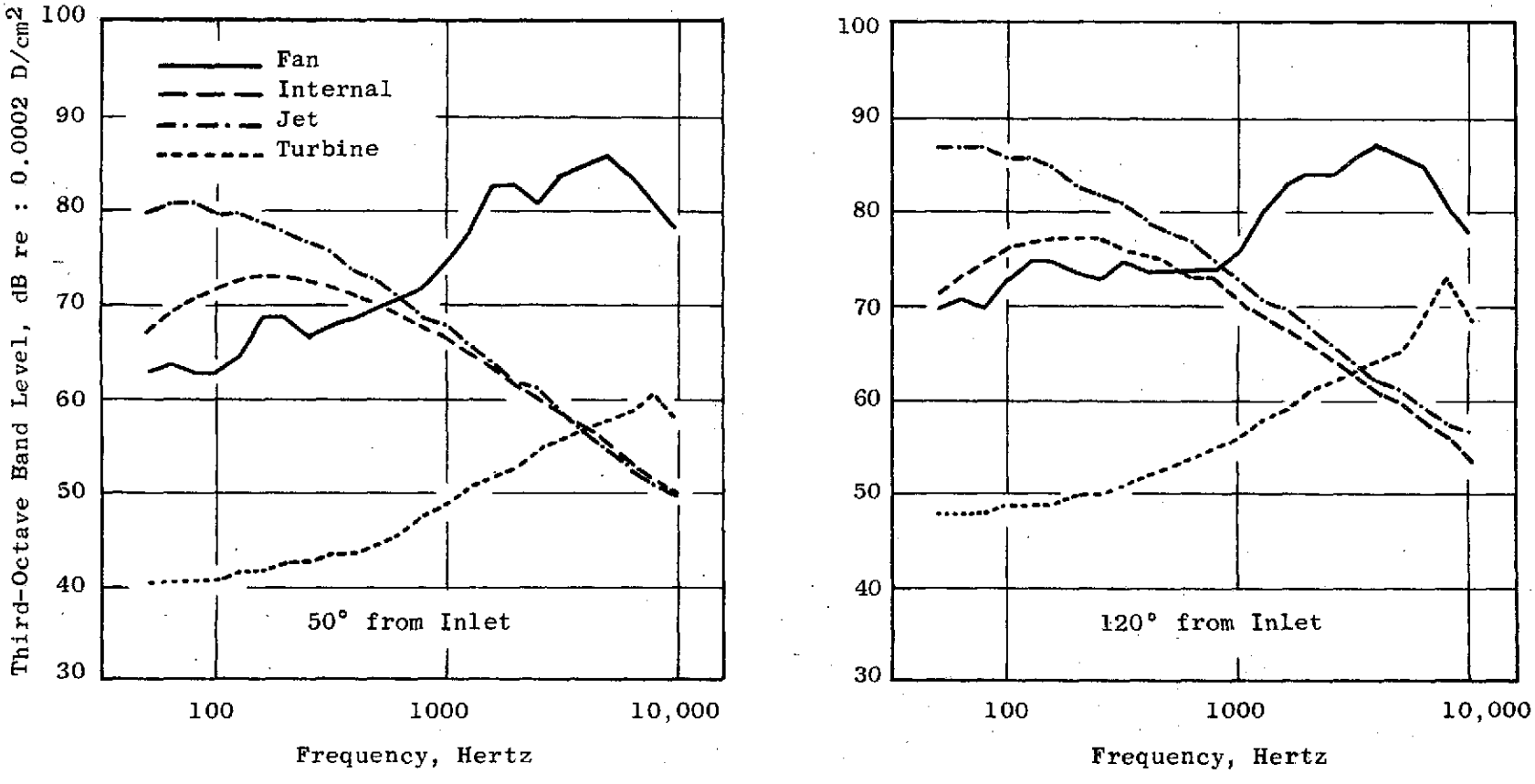

Figure 8. 1/3 Octave Band Spectral Distributions at Approach Power, Unsuppressed Low Speed Engine.

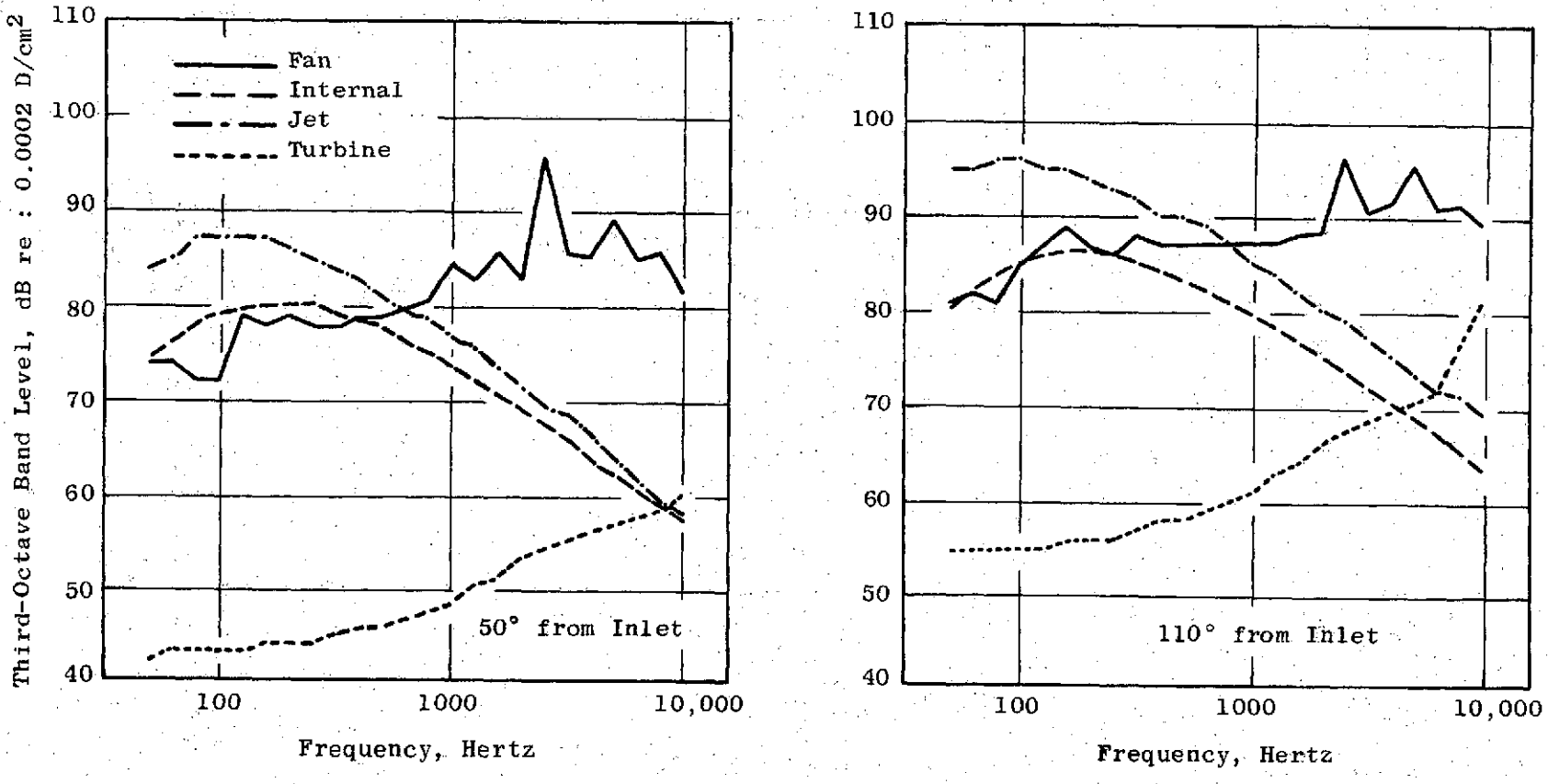

Figure 9. 1/3 Octave Band Spectral Distributions at Takeoff Power, Unsuppressed Low Speed Engine.

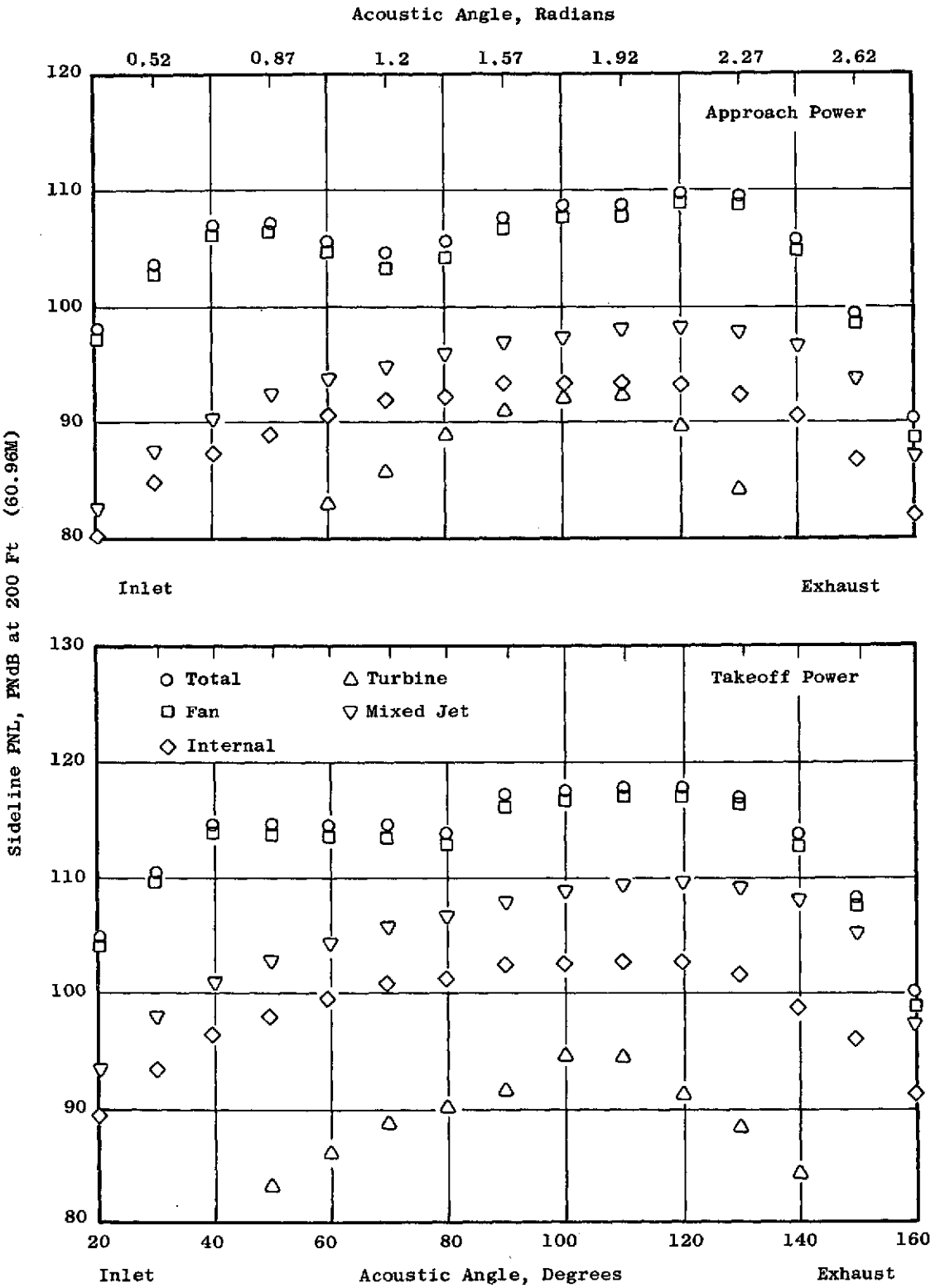

Figure 10. Unsuppressed Low Speed Engine Component Noise, 200-ft (60.96 m) Sideline PNL Vs. Acoustic Angle.

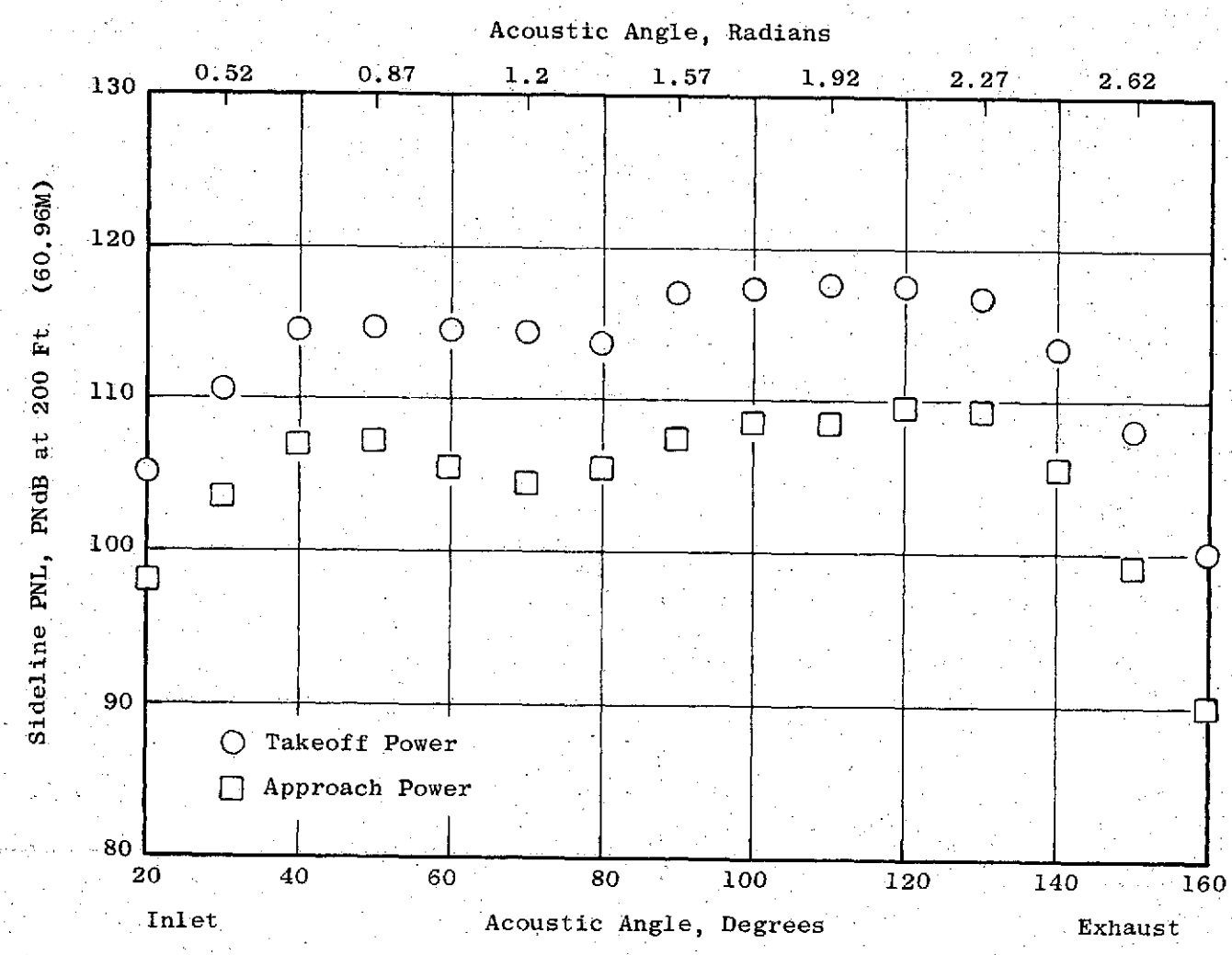

Figure 11. Overall 200-ft (60.96 m) Sideline PNL Vs. Acoustic Angle, Unsuppressed Low Speed Engine.

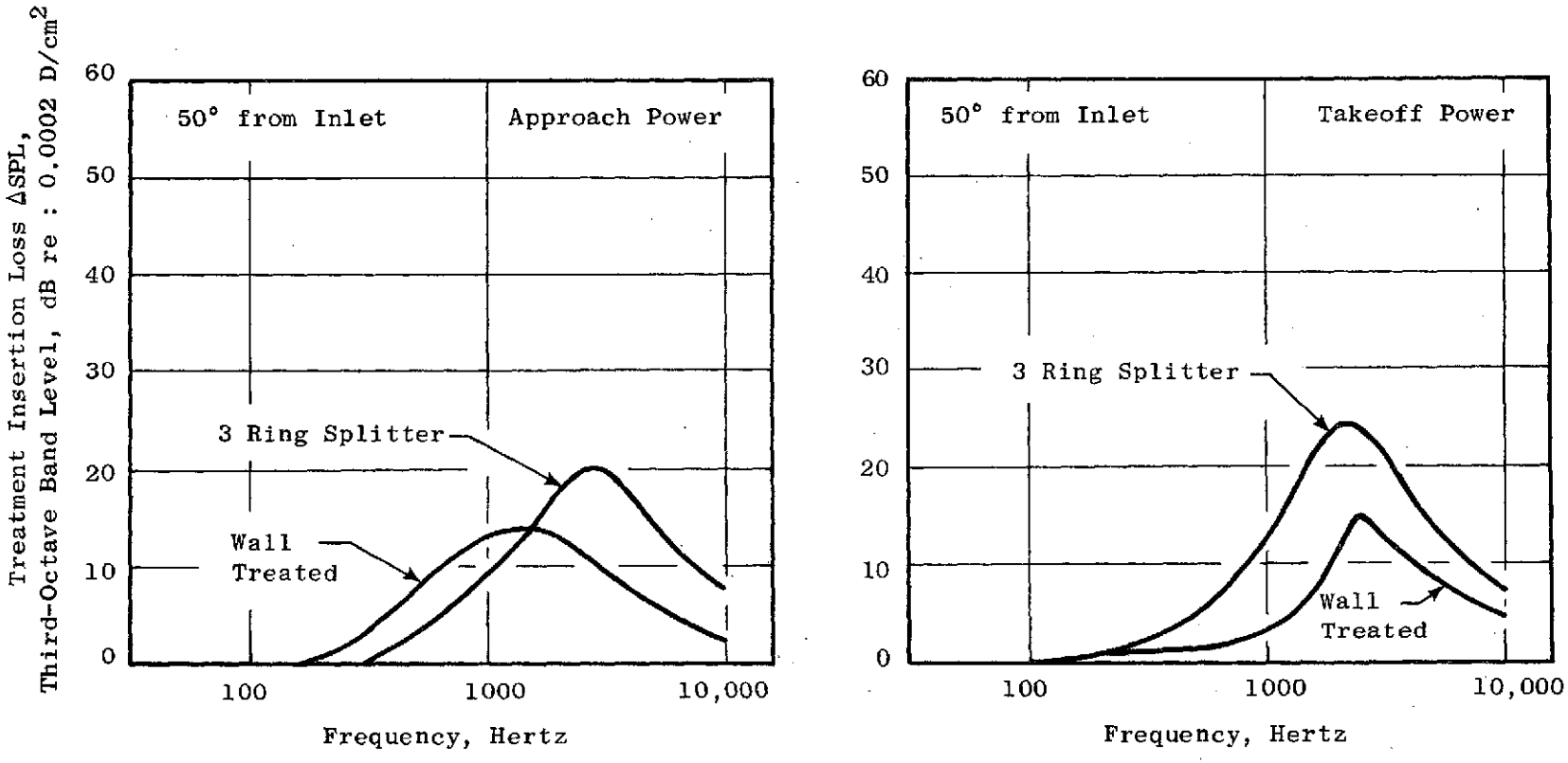

Figure 12. Fan Inlet Suppression, Low Speed Engine.

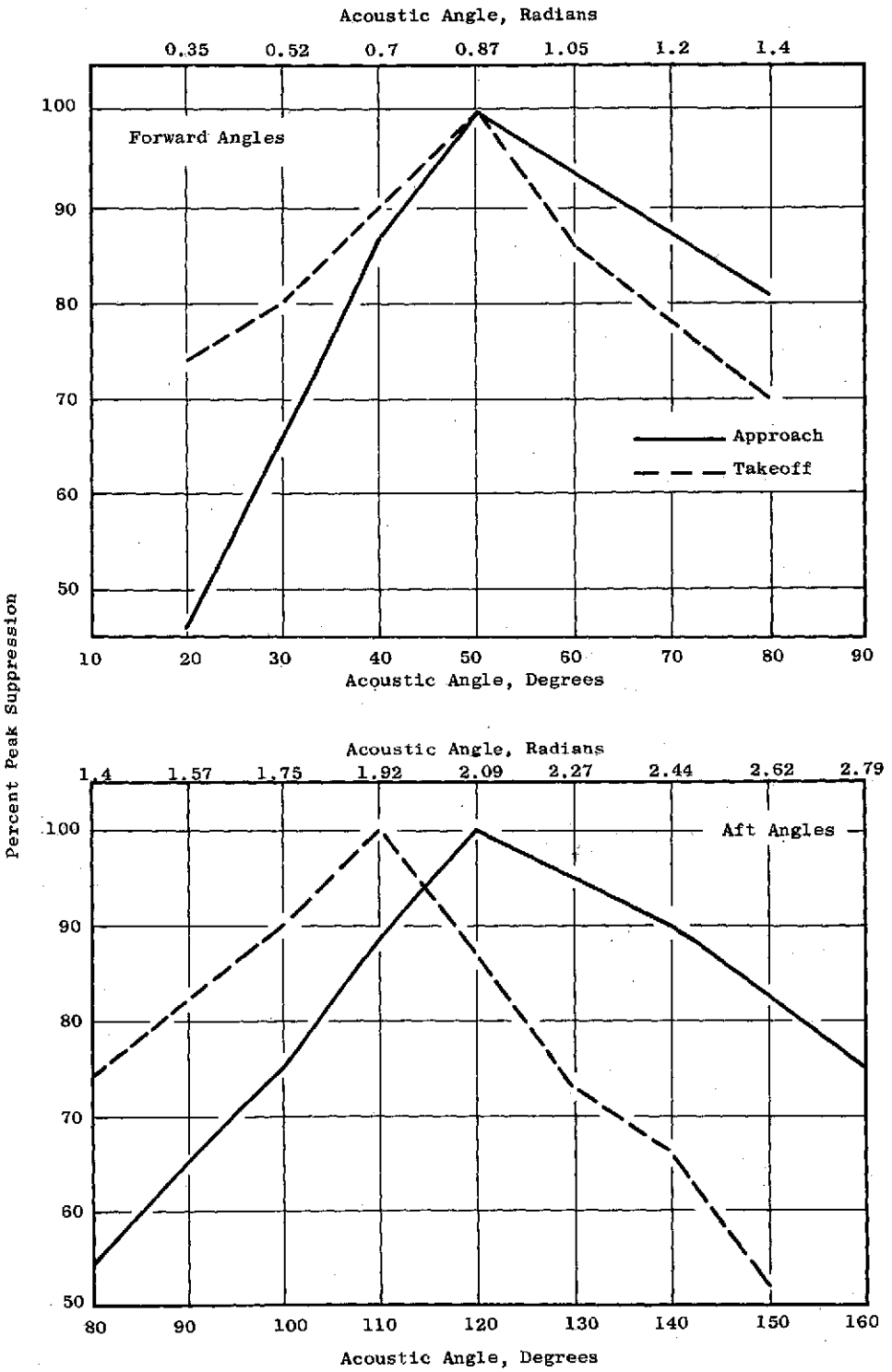

Figure 13. Suppression Directivity, Low Speed Engine.

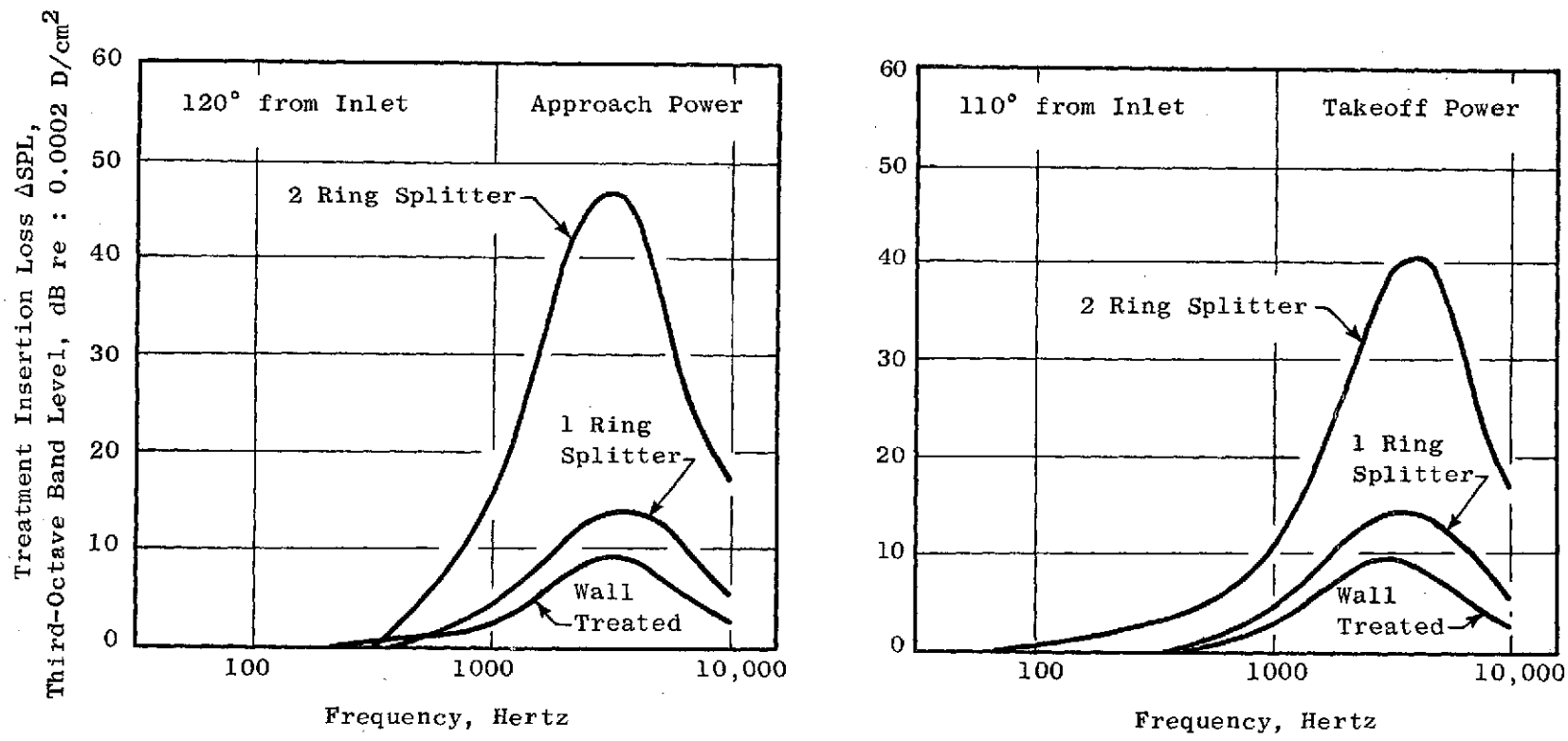

Figure 14. Fan Exhaust Suppression, Low Speed Engine.

designed to obtain maximum suppression with the duct annulus area adjusted for the optimum Mach number distribution through the duct and splitter. As a consequence, the nacelle diameter had to be increased, the thrust reverser had to be moved aft, and the overall length of the nacelle had to be increased. The specific changes required in the nacelle to accommodate the two aft splitters are shown in Section 3.2 and the effects on inlet installed performance are described in Section 3.3.

In the case where maximum suppression of the fan is utilized (that is the three-ring inlet splitter and the two-ring exhaust splitter), the fan noise was suppressed enough such that the turbine and internal source noises also contributed significantly to the overall noise. In this case, additional acoustic treatment was incorporated aft of the core to suppress both the high frequency turbine tones and low frequency internal noise. The geometry characteristics of this treatment are shown in Figure 15. The insertion losses obtained from this treatment at the angle of maximum noise from the inlet (110°) is shown in Figure 16. The suppression effectiveness was slightly different between the takeoff and approach cases (due to the change in the speed of sound with the change in temperature).

4.1.3 Suppressed Engine Noise Characteristics

The unsuppressed engine noise characteristics described in Section 4.1.1 were modified by reducing the 1/3 octave band spectral distributions of the separate components by the insertion losses described in Section 4.1.2. By summing these modified sources at each angle along the 200-ft (60.96 m) sideline the overall directivity characteristics of the suppressed nacelles are obtained. Figure 17 shows the directivity characteristics of the low speed engine at approach and takeoff power for the four installation configurations considered. The use of wall treatment is seen to be effective in reducing the overall noise levels 5 to 6 PNdB in both the forward and aft quadrants. The use of the single exhaust splitter reduced the aft end noise about 3 PNdB at approach and takeoff. This splitter also reduced the front end noise slightly, particularly for the takeoff condition where the total noise level is clearly aft dominated. The fully suppressed case with three inlet and two exhaust splitters produces an additional overall noise reduction but the amount of reduction is not as much as would be anticipated when comparing the insertion losses for the splitters as shown in Figure 14. In this case the overall noise levels are held up by contributions from jet noise at takeoff power and internal and turbine noise in both takeoff and approach.

4.1.4 Comparisons with Quiet Engine "A"

While directly analogous configurations of the low speed engine and Engine A are not available, Engine A was tested with acoustically treated duct walls with treatment areas as shown in Table XI.

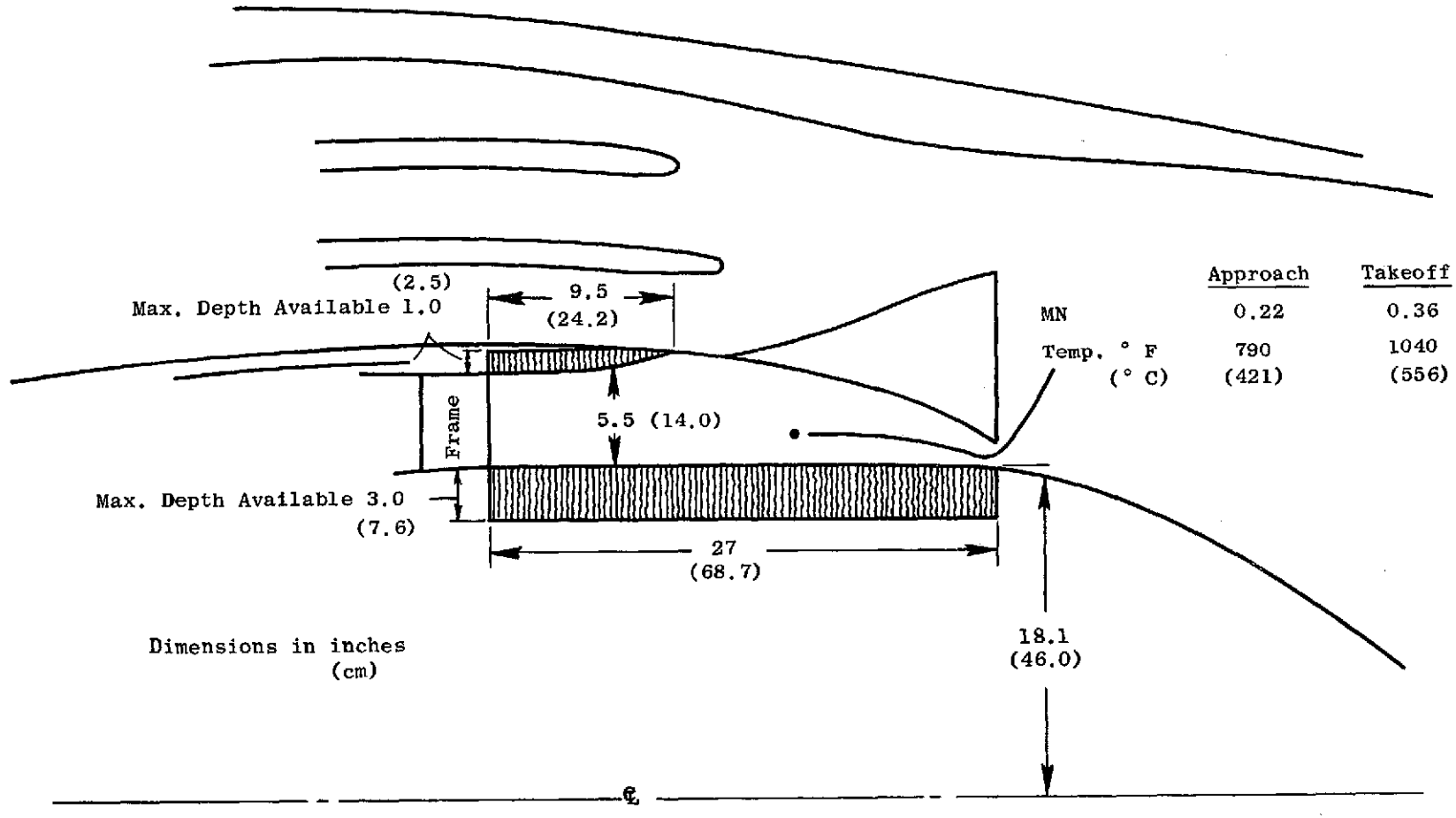

Figure 15. Core Exhaust Duct Treatment, Low Speed Engine.

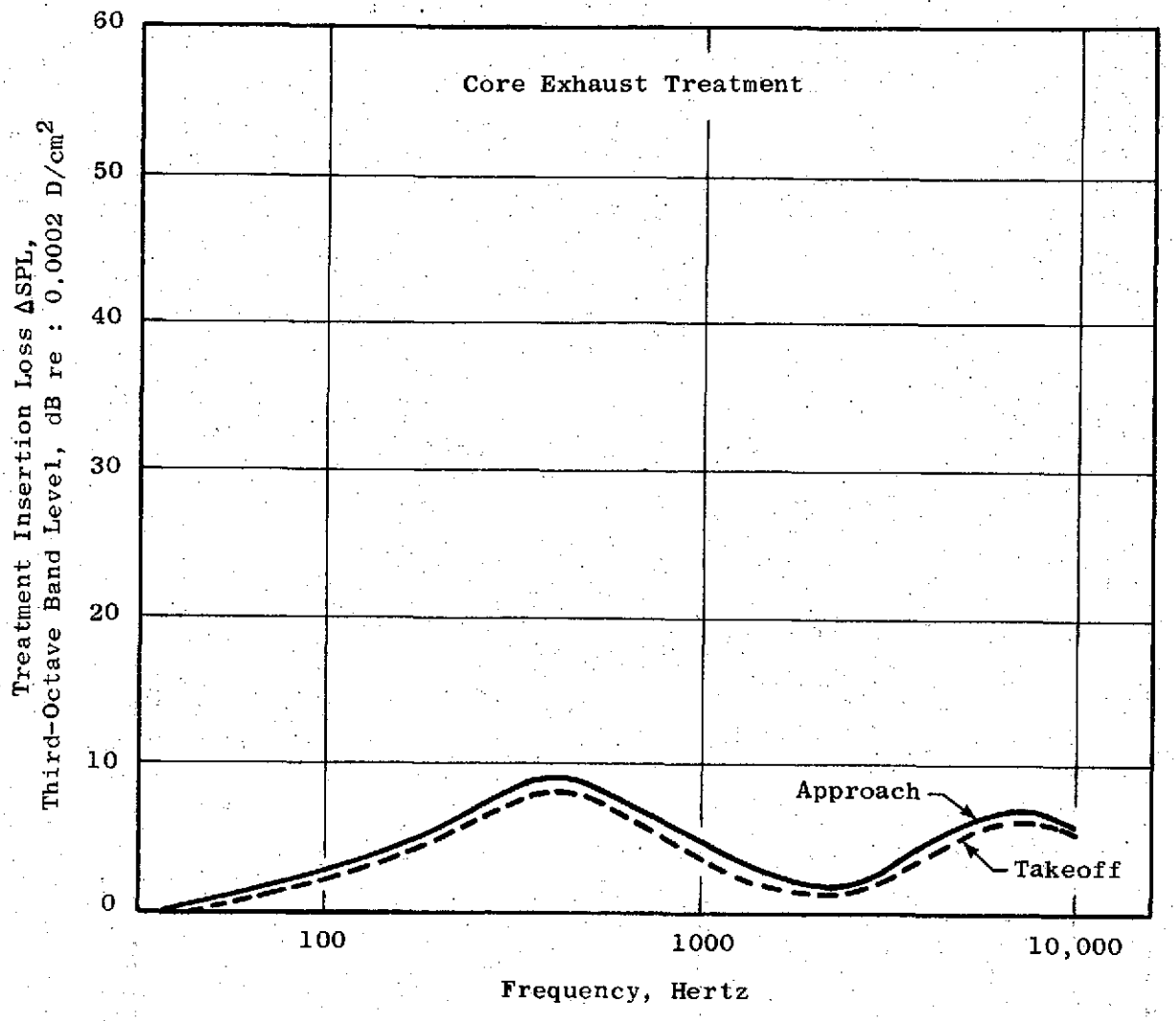

Figure 16. Core Exhaust Suppression, Low Speed Engine.

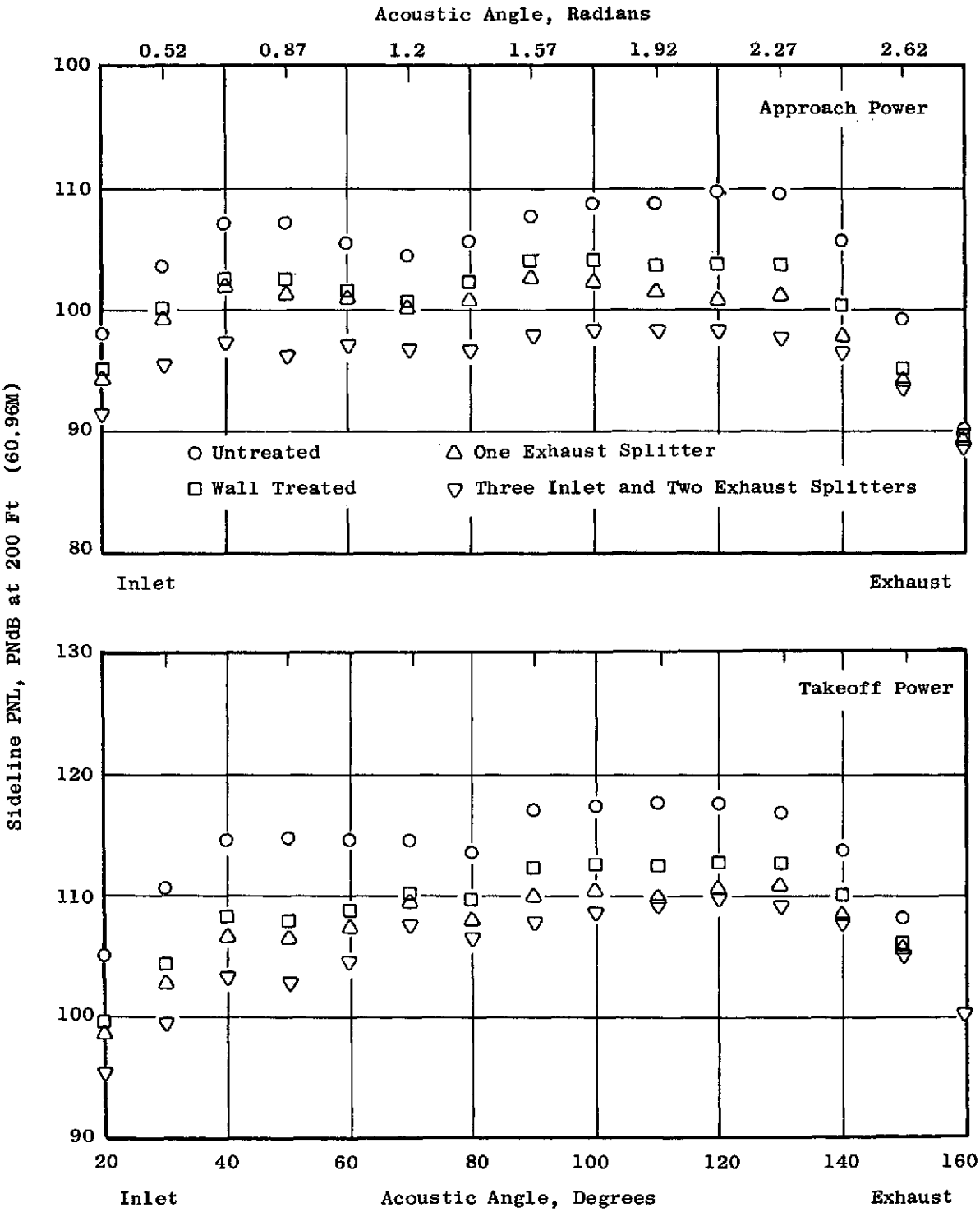

Figure 17. Directivity Characteristics of the Low Speed Engine at Approach and Takeoff Power.

Table XI. Treatment Area Comparison.

	Fan Inlet ft^2 (m^2)	Fan Exhaust ft^2 (m^2)
Duct Wall Treatment		
Engine A (MDOF)	51 (4.74)	147 (13.68)
Low Speed Engine (SDOF)	69 (64.1)	179 (16.65)
Fully Suppressed		
Engine A	276 (25.65)	230 (21.4)
Low Speed Engine	220 (20.45)	317 (29.5)

The wall-treated Engine A configuration is seen to compare reasonably well with the wall-treated case for the low speed engine. The 200-ft (60.96 m) sideline characteristics of Engine A and the low speed engine are compared in Figure 18 for both approach and takeoff power settings.

The fully suppressed configuration for Engine A which used three inlet splitters and a long, single exhaust splitter also compares favorably with the fully suppressed nacelle for the low speed engine. The 200-ft (60.96 m) sideline comparisons are shown in Figure 19 for approach and takeoff.

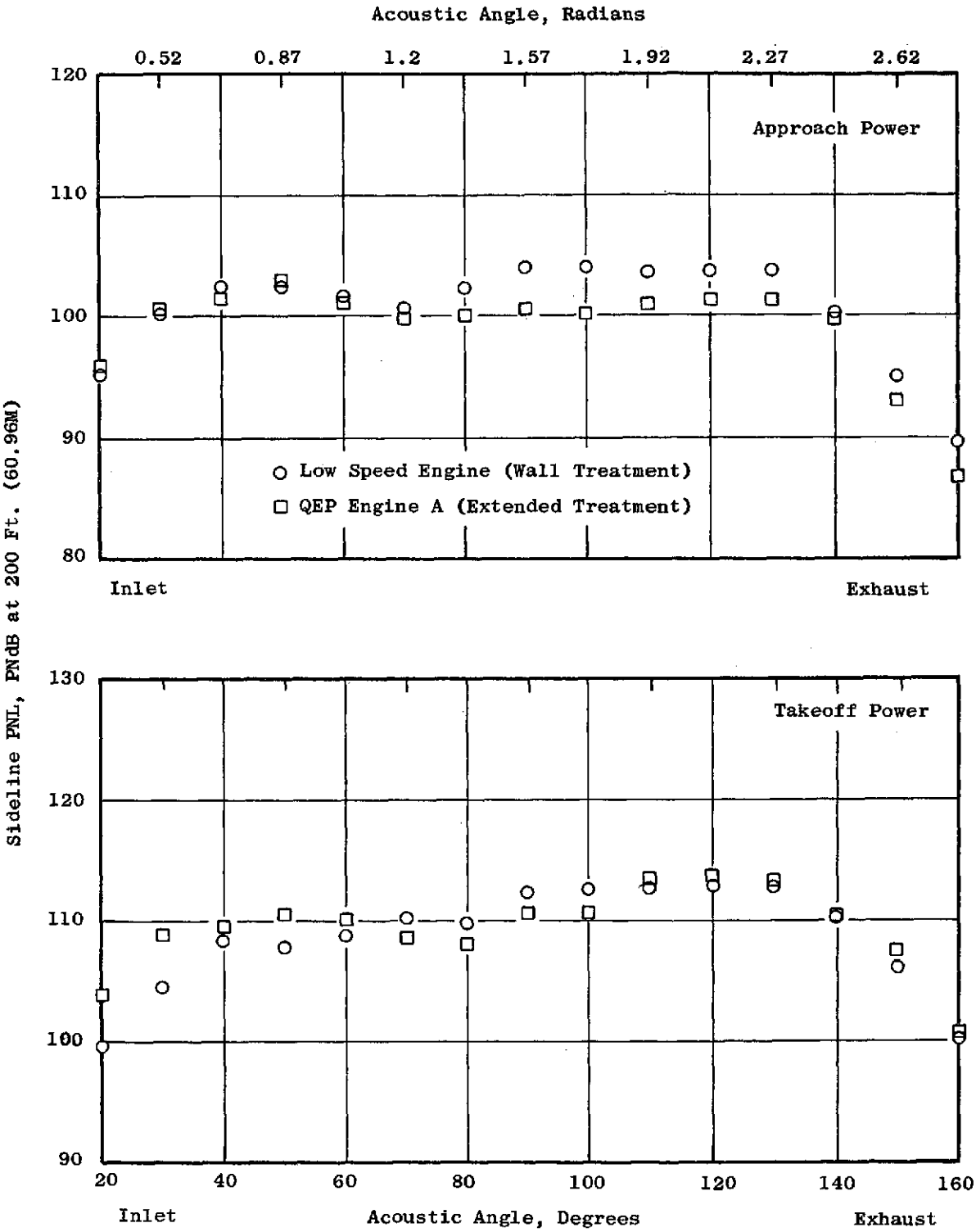

Figure 18. Comparison of 200-ft (60.96 m) Sideline Characteristics of QEP Engine A and Low Speed Engine.

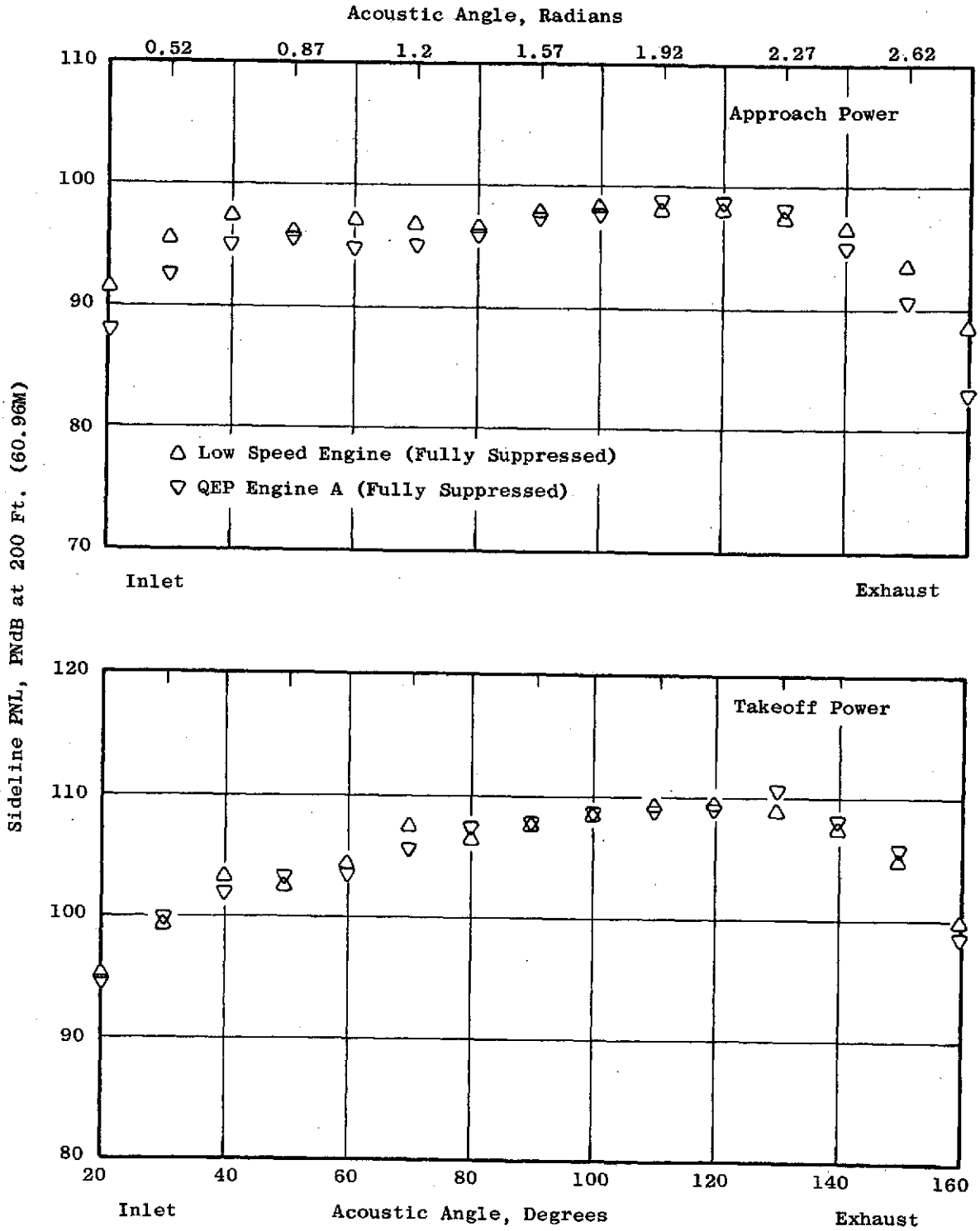

Figure 19. Comparison of 200-ft (60.96 m) Sideline Characteristics of Fully Suppressed QEP Engine A and Low Speed Engine.

5.0 HIGH SPEED ENGINE CHARACTERISTICS

5.1 BASIC ENGINE

The high speed engine, representing current levels of technology, was derived from the Quiet Engine Program Fan C, adapted to a modern core and sized for a SLS takeoff thrust of 22,000 lb (97,900 N) with nominal installation losses. The primary cycle characteristics are tabulated in Table XII. An engine cycle representative of CTOL applications has been selected to provide for a mixed core and fan stream ahead of the nozzle. The jet velocity shown in Table XII represents the velocity after mixing. Inlet recoveries, duct losses, mixing losses and nozzle thrust coefficients used in the cycle are shown in Table XIII. The engine flowpath configuration is shown in Figure 20. A short tabulation of the major component characteristics is contained in Table XIV.

The high speed engine fan applies the measured performance characteristics of Fan C in the bypass flow modified to a higher aspect ratio, tip-shrouded configuration with 46 blades. The fan pressure ratio of 1.55 was selected as a near optimum value for CTOL installations balancing the installed performance characteristics with a takeoff jet noise level of about FAR 36-20. A clean stall margin in excess of 17% should provide stall-free operation in the most severe operational environment anticipated for this engine. The Fan C radius ratio of 0.38 was retained, with booster stages added to provide the desired core supercharging pressure ratio of 2.5. Three booster stages were selected to meet the requirement of boost pressure ratio plus an adequate stall margin, and this selection was based on aerodynamic loadings consistent with the CF6-50 engine booster stages.

A four-stage low pressure turbine was selected to provide a moderately highly loaded turbine consistent with the design efficiency objective.

The overall nominal (hardwall) engine takeoff thrust is shown in Figure 21 and attitude cruise SFC is shown in Figure 22.

5.2 NACELLE CONFIGURATIONS

Overall arrangement: The engine is installed in a long duct nacelle, illustrated in Figure 23. As in the low speed engine, the major features are:

1. Mixed core and fan flows
2. Fan thrust reverser upstream of the mixing plane

The impact of incorporating various degrees of acoustical treatment was investigated by comparing the following configurations:

1. Basic Nacelle without treatment
2. With wall treatment only

Table XII. QEP Trade Study, High Speed Fan Cycle.

	M=0, SL T/O 86° F (30° C) Day	M=.85, 35K Max Cruise Std. + 10° C Day
Thrust - lb (N)	22,000 (97,900)	4950 (22,000 N)
$W\sqrt{\theta}/\delta$ - lb/sec (kg/sec)	814 (370)	911 (414)
Fan Pressure Ratio	1.47	1.55
Bypass Ratio	6.35	6.4
Turbine Rotor (Cycle) Temperature, ° F (° C)	2330 (1277)	2140 (1172)
Core Supercharging Pressure Ratio	1.6	2.4
Core Corrected Flow - lb/sec (kg/sec)	58 (26.4)	59 (26.8)
Overall Pressure Ratio	24	28
Jet Velocity - ft/sec (m/sec)	920 (280)	---

Table XIII. Nominal Installation Allowances, High Speed Engine.

		M=0, SL T/O 86° F (30° C) Day	M=.85, 35K Max Cruise Std. + 10° C Day
Inlet Recovery	P/P_o	0.9982	0.9974
Duct Loss (includes mixer friction loss)	$\Delta P/_P\%$	0.97	1.15
Mixing Loss	$\Delta P/_P\%$	0.26	0.91
Nozzle Thrust Coefficient, Cv		0.996	0.996

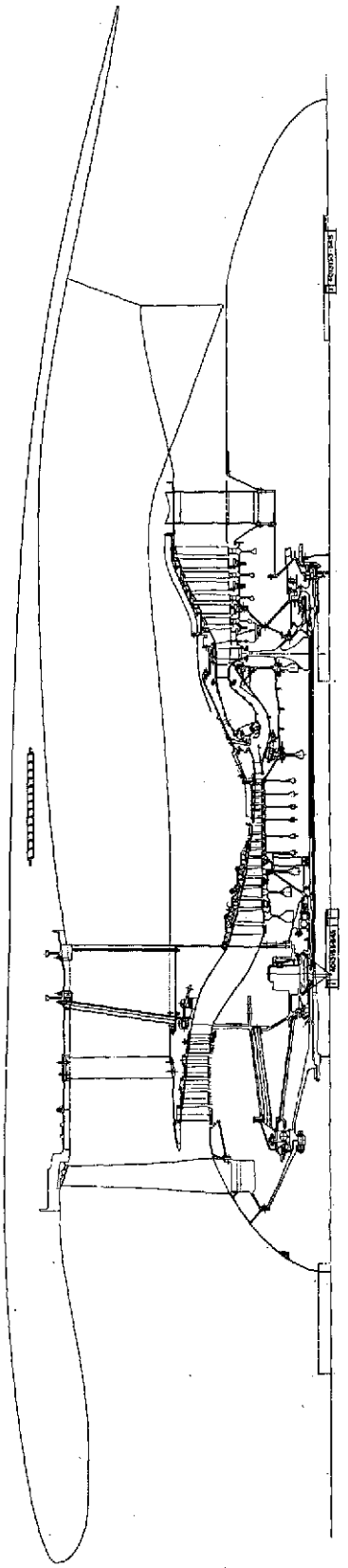

Figure 20. Engine with High Speed Fan.

Table XIV. QEP Trade Study, Design Summary - High Speed Fan.

Fan Aero		
Diameter, inches (m)	68.3 (1.74)	
Corrected Flow, lb/sec (kg/sec)	911 (414)	
Pressure Ratio	1.55	
Corrected Tip Speed, Design Takeoff, ft/sec (m/sec)	1550/1440 (472/439)	Same T.O. as CF6-6
Corrected Flow/Annulus Area, lb/sec-ft^2	41.8	
Fan Blade		
Material	ti	
Shroud Location	Tip	
Tip Chord, inches (m)	6-6.5 (0.15-0.17)	
Blade-Vane Spacing	2 chords	
N_B	45-50	
Bypass OGV		
N_V	90	
Booster		
Core Supercharging Pressure Ratio	2.4	
Number of Booster Stages	3	
Booster Corrected Flow, lb/sec (kg/sec)	122 (55.5)	
Low Pressure Turbine		
Number of Stages	4	
Average Pitch Line Loading	1.1	
Last Stage Tip Diameter, inches (m)	39.1 (.99)	
Core Design		
Core Corrected Flow, lb/sec (kg/sec)	59.1 (26.9)	
Number of Compressor Stages	9	
Core Compressor Ratio	11.5	
Number of Turbine Stages	1	

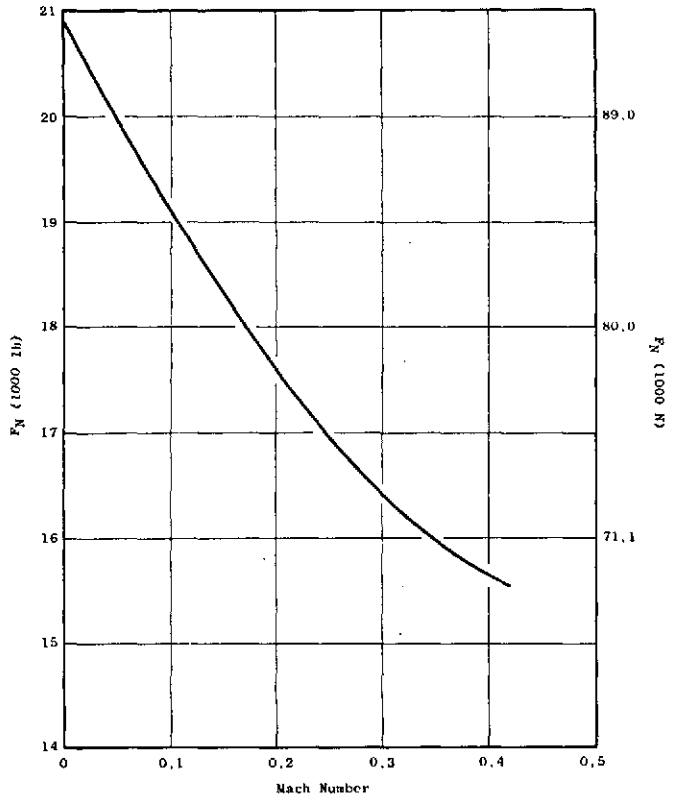

Figure 21. Hardwall Engine Takeoff Performance, High Speed Engine.

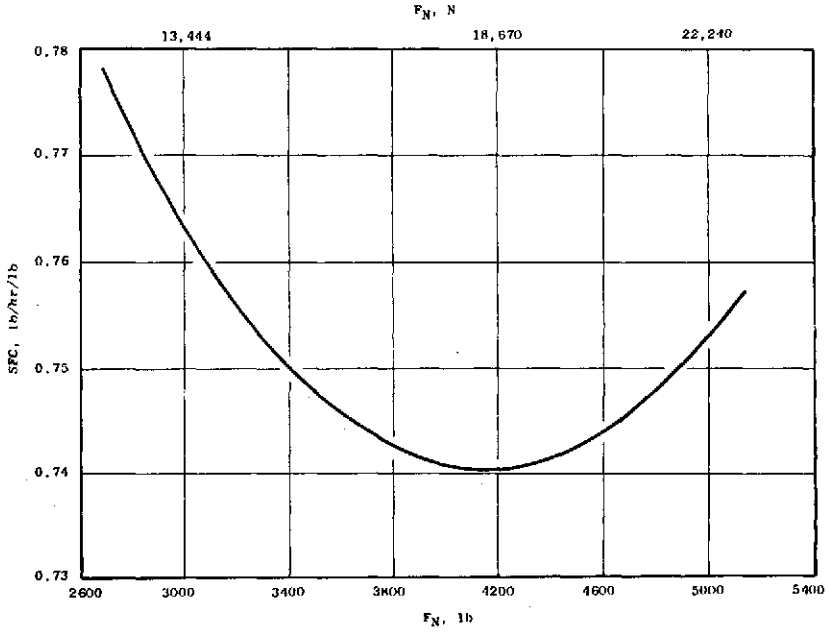

Figure 22. Hardwall Engine Cruise Performance, High Speed Engine.

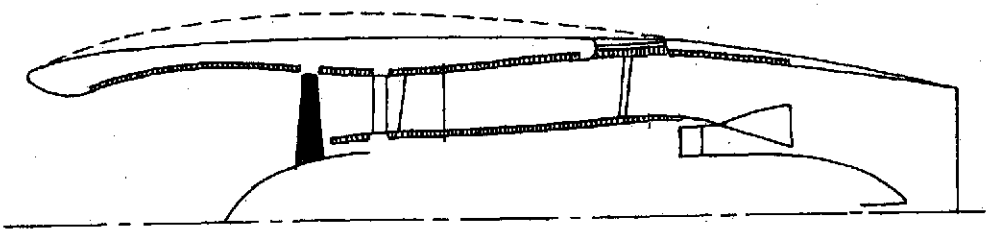

a. Wall Treatment

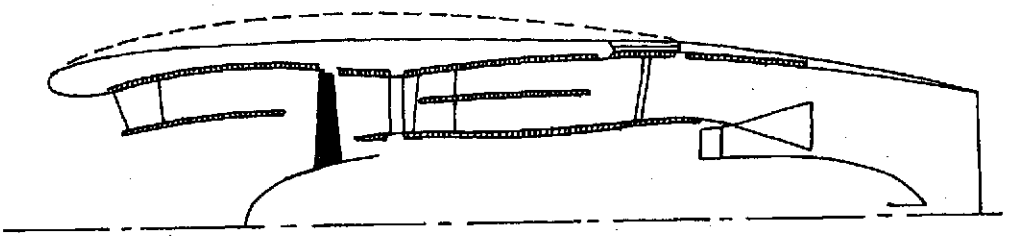

b. Wall Treatment Plus 1 Inlet Splitter and 1 Aft Splitter

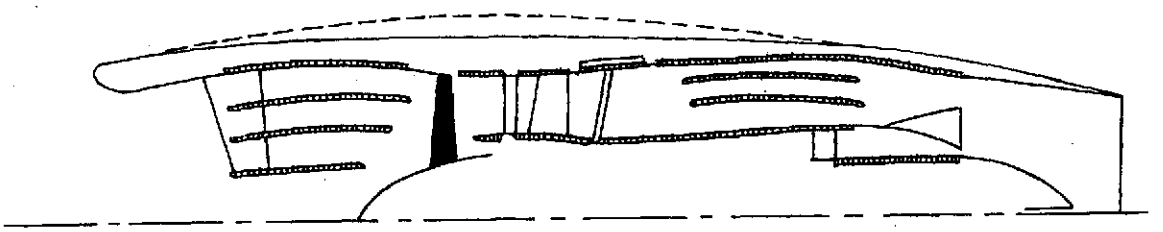

c. Wall Treatment Plus 3 Inlet Splitters and 2 Aft Splitters Plus Core Treatment

Figure 23. QEP High Speed Engine.

3. With wall treatment and single inlet and aft splitter

4. With wall treatment

   + 3 inlet splitters

   + 2 aft splitters

Schematics of these installations are shown in Figure 23. Configuration 23(b) (with single inlet and aft splitter) was selected since the high speed engine with wall treatment is nearly balanced between inlet and aft noise at takeoff and, in order to make full impact on flyover EPNdB, both fore and aft noise constituent must be reduced. Configuration 23(c) incorporates massive suppression in both fan inlet and exhaust ducts and requires turbine and core noise suppression as well. This arrangement represents the minimum noise level that could be reasonably achieved with this engine and entails significant compromise in the nacelle.

As with the low speed engine, the only type of acoustic liner is the single-layer lining. Combinations of different lining constructions are used to broaden the effective bandwidth of the single-layer type.

The external aerodynamic characteristics and pertinent internal characteristics are summarized in Table XV. The nacelle weights and costs are tabulated in Table XVI.

5.3 INSTALLED PERFORMANCE

The internal installation losses are summarized in Table XVII for the takeoff thrust and Table XVIII for altitude cruise SFC. The installed takeoff thrusts and cruise SFC characteristics are compared in Figures 24 and 25.

Table XV. High Speed Engine Nacelle Description.

Nacelle Configuration	Hardwall	Treated Walls	Treated Walls + 1 Inlet Splitter + 1 Aft Splitter	Treated Walls + 3 Inlet Splitters + 2 Aft Splitters
External Characteristics				
Nacelle Length, in (m)	207 (5.27)	207 (5.27)	207 (5.27)	240 (6.10)
Maximum Dia, in (m)	83 (2.11)	83 (2.11)	83 (2.11)	85 (2.16)
Accessory Bulge, in (m)	6.1 (0.15)	6.1 (0.15)	6.1 (0.15)	5.1 (0.13)
Highlight Dia, in (m)	68.7 (1.75)	68.7 (1.75)	68.7 (1.75)	68.7 (1.75)
Fan Cowl Afterbody Angle ($\theta_{wrv}/\theta_{T/E}$)	6°/15°	6°/15°	6°/15°	6°/15°
Internal Characteristics				
Inlet Length (Highlight to Fan), in (m)	61 (1.5)	61 (1.5)	61 (1.5)	84 (2.13)
Wall Treated Area, ft^2 (m^2)	---	62 (5.76)	62 (5.76)	58
Splitter Tested Area, ft^2 (m^2)	---	---	62 (5.76)	167.5/225.5 (net) (15.56/20.95)
Fan Exhaust				
Length (OGV - Mixer), in (m)	9 (2.38)	94 (2.38)	94 (2.38)	104 (2.64)
Wall Treated Area, ft^2 (m^2)	---	134 (12.46)	134 (12.46)	159 (14.78)
Splitter Tested Area, ft^2 (m^2)	---	---	67 (6.23)	157/316 (net) (14.6/29.4)
Core Exhaust				
Length (Frame - Mixer), in (m)	20 (0.51)	20 (0.51)	20 (0.51)	30 (0.76)
Nozzle				
Length (Mixer - Exit), in (m)	37 (0.94)	37 (0.94)	37 (0.94)	37 (0.94)

Table XVI. High Speed Engine Nacelle Weights and Price.

Nacelle Configuration	Hardwall		Treated Walls		Treated Walls + 1 Inlet Splitter + 1 Aft Splitter		Treated Walls + 3 Inlet Splitters + 2 Aft Splitters	
	Weight lb (kg)	Price ($1000)	Weight lb (kg)	Price ($1000)	Weight lb (kg)	Price ($1000)	Weight lb (kg)	Price ($1000)
Inlet								
Cowl + Treatment	388 (177)	37	397 (181)	38	397 (181)	38	532 (242)	75
Splitter(s)	---	---	---	---	168 (77)	8	429 (195)	20
Nose Cone	17 (7.7)	1	17 (7.7)	1	17 (7.7)	1	17 (7.7)	1
Fan Cowl	123 (56)	16	125 (57)	16	125 (57)	16	133 (61)	17
Fan Exhaust Duct								
Walls	229 (104)	26	251 (114)	28	251 (114)	27	304 (138)	32
Splitter(s)	---	---	---	---	63 (28.7)	4	214 (97)	11
Thrust Reverser								
Cascade - Blocker	560 (255)	118	560 (255)	118	560 (355)	118	560 (255)	118
Translating Cowl	346 (157)	32	367 (167)	34	367 (167)	34	386 (176)	34
Mixer	160 (73)	17	160 (73)	17	160 (73)	17	160 (73)	17
Core Plug	45 (20.5)	2	45 (20.5)	2	45 (20.5)	2	53 (24.1)	3
Engine Mount	90 (41)	---	90 (41)	---	90 (41)	---	90 (41)	---
Nacelle Equipment	725 (330)	---	725 (330)	---	725 (330)	---	725 (330)	---
Total	2683 (1221)	249	2737 (1246)	254	2968 (1352)	265	3603 (1640)	328

Table XVII. High Speed Engine Installation Loss Comparisons.
Takeoff, Vp = 100 Kts., Sea Level, 86° F (30° C) Day

Configuration	Hardwall		Treated Duct Walls		Treated Wall + 1 Inlet Splitter + Aft Splitter		Treated Walls + 3 Inlet Splitters + 2 Aft Splitters	
	ΔP/P%	Δ% F_N/F_N	ΔP/P%	Δ% F_N/F_N	ΔP/P%	Δ% F_N/F_N	ΔP/P%	Δ% F_N/F_N
Inlet Loss (1)	0	0	.062	-0.16	.385	-1.00	.792	-2.06
Fan Duct Loss (1)	0	0	0	0	.323	-0.40	.690	-0.75
Total Thrust Loss $\Delta F_N/F_N$		0		-0.16		-1.40		-2.81
Installed F_N, lb (N)		18,555 (82,500)		18,525 (82,400)		18,295 (81,300)		-18,037 (80,200)

1 Losses in addition to those incorporated in nominal (hardwall) engine
Nozzle Cv = 0.996 for all cases.

Table XVIII. High Speed Engine Installation Loss Comparisons.
M = 0.8, 30 K, Standard Day

Configuration	Hardwall[1]		Treated Duct Walls (1)		Treated Wall + 1 Inlet Splitter + Aft Splitter[1]		Treated Wall + 3 Inlet Splitters + 2 Aft Splitters[2]	
	ΔP/P%	Δ%SFC/SFC	ΔP/P%	Δ%SFC/SFC	ΔP/P%	Δ%SFC/SFC	ΔP/P%	Δ%SFC/SFC
Inlet Loss	0	0	0.089	+ 0.14	0.560	+ 0.77	1.159	+ 1.76
Fan Duct Loss	0	0	0	0	0.379	+ 0.46	0.82	+ 1.00
Air Condition, Bleed 1 pps Horsepower Extraction 50 HP		+4.30		+4.30		+4.30		+4.30
Total Installed $\frac{\Delta\%SFC}{SFC}$ SFC Increase		+ 4.30		+ 4.44		+ 5.53		+ 7.06
Installed SFC Mx Cruise		0.6706		0.6714		0.6791		0.6891

(1) Nacelle and Pylon Drag = 402 lb (183 kg)

(2) Nacelle and Pylon Drag = 426 lb (194 kg)

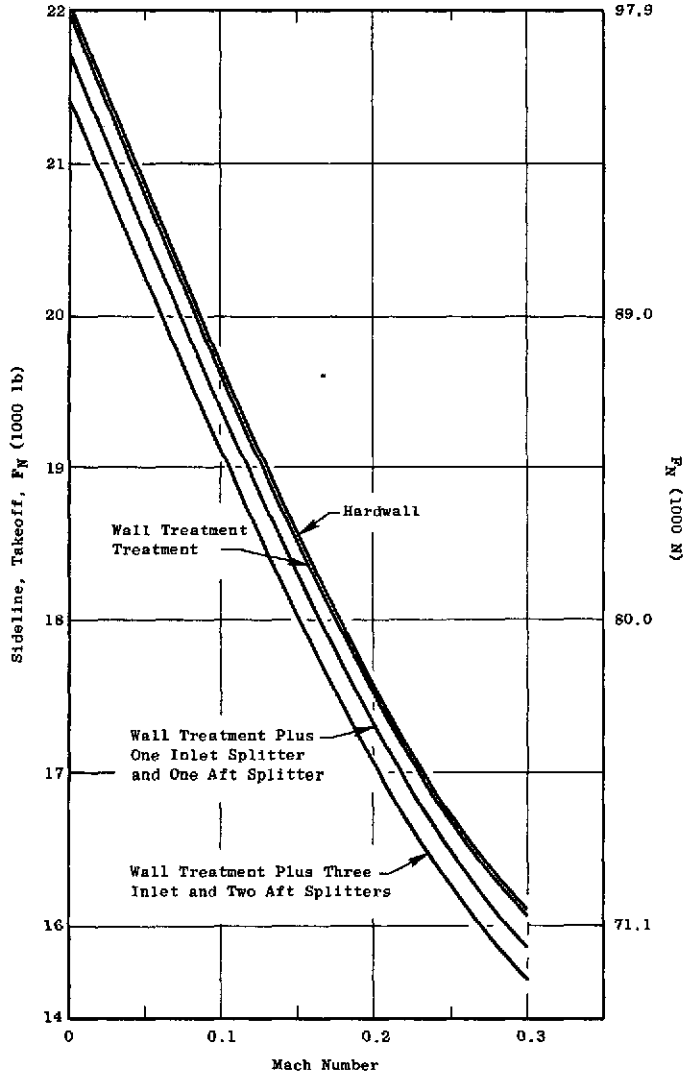

Figure 24. Installed Takeoff Performance Comparison, High Speed Engine.

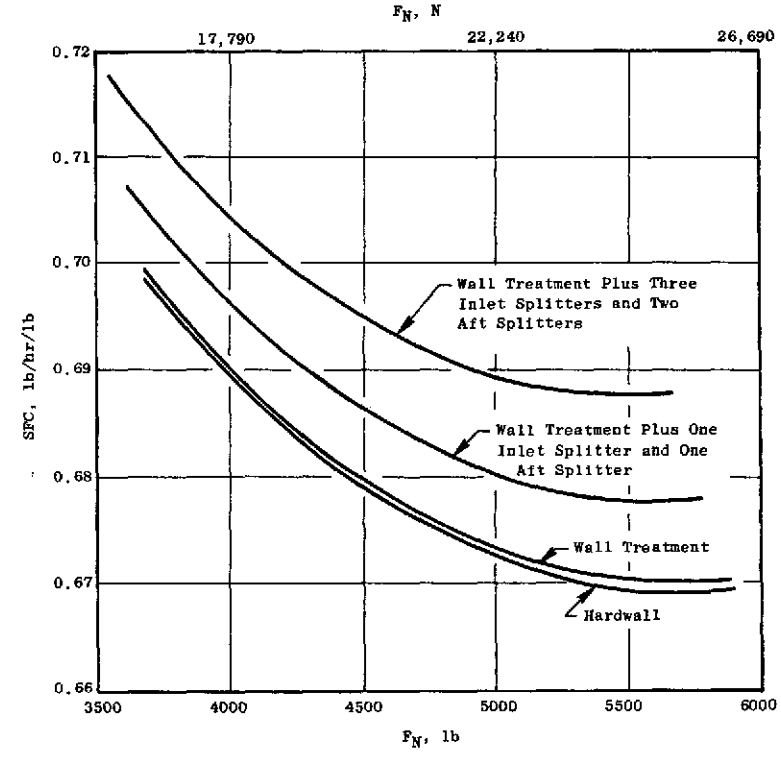

Figure 25. Installed Cruise Performance Comparison, High Speed Engine.

6.0 HIGH SPEED ENGINE STATIC NOISE CHARACTERISTICS

6.1 UNSUPPRESSED ENGINE CHARACTERISTICS

The 200-ft (60.96 m) sideline static characteristics for the high speed engine are obtained using the same procedure as with the low speed engine by summing the individual contributions of the four primary component noise sources. The fan component used the NASA test data for the 26-bladed fan, with the measured spectral distribution shifted to account for the higher blade passing frequency caused by increasing the blade number to 46. The parameters used in the turbine noise estimates are listed in Table XIX. The turbine, mixed jet, and internal noise sources were estimated using the procedures described in Appendix A. Figure 26 shows the spectral distributions for the four noise sources at approach power for the angle corresponding to the maximum forward noise (at 50°) and for the maximum aft noise at 120°. Figure 27 shows the corresponding 1/3 octave band spectral distribution at takeoff power. (The high tones at 1000 Hz in Figure 27 are the MPT's which are radiated from the fan inlet - but are also prominent in the aft angles.) Corresponding distributions are used at every 10° increment from 20° to 160°.

The noise sources expressed as PNdB at the 200-ft (60.96 m) sideline at the approach power setting are shown in Figure 28 for sideline angles from 20° to 150°. (Fan rpm at approach is 60% of aero design.) The total PNdB from these sources and corresponding directivity plot for the takeoff condition are also shown in Figure 28. The fan is clearly the dominant noise source at takeoff with the front end noise being high because of strong multiple pure tones characteristic of high speed (supersonic) fans. The overall 200-ft (60.96 m) sideline perceived noise levels as a function of the acoustic angle are summarized in Figure 29 for the takeoff and approach power settings.

6.2 NOISE SUPPRESSION

Again, the initial step in suppressing engine noise is the use of acoustic material in the fan duct. The treatments selected for the high speed fan duct were tuned to the dominant frequencies which controlled the PNdB level at takeoff. The predicted effectiveness of this treatment was based on both static duct tests as well as measurements obtained from Engine C. The suppression characteristics at the various 1/3 octave band frequencies are shown in Figure 30. Corresponding suppression was incorporated at other angles, again based as a fraction of that obtained at the angle of maximum suppression as shown in Figure 31.

The suppression obtained from the treatment in the aft fan ducts is shown in Figure 32 for approach and takeoff power settings. Again, the suppression at other angles was related to that at the maximum angle as shown in Figure 31.

Corresponding insertion losses were estimated using a single splitter and a three-ring splitter in addition to the wall treatment at the inlet, with the overall suppression also shown in Figure 30. The two cases where splitters

Table XIX. High Speed Engine Parameters.

Turbine	
3rd Stage Blade Number	146
4th Stage Blade Number	142
Takeoff	
Speed, rpm	4940
Weight Flow, lb/sec (kg/sec)	112 (51)
Third Stage Blade Passing Frequency	12,500 Hz
Fourth Stage Blade Passing Frequency	12,500 Hz
Approach	
Speed, rpm	3650
Weight Flow, lb/sec (kg/sec)	71 (32.3)
Third Stage Blade Passing Frequency	8,000 Hz
Fourth Stage Blade Passing Frequency	8,000 Hz
Combustor	
Takeoff	
Corrected rpm	4950
Combustor Inlet Temperature T3, °R (°C)	1479 (548)
Turbine Inlet Temperature T4, °R (°C)	2788 (1277)
Compressor Discharge Pressure P3, lb/in^2 (kg/cm^2)	353.6 (24.9)
Compressor Discharge Weight Flow W3, lb/sec (kg/sec)	104.1 (47.4)
Approach	
Corrected rpm	3650
Combustor Inlet Temperature T3, °R (°C)	1225 (407)
Turbine Inlet Temperature T4, °R (°C)	2136 (913)
Compressor Discharge Pressure P3, lb/in^2 (kg/cm^2)	199.2 (14.03)
Compressor Discharge Weight Flow W3, lb/sec (kg/sec)	67.2 (30.6)

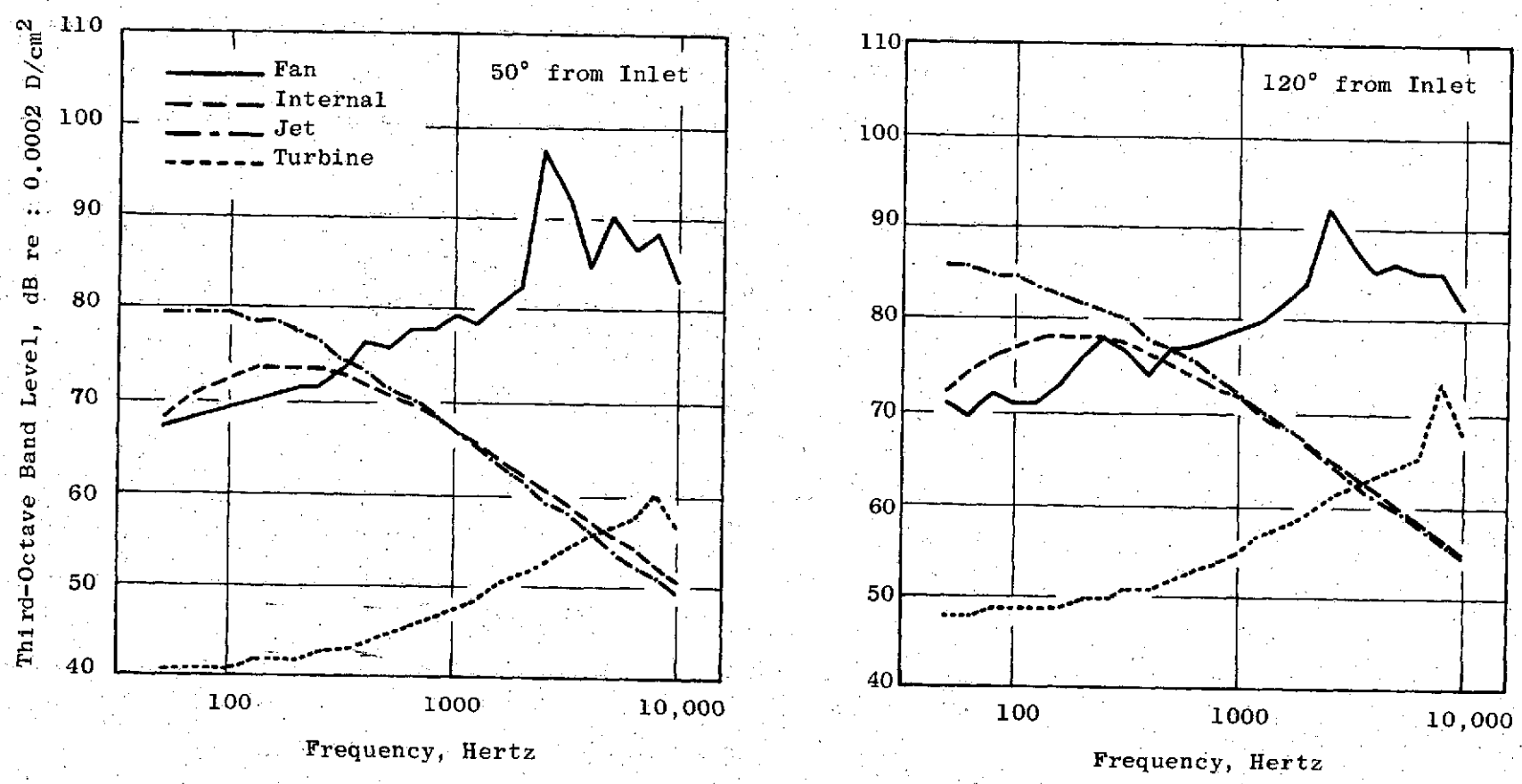

Figure 26. 1/3 Octave Band Spectral Distributions at Approach Power, Unsuppressed High Speed Engine.

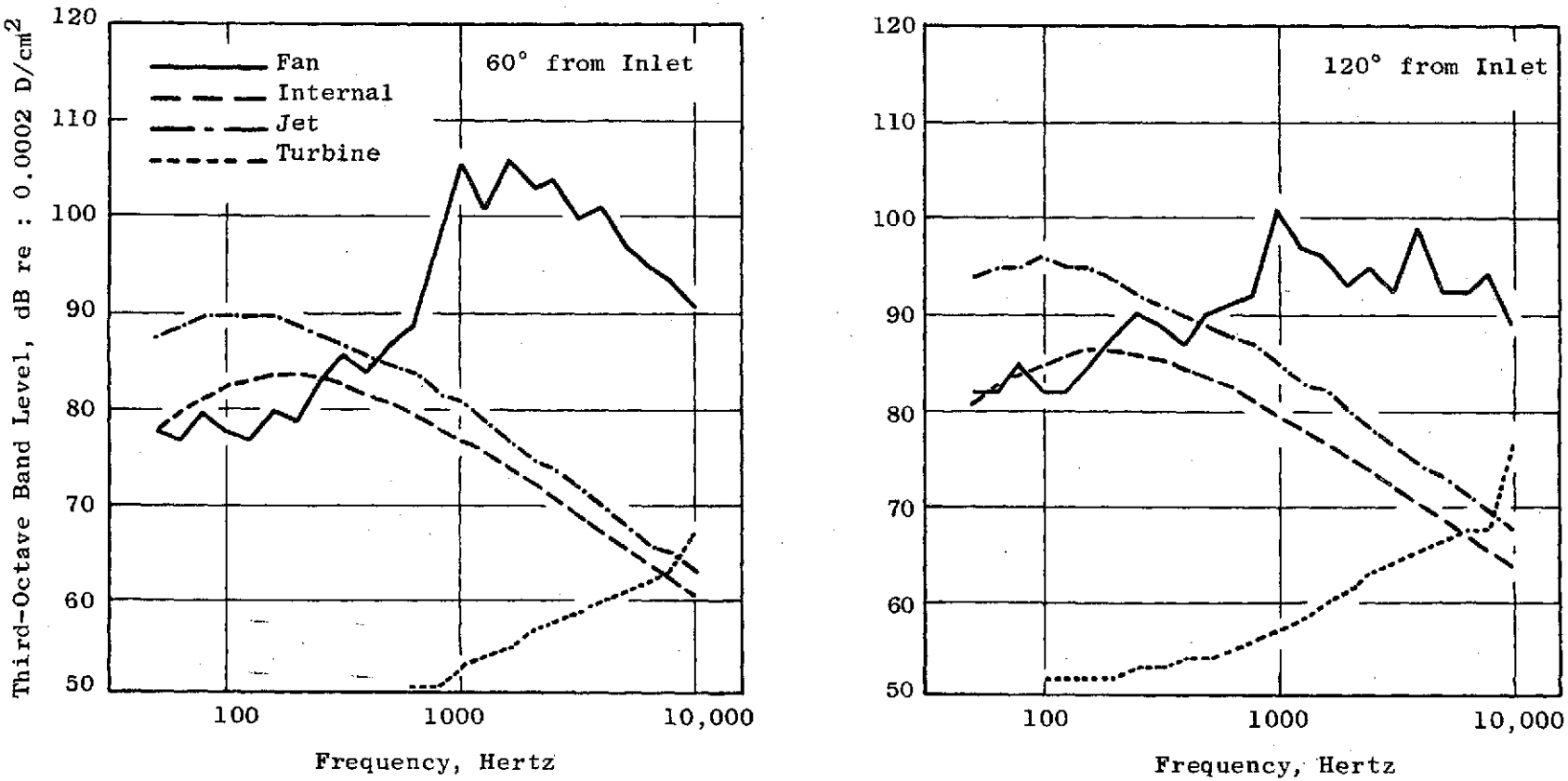

Figure 27. 1/3 Octave Band Spectral Distributions at Takeoff Power, Unsuppressed High Speed Engine.

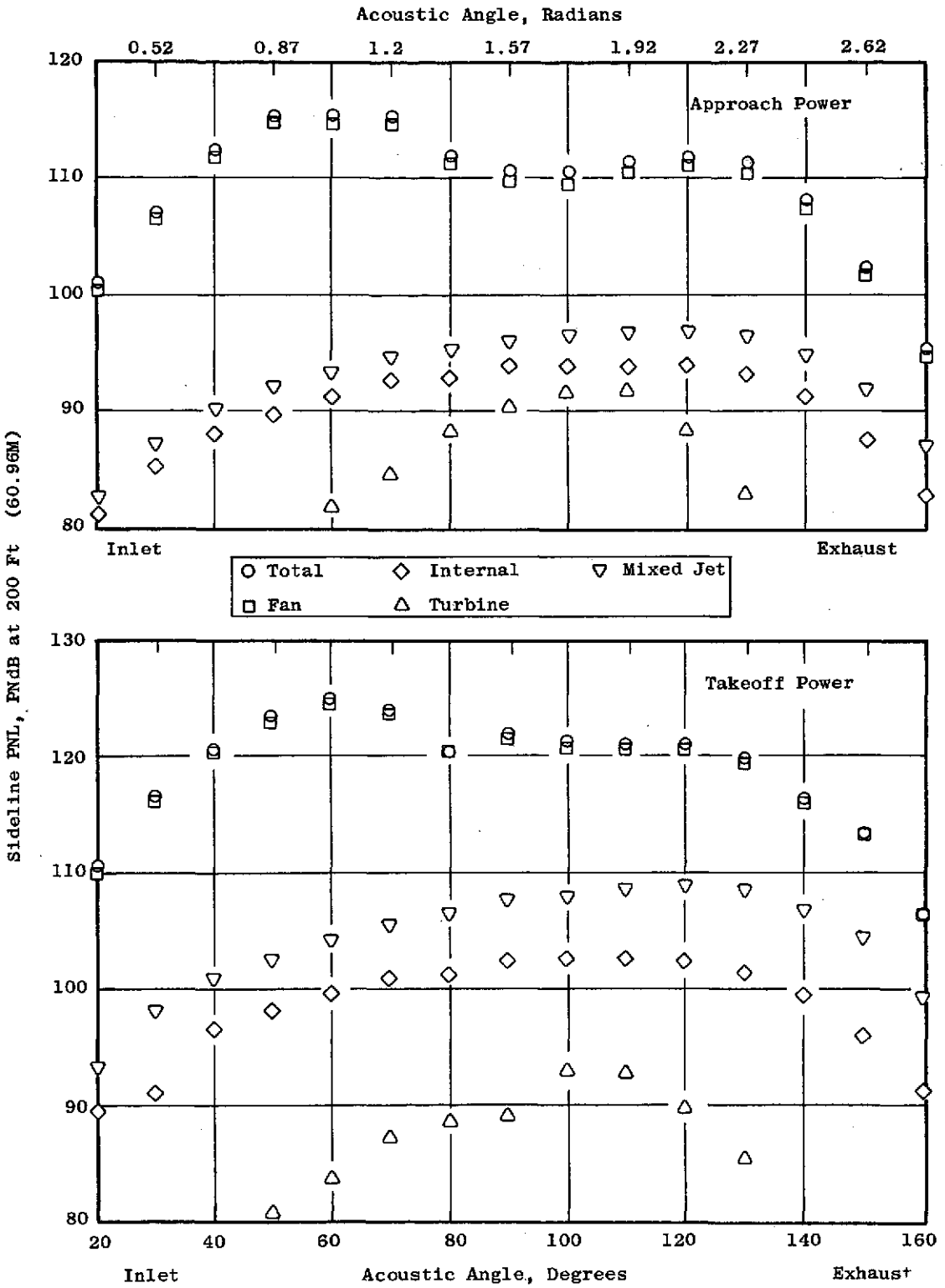

Figure 28. Unsuppressed High Speed Engine Component Noise, 200-ft (60.96 m) Sideline PNL Vs. Acoustic Angle.

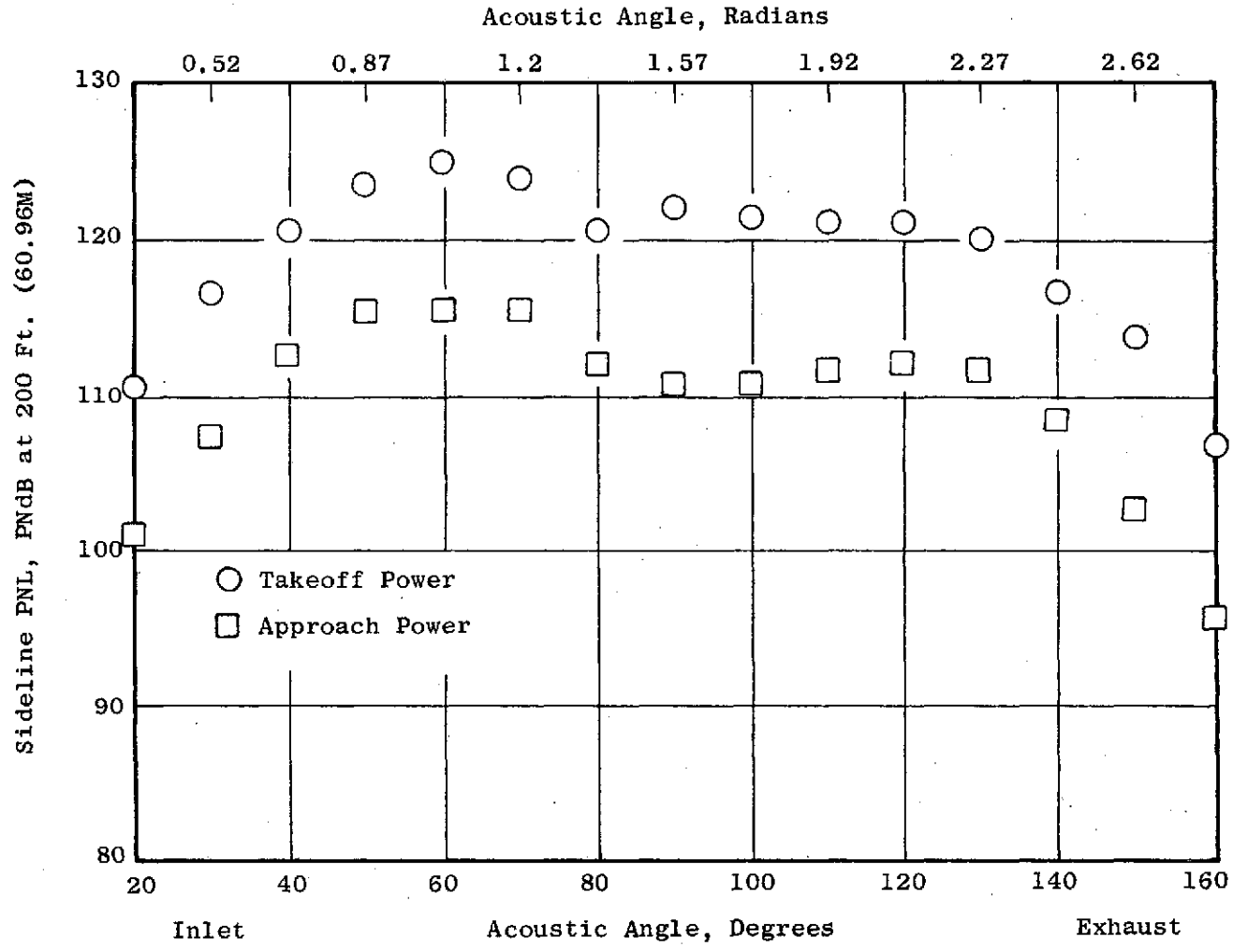

Figure 29. Overall 200-ft (60.96 m) Sideline PNL Vs. Acoustic Angle, Unsuppressed High Speed Engine.

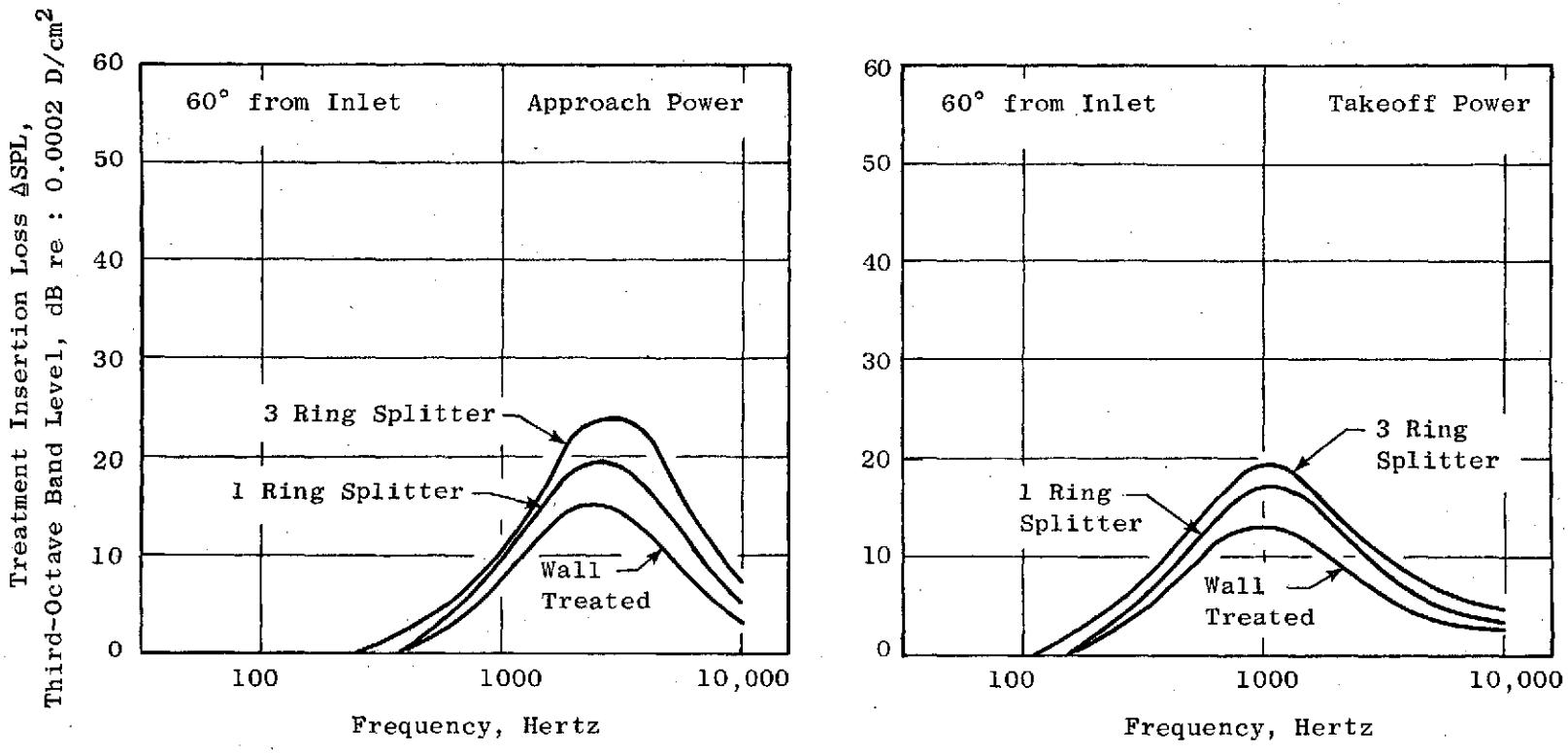

Figure 30. Fan Inlet Suppression, High Speed Engine.

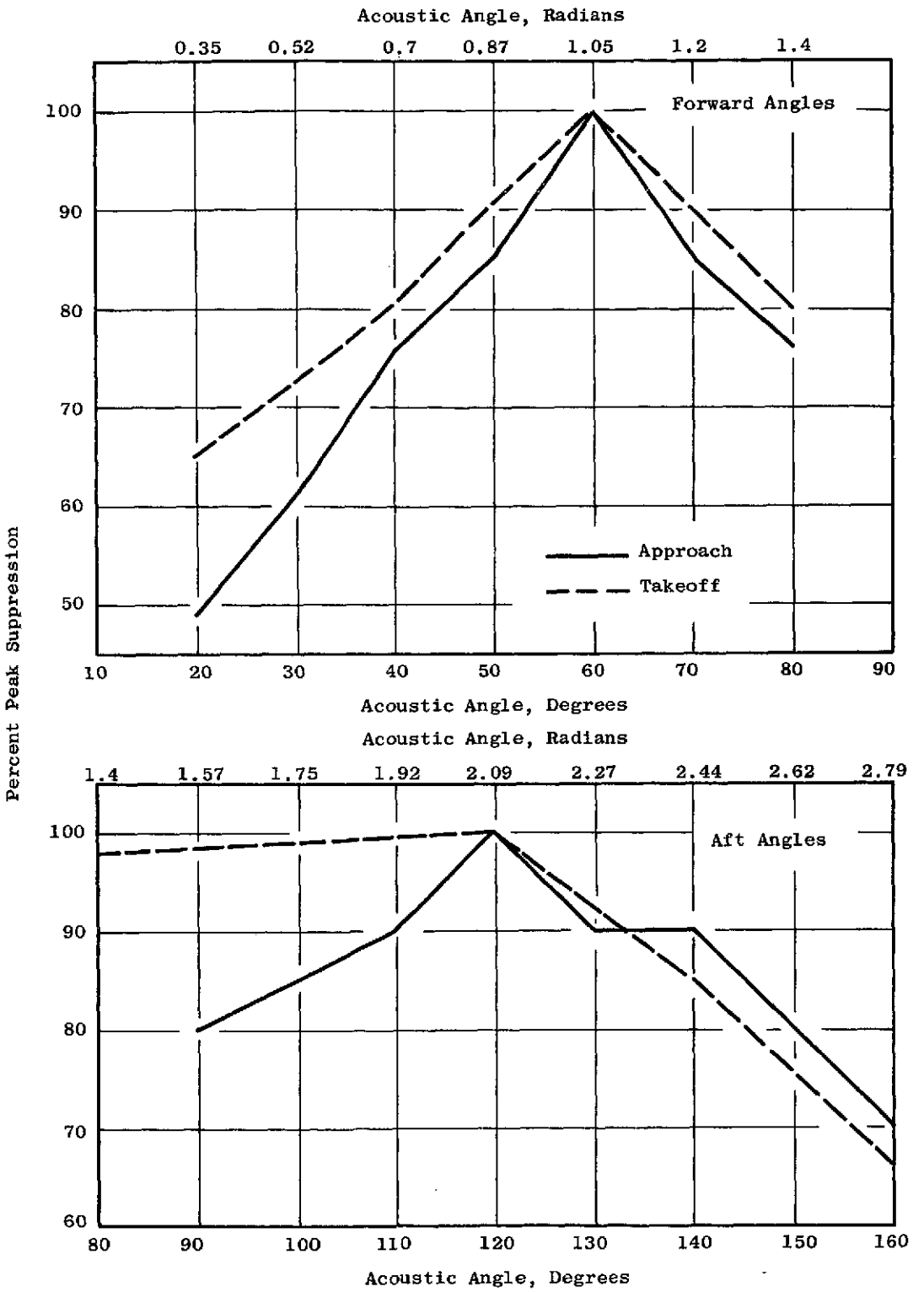

Figure 31. Suppression Directivity, High Speed Engine.

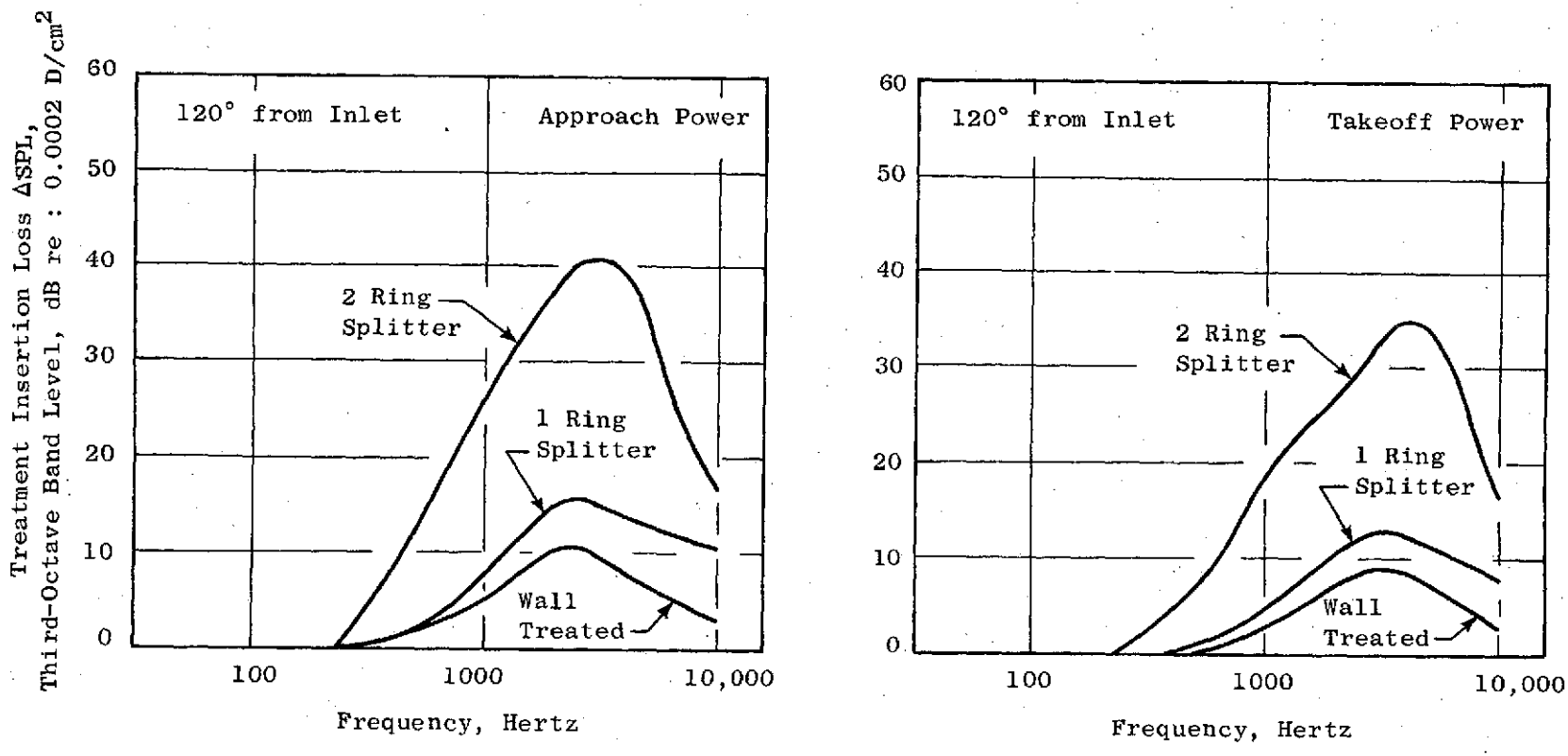

Figure 32. Fan Exhaust Suppression, High Speed Engine.

are used in the aft duct are shown in Figure 32. Again, the single splitter was limited in effectiveness since it was inserted into the initial fan duct with the constraints of no increase in nacelle diameter and was compatible with the original thrust reverser. The two-ring splitter was designed to obtain maximum suppression with the duct annulus area adjusted for optimum Mach number distribution through the duct and splitter. As a consequence, the nacelle diameter had to be increased, the thrust reverser had to be moved aft, and the overall length of the nacelle had to be increased. The specific changes required in the nacelle are listed in Section 5.2 and the effects on inlet installed performance are described in Section 5.3.

In the case where maximum suppression of the fan is utilized (that is the three-ring inlet splitter and the two-ring exhaust splitter), the fan noise was suppressed enough such that the turbine noise and internal source noises also contributed significantly to the overall. In this case, additional acoustic treatment was incorporated aft of the core to suppress both the high frequency turbine tones and low frequency internal noise. The insertion losses obtained from this treatment at the angle of maximum noise from the inlet (110°) is shown in Figure 33. The suppression effectiveness was slightly different between the takeoff and approach cases.

6.3 SUPPRESSED ENGINE NOISE CHARACTERISTICS

The initial engine noise characteristics described in Section 4.1.1 were modified by reducing the 1/3 octave band spectral distributions of the separate components by the insertion losses described in Section 4.1. By summing these modified sources at each angle along the 200-ft (60.96 m) sideline the overall directivity characteristics of the suppressed nacelles are obtained. Figure 34 shows the directivity characteristics of the High Speed Engine at approach and takeoff power for the four installation configurations considered. The use of wall treatment is seen to be effective in reducing noise levels about 6 PNdB at the aft angles. The higher suppression at forward angles (up to 8 PNdB) is based on observed results from Engine C, where the high MPT levels were concentrated near the duct wall and responded more effectively than the more nearly radially constant blade passing tones. The use of the single exhaust splitter reduced the aft end noise about 3 to 4 PNdB at approach and takeoff. The single inlet splitter reduced the front end noise by about 3 PNdB at approach and takeoff.

The fully suppressed case with three inlet and two exhaust splitters produces an additional overall noise reduction but again the amount of reduction in the aft angle is not as much as would be anticipated when comparing the insertion losses for the splitters as shown in Figure 32. The overall noise levels are also held up by contributions from jet noise at takeoff power and internal and turbine noise in both takeoff and approach.

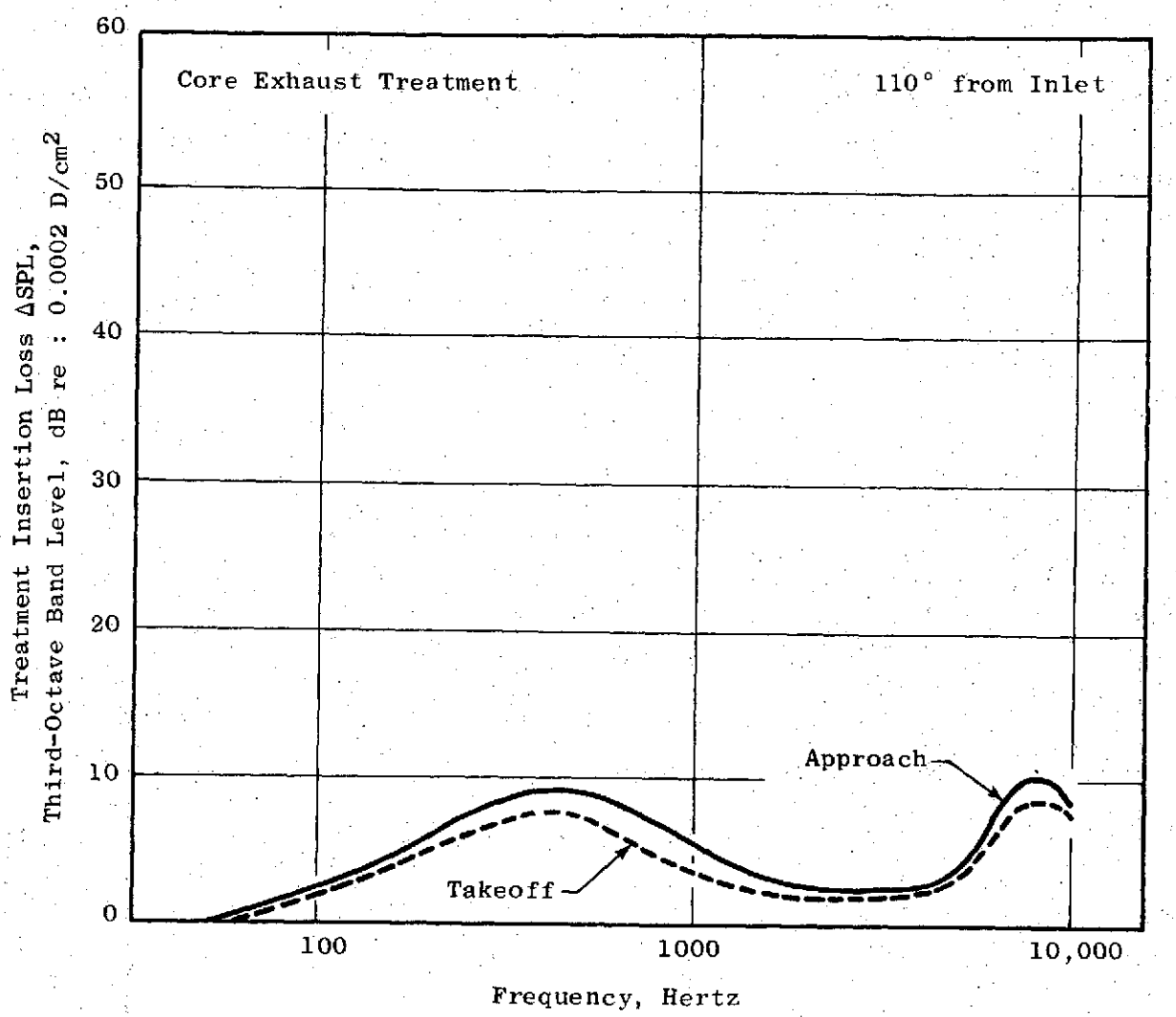

Figure 33. Core Exhaust Suppression, High Speed Engine.

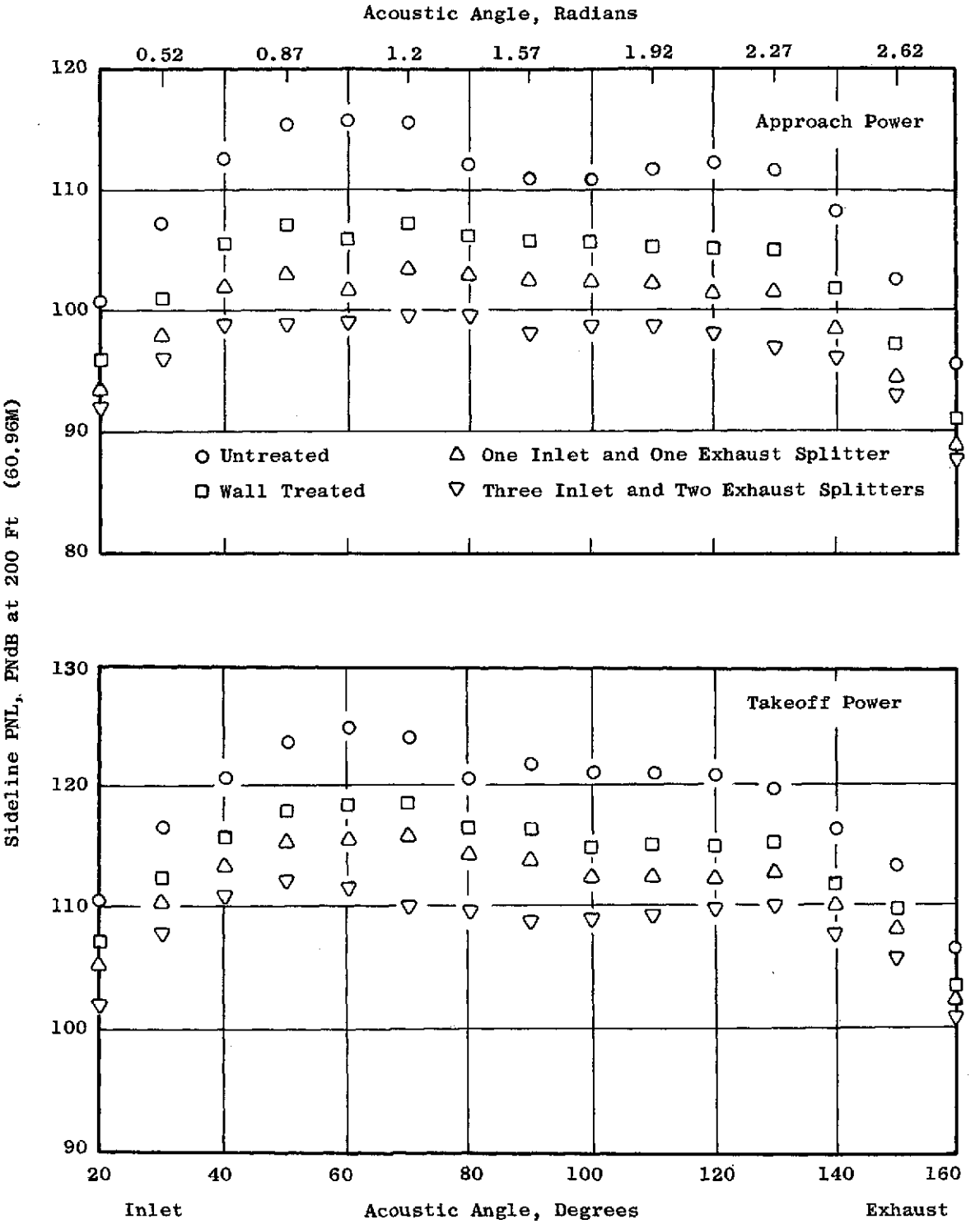

Figure 34. Directivity Characteristics of the High Speed Engine at Approach and Takeoff Power.

6.4 COMPARISONS WITH QUIET ENGINE "C"

The most directly analogous configurations of the high speed engine and Quiet Engine C are the fully suppressed configurations compared in Table XX.

Table XX. Treatment Area Comparison.

Duct Wall Treatment	Fan Inlet ft^2 (m^2)	Fan Exhaust ft^2 (m^2)
Engine C	62 (5.76)	134 (12.46
Fully Suppressed		
Engine C	286.5(26.65)	373.5 (34.7)
High Speed Engine	225.5(20.95)	316 (29.40)

The 200-ft (60.96 m) sideline characteristics are compared in Figure 35 for both approach and takeoff power settings. Note that Engine C has more treatment area than the high speed engine.

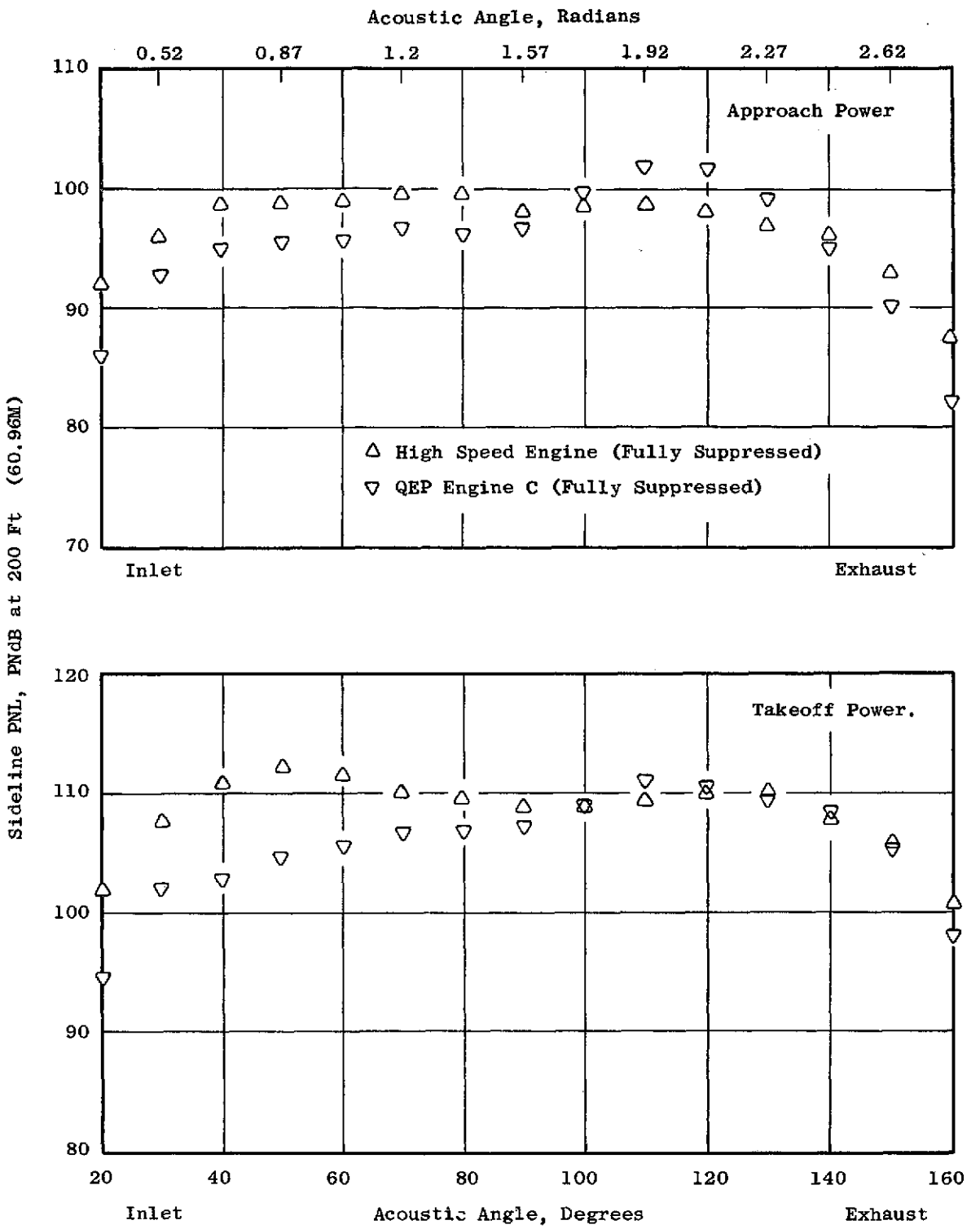

Figure 35. Comparison of 200-ft (60.96 m) Sideline Characteristics of Fully Suppressed QEP Engine C and High Speed Engine.

7.0 APPLICATION STUDIES

7.1 APPROACH

The engines and nacelles described in Sections 3 through 6 were used in aircraft application studies for a new tri-jet aircraft. The new tri-jet aircraft was considered adjustable in size and gross weight in order to maintain a fixed payload and range for each engine/nacelle combination. (A brief study of these engines and nacelles in a DC-8-Type aircraft is presented in Appendix C).

7.2 TRI-JET AIRCRAFT

The baseline aircraft used for the tri-jet studies was selected to meet the following criteria.

Payload, lb (kg)	35,400 (16,100)
Number of passengers	177
Range, N. Mi. (km)	1,850 (3,480)
Wing Loading, W/S, lb/ft^2 (kg/m^2)	104 (510)
Cruise Altitude, ft (m)	30,000 (9,144)
Cruise Mach No.	0.84

The resultant baseline aircraft characteristics were:

Takeoff Gross Weight, lb (kg)	200,500 (91,200)
OWE, lb (kg)	112,000 (50,900)
Avg. Installed Cruise Thrust/eng, lb/eng (N/eng)	4,560 (20,300)
Static Takeoff Thrust,eng, lb/eng (N/eng)	22,000 (97,900)
Block Time, Hour	4.22
Block Speed, N. Mi/hr (km/hr)	438 (825)

The DOC estimates for this aircraft were obtained using the procedure applied in the ATT studies (Reference 4). The procedure is described in Appendix B. Comparisons are included with prior NASA studies (Reference 5). The sensitivity factors for the tri-jet were estimated for the case of a constant payload and mission. The base aircraft and engines are scaled for SFC and pod weight changes. The cost effects of scaling the aircraft size are included in the overall DOC sensitivity factors. (The DOC calculation procedure is discussed in Appendix B.) The resultant sensitivity factors for the major engine and nacelle characteristics are:

	Δ% DOC*	Δ% TOGW
1% total ΔSFC	0.55	0.66
100 lb Δ Pod Weight (each)	0.26	0.36
$10,000 Δ Engine Price	0.26	---
$10,000 Δ Nacelle Price	0.15	---

* Δ% DOC also includes change in DOC due to change in aircraft size.

7.3 TRI-JET COMPARISONS

7.3.1 Low Speed Engine

The installed engine characteristics described in Section 4 represent basic hardwall engine installation with decrements in performance and weight for nacelles with varying degrees of acoustic suppression. In order to apply these results to the tri-jet study, the engines must be scaled to the required nominal takeoff thrust. The effects on DOC and TOGW are then estimated using the costs and weights associated with the scaled engine.

The necessary scaling factors and scaled engine characteristics are summarized in Table XXI for the various low speed engine configurations.

The wall-treated nacelle configuration is used as the baseline. The incremental Δ's are shown relative to the wall-treated case.

7.3.2 High Speed Engine

The high speed engine characteristics are summarized in Table XXII in a format corresponding to that used for the low speed engine. The baseline case is again the wall-treated low speed engine configuration, with all Δ's shown relative to that case.

7.4 TRI-JET NOISE COMPARISON

7.4.1 Prediction Procedure

The noise characteristic produced at a ground measurement point by an aircraft flyover along a given flight path is estimated using the following procedure:

(1) The engine noise sources are approximated by substituting the predicted ground static data at 10° angle increments to the engine inlet.

(2) At a given instant in time the range from the ground observer to

Table XXI. Low Speed Engine DOC Comparisons.

Nacelle Configuration	Hardwall	Treated Wall	Treated Wall +1 Aft Splitter	Treated Wall +3 Inlet Splitters +2 Aft Splitters
From Section 2				
Installed F_N @ Takeoff, lb (N)	18,443 (82,000)	18,397 (81,900)	18,321 (81,500)	17,862 (79,500)
Installed SFC @ Alt Mx Cruise	.6578	.6595	.6626	.6789
Pod Weight, lb (kg)	6682 (3040)	6831 (3110)	6900 (3140)	7730 (3520)
ΔEngine Price, K$ from Base	Base	Base	Base	Base
Nacelle Price	274	280	284	366
Scale Factor (Scaled to F_N)	.9975	1.0	1.0041	1.029
Scaled F_N @ Takeoff, lb (Base) (N)	18,397 (81,900)	18,397 (81,900)	18,397 (81,900)	18,397 (81,900)
Scaled Nacelle Weight, lb (kg)	2735 (1244)	2891 (1315)	2973 (1352)	3905 (1770)
Scaled Engine Weight, lb (kg)	3928 (1782)	3940 (1787	3960 (1796)	4083 (1852)
Scaled Nacelle Price	273	280	285	377
ΔScaled Engine Price, K$ from Base (Base is $380K)	-1	Base	+2	+11
% Total ΔSFC* TRIJET	-.2	---	+.5	+4.4
ΔPod Weight, lb (kg)	-168 (76.4)	---	+102 (46.3)	+1157 (526)
$1,000 ΔEngine Price	-1	---	+2	+11
$1,000 ΔNacelle Price	-7	---	+5	+97
Δ% DOC, SFC	-.1	---	+.3	+2.4
Δ% DOC, Pod Weight	-.4	---	+.3	+3.1
Δ% DOC, Engine Price	---	---	---	+.3
Δ% DOC, Nacelle Price	-.1	---	+.1	+1.4
Total Δ% DOC	-.6	0	+.7	+7.2

* Effective SFC Includes Pod Drag and Power Setting Effects.

Table XXII. High Speed Engine DOC Comparisons.

Nacelle Configuration	Hardwall	Treated Wall	Treated Wall + 1 inlet splitter + 1 Aft splitter	Treated Wall + 3 Inlet Splitters + 2 Aft Splitters
From Section 2				
Installed F_N @ Takeoff, lb (N)	18,555 (82,500)	18,525 (82,400)	18,295 (81,400)	18,037 (80,200)
Installed SFC @ Alt Mx Cruise	.6706	.6714	.6791	.6891
Pod Weight, lb (kg)	6183 (2810)	6237 (2840)	6468 (2940)	7103 (3230)
ΔEngine Price, K$ from Base	-53	-53	-53	-53
Nacelle Price	249	254	265	328
Scale Factor	.9914	.993	1.005	1.02
Scaled F_N @ Takeoff, lb (N)	18,397 (81,900)	18,397 (81,900)	18,397 (81,900)	18,397 (81,900)
Scaled Nacelle Weight, lb (kg)	2659 (1210)	2717 (1244)	2984 (1358)	3678 (1673)
Scaled Engine Weight, lb (kg)	3462 (1574)	3469 (1578)	3522 (1602)	3588 (1632)
Scaled Nacelle Price	247	252	266	335
ΔScaled Engine Price, K$ from Base	-57	-56	-51	-46
% Total ΔSFC* TRIJET	+1.3	+1.5	+3.2	+5.0
ΔPod Weight, lb (kg)	-710 (323)	-645 (293)	-325 (148)	+435 (198)
$1,000 Δ Engine Price	-57	-56	-51	-46
$1,000 Δ Nacelle Price	-33	-28	-14	+55
Δ% DOC, SFC	+.8	+.9	+1.8	+2.8
Δ% DOC, Pod Weight	-1.9	-1.6	-.9	+1.1
Δ% DOC, Engine Price	-1.5	-1.4	-1.3	-1.2
Δ% DOC, Nacelle Price	-.4	-.3	-.2	+.8
Total Δ% DOC	-3.0	-2.4	-.6	+3.5

*Effective SFC Includes Pod Drag and Power Setting Effects.

the moving aircraft is determined as a function of angle to the inlet axis.

(3F The engine data is interpolated to match the flyover acoustic angle.

(4) Correction factors are applied to the static data depending on separation distance and aircraft velocity. These correction factors are (1) the spherical divergence dissipation of sound energy, (2) the atmospheric absorption as specified in SAE Specification ARP 866, and (3) a ground boundary attenuation as specified in SAE Specification AIR 923. The ground boundary layer or EGA factor is further modified by GE/Acoustic Engineering with the assumption that it applies only in a layer below a 100-ft (30.48 m) altitude. Noise transmission above a 100-ft (30.48 m) altitude is not attenuated with EGA.

(5) The jet noise is reduced by the change in relative velocity between the static test exhaust velocity and the relative velocity for the moving aircraft.

(6) Frequency is shifted to account for the doppler effect.

A sophisticated computer program has been prepared to perform the flyover calculations. The program solves the complex geometry of an aircraft traversing a selected path with varying engine angles and frequencies and a flight noise spectrum is prepared. This spectrum is then transmitted over the appropriate acoustic range with the necessary corrections to prepare a spectrum at the ground position desired. From this predicted spectrum PNL and PNLT values are calculated. This information is then used to calculate an EPNL value for the flyover event as specified in FAR 36. However, the 90 EPNdB floor of the current regulation was not used in this study.

7.4.2 Tri-Jet Flight Path Characteristics

The flight path data corresponding to the new tri-jet aircraft are based on single segment climb and approach patterns. Power cutback was not explored for these studies. The pertinent data are summarized in Table XXIII.

7.4.3 Low Speed Engine Flyover Noise

Takeoff

The low speed engine acoustic characteristics described in Section 3 were incorporated in the flyover noise prediction procedure on the flight paths shown in Table XXIII. The resultant noise history at the takeoff measuring point is plotted in Figure 36 showing PNLT as a function of time. The acoustic angle relative to the engine is also indicated. The flyover characteristics are shown for each nacelle configuration. The EPNL - calculated as described in FAR 36 but without the noise floor - is indicated on the right of the plot.

Table XXIII. QEP Trade Study, Flight Path Data.

	New Tri-Jet
Takeoff	
Climb Angle, 100% P.S., degrees	6.5
Flap Angle, degrees	15
Angle of Attack, degrees	12
Engine Angle, degrees	3
Engine Angle to Ground, degrees	21.5
Altitude @ 3.5 N. Miles, ft (m)	1600 (488)
Flight Mach No.	0.25
Descent	
Descent Angle, degrees	-3
Flap Angle, degrees	40
P.S., %	34
Angle of Attack, degrees	6
Flight Mach No.	0.20

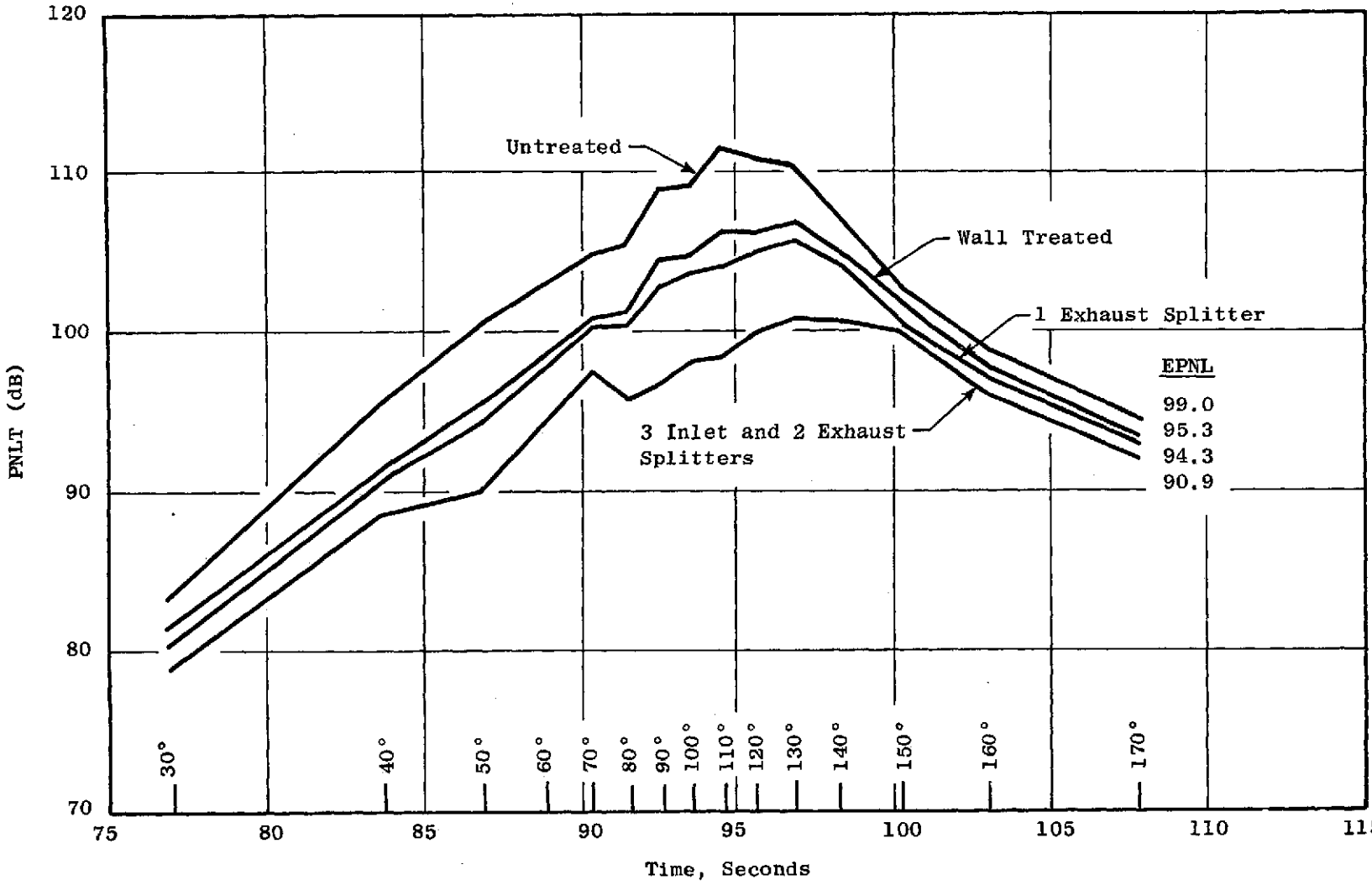

Figure 36. PNLT Vs. Time, Tri-Jet Takeoff, Low Speed Engine Totals.

The overall PNLT is the sum of all the major noise sources. The constituent breakdown for the individual sources is shown in a corresponding plot in Figure 37. The fan noise dominates for the hardwall nacelle, the wall treated nacelle and the single exhaust splitter configurations. Internal (combustion and core) noise is also above the jet noise level (when relative velocity effects are considered). Turbine noise is not a major contributor. The EPNL that would result from the individual sources is also shown on the right. For the bypass ratio and mixed-jet cycle selected, jet noise is more than 10 PNLT below the fan noise when the relative velocity effect is included.

The configuration with three fan inlet and two fan exhaust splitters reduced the fan noise to a level such that core noise became a significant contributor even on takeoff. Additional core suppression (as well as turbine suppression) was incorporated in this configuration to produce the relative constituent levels shown in Figure 38.

Approach

Corresponding overall flyover time histories are shown for the 40% F_N approach condition in Figure 39 with the resultant EPNL indicated on the right for each configuration. These levels are reduced by 1.5 EPNdB to account for a revised tri-jet approach power setting of 34% F_N (rather than 40% F_N). The relative constituent levels at approach are shown in Figure 40. At approach both turbine and core noise are contributing to the suppressed fan levels leading to the need for the turbine suppression mentioned above. The flyover constituent levels for the fully suppressed configuration at approach are shown in Figure 41.

The above estimates are obtained using component data taken over a hard surface without correction for ground nulls, etc. Experience has shown that use of static data obtained with a hard surface for flyover predictions will generally overpredict the EPNL by about 2 EPNL when compared with actual measurements. A significant factor in this difference is considered to be a result of the use of normal sod surfaces during certification rather than hard surfaces. As a consequence the anticipated noise levels corresponding to a normal certification measurement would be the above estimates (shown in the preceding figures) reduced by 2.0 EPNL. The final EPNL values, (reflecting this 2 EPNL reduction) for the tri-jet aircraft at the FAR 36 takeoff and approach certification conditions are summarized in Table XXIV.

The results shown in Table XXIV are considered representative of "status" levels, that is, expected levels based on demonstrated components, suppression effectiveness with current materials, etc.

7.4.4 High Speed Engine Flyover Noise

Takeoff

The high speed engine acoustic characteristics described in Section 5 were incorporated in the Flyover Noise Prediction procedure on the flight paths shown in Table XXIII. The resultant noise history at the takeoff measuring

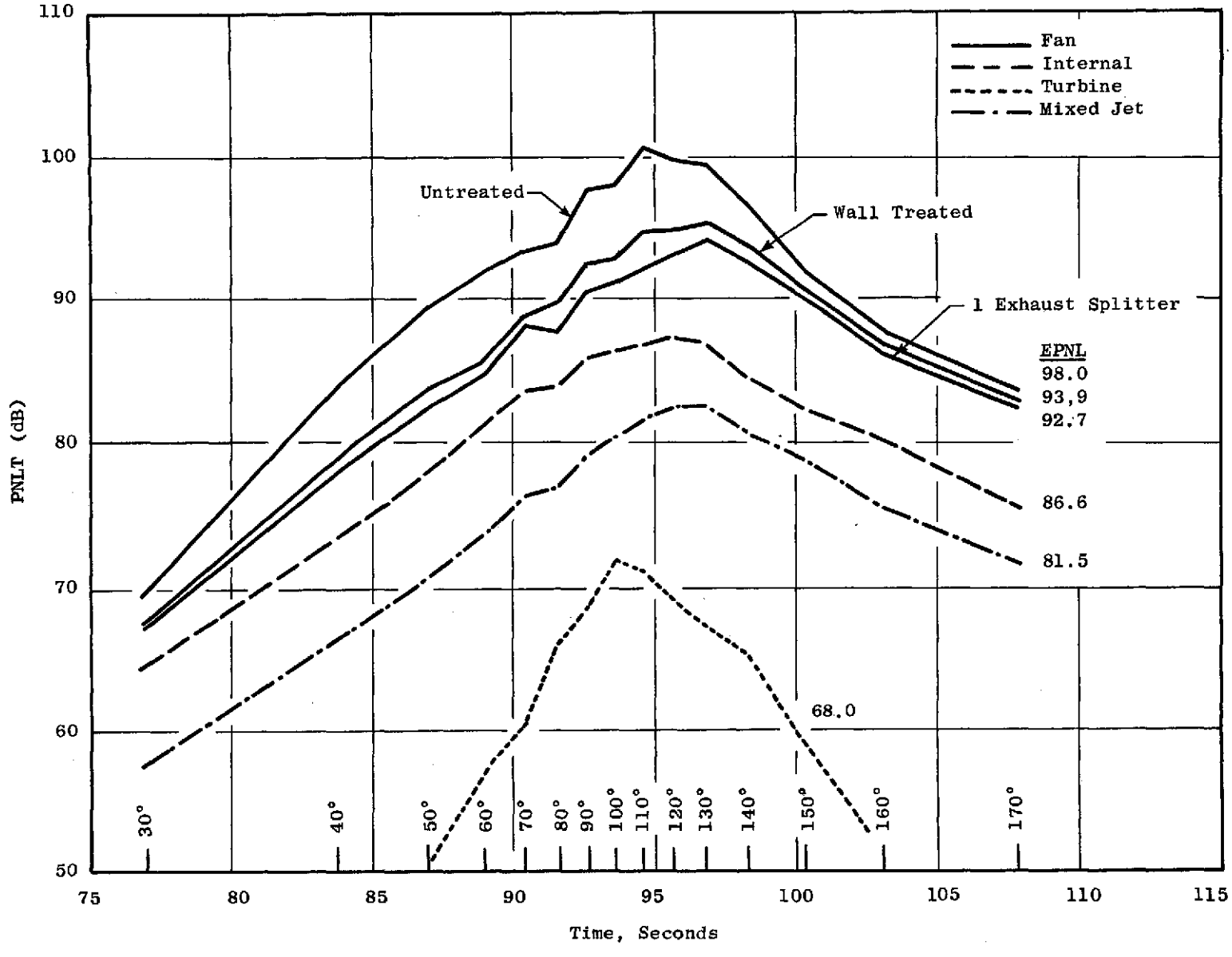

Figure 37. PNLT Vs. Time, Tri-Jet Takeoff, Low Speed Engine Components.

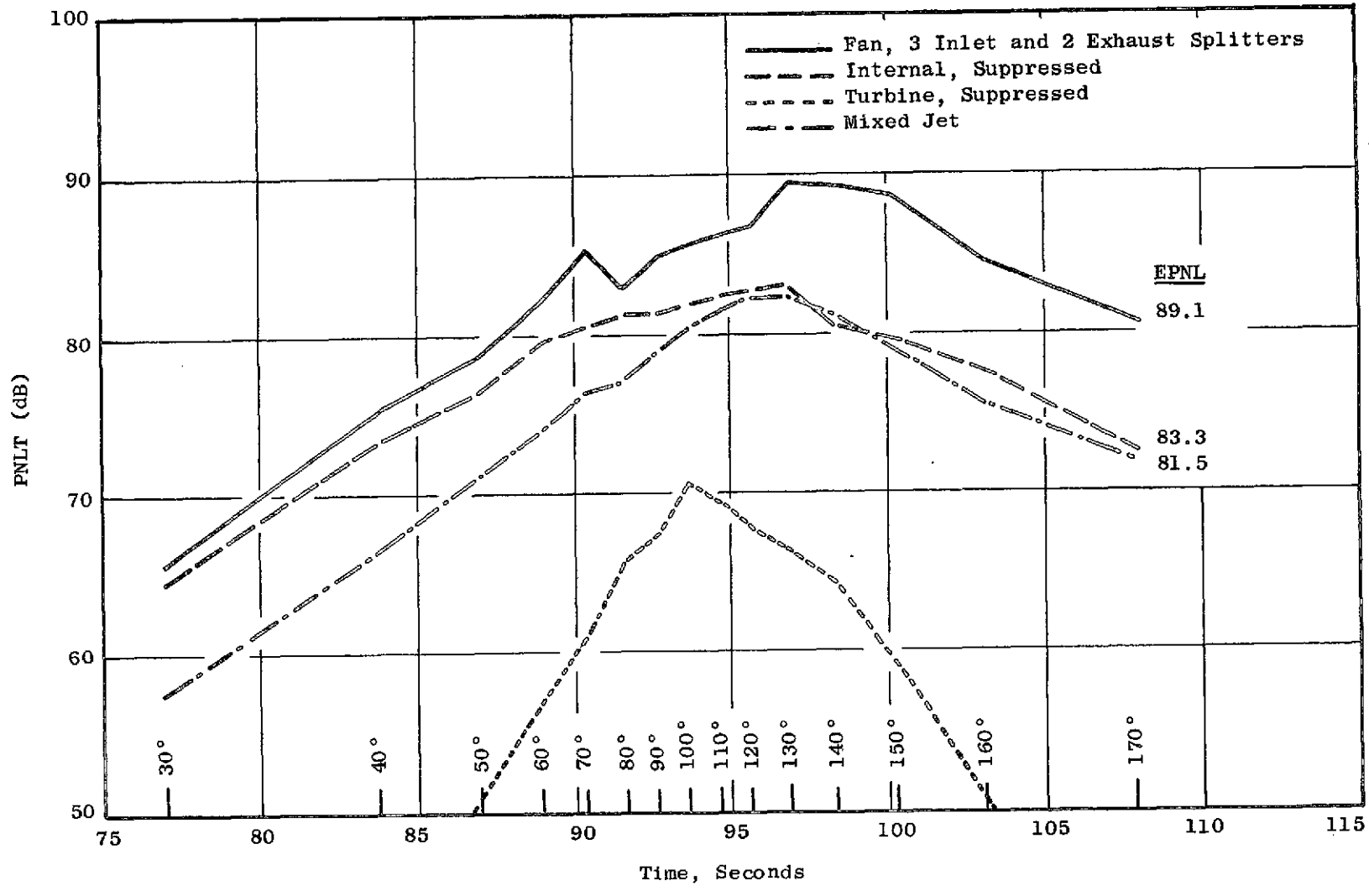

Figure 38. PNLT Vs. Time, Tri-Jet Takeoff, Low Speed Engine.

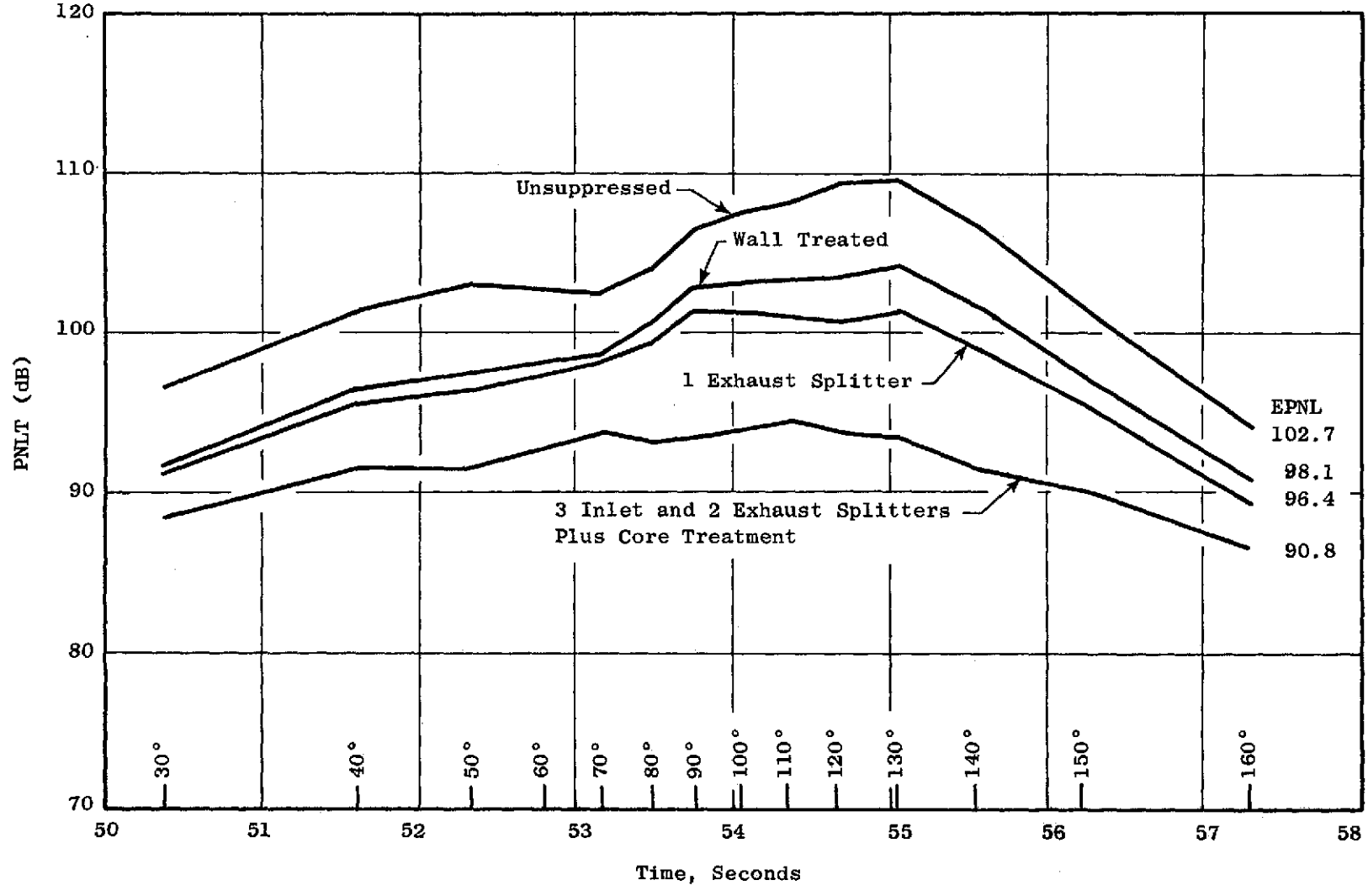

Figure 39. PNLT Vs. Time, Tri-Jet Approach, Low Speed Engine Totals.

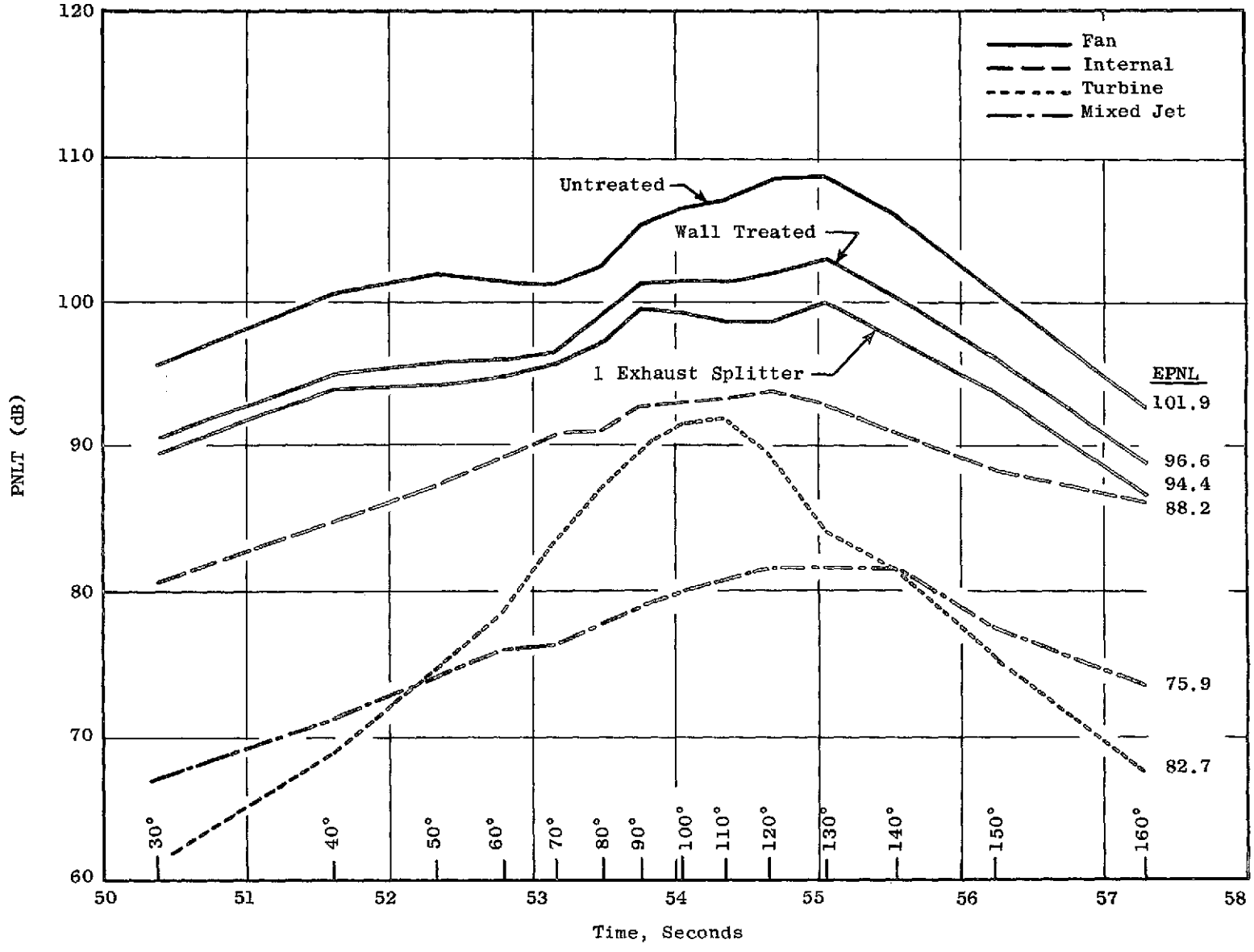

Figure 40. PNLT Vs. Time, Tri-Jet Approach, Low Speed Engine Components.

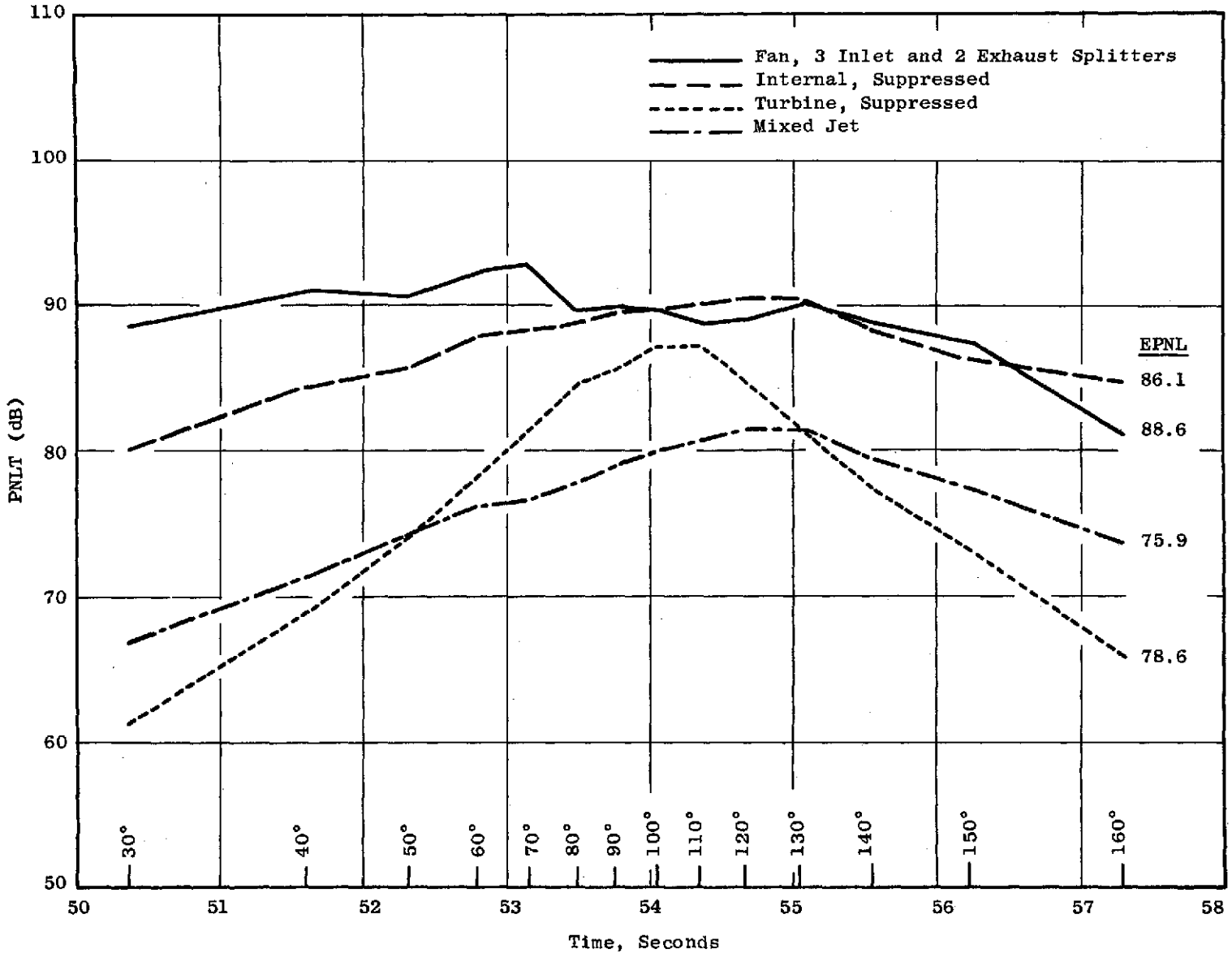

Figure 41. PNLT Vs. Time, Tri-Jet Approach, Low Speed Engine.

Table XXIV. Tri-Jet Low Speed Engine EPNL Values.
Nominal TOGW = 200,500 lb

Configuration	Takeoff	Approach
Hardwall Nacelle	97	99
Treated Wall	93.5	94.5
Treated Wall plus 1 aft splitter	92.5	93
Treated Wall plus 3 inlet splitters plus 2 aft splitters	89	87.5
FAR 36	100	105

point is plotted in Figure 42 showing PNLT as a function of time. The acoustic angle relative to the engine is also indicated. The flyover characteristics are shown for each nacelle configuration. The EPNL calculated as described in FAR 36 but without the noise floor, is indicated on the right of the plot.

The constituent breakdown for the individual sources is shown in a corresponding plot in Figure 43. The fan noise dominates for the hardwall nacelle, the wall-treated nacelle and the single exhaust splitter configurations. Internal (combustion and core) noise is also above the jet noise level. Turbine noise is not a major contributor. The EPNL that would result from the individual sources is also shown on the right. For the bypass ratio and mixed jet cycle selected for the high speed engine the jet noise is also more than 10 EPNLT below the fan noise when the relative velocity effect is included.

The configuration with three fan inlet and two fan exhaust splitters reduced the fan noise to a level such that the core noise became a significant contributor even on takeoff. Additional core suppression (as well as turbine suppression) was incorporated in this configuration to produce the relative constituent levels shown in Figure 44.

Approach

Corresponding overall flyover time histories are shown for the 40% F_N approach condition in Figure 45 with the resultant EPNLT indicated on the rignt for each configuration, these levels are reduced by 1.5 EPNdB to account for the tri-jet approach power setting of 34% F_N. The relative constituent levels at approach are shown in Figure 46. At approach, both turbine and core noise are contributing to the suppressed fan levels leading to the need for the turbine suppression mentioned above when the fan is fully suppressed. The flyover constituent levels for the fully suppressed configuration at approach are shown in Figure 47.

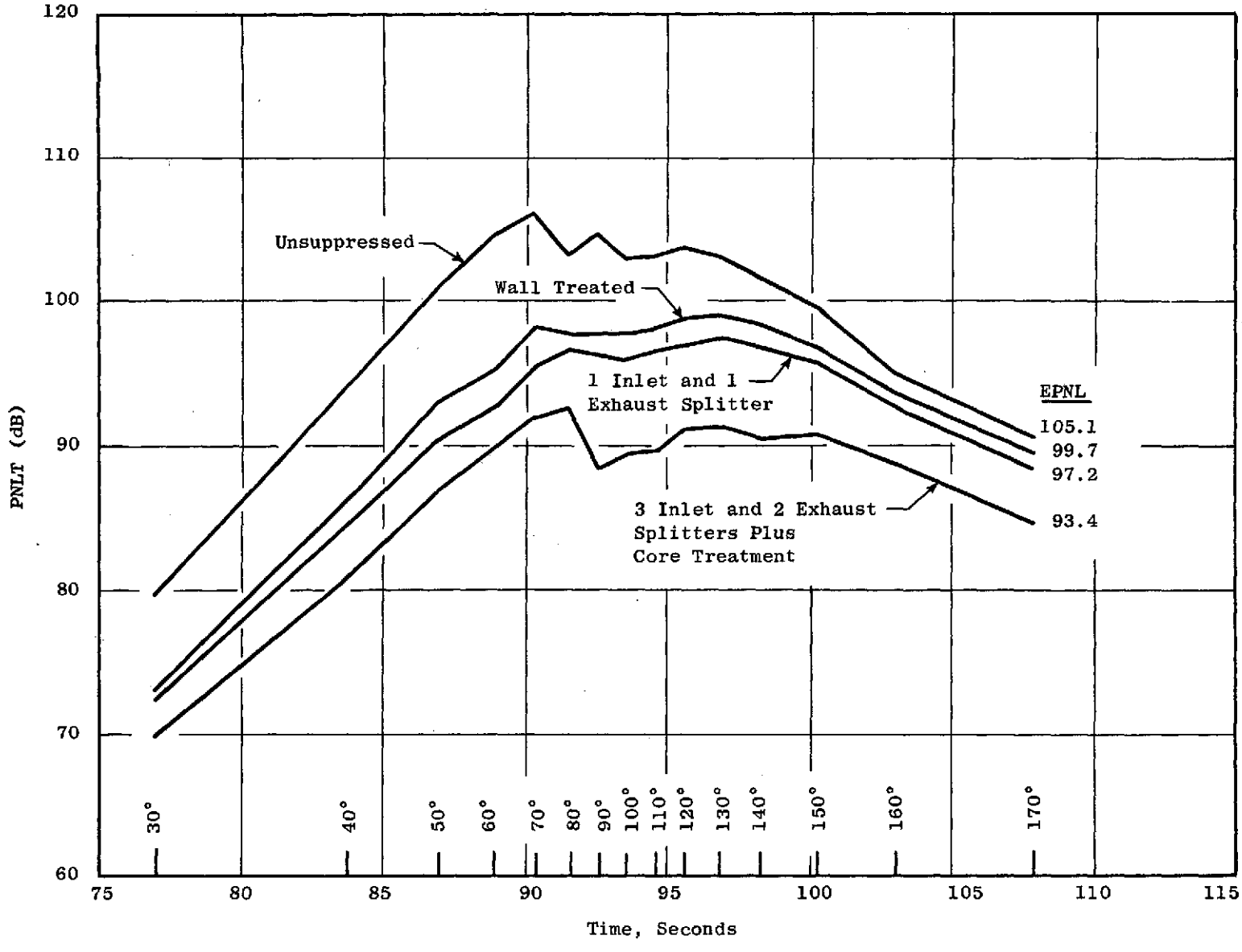

Figure 42. PNLT Vs. Time, Tri-Jet Takeoff, High Speed Engine Totals.

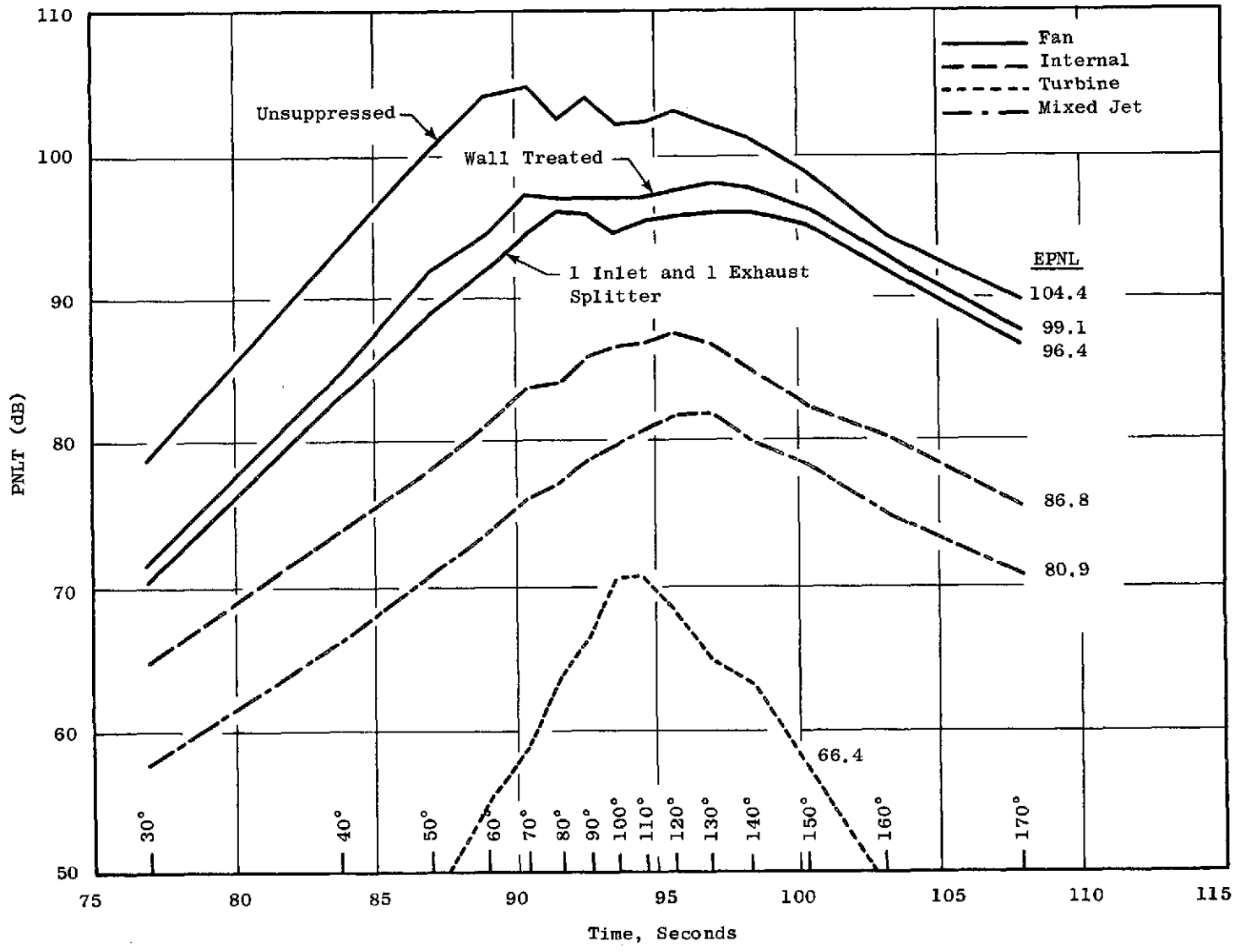

Figure 43. PNLT Vs. Time, Tri-Jet Takeoff, High Speed Engine Components.

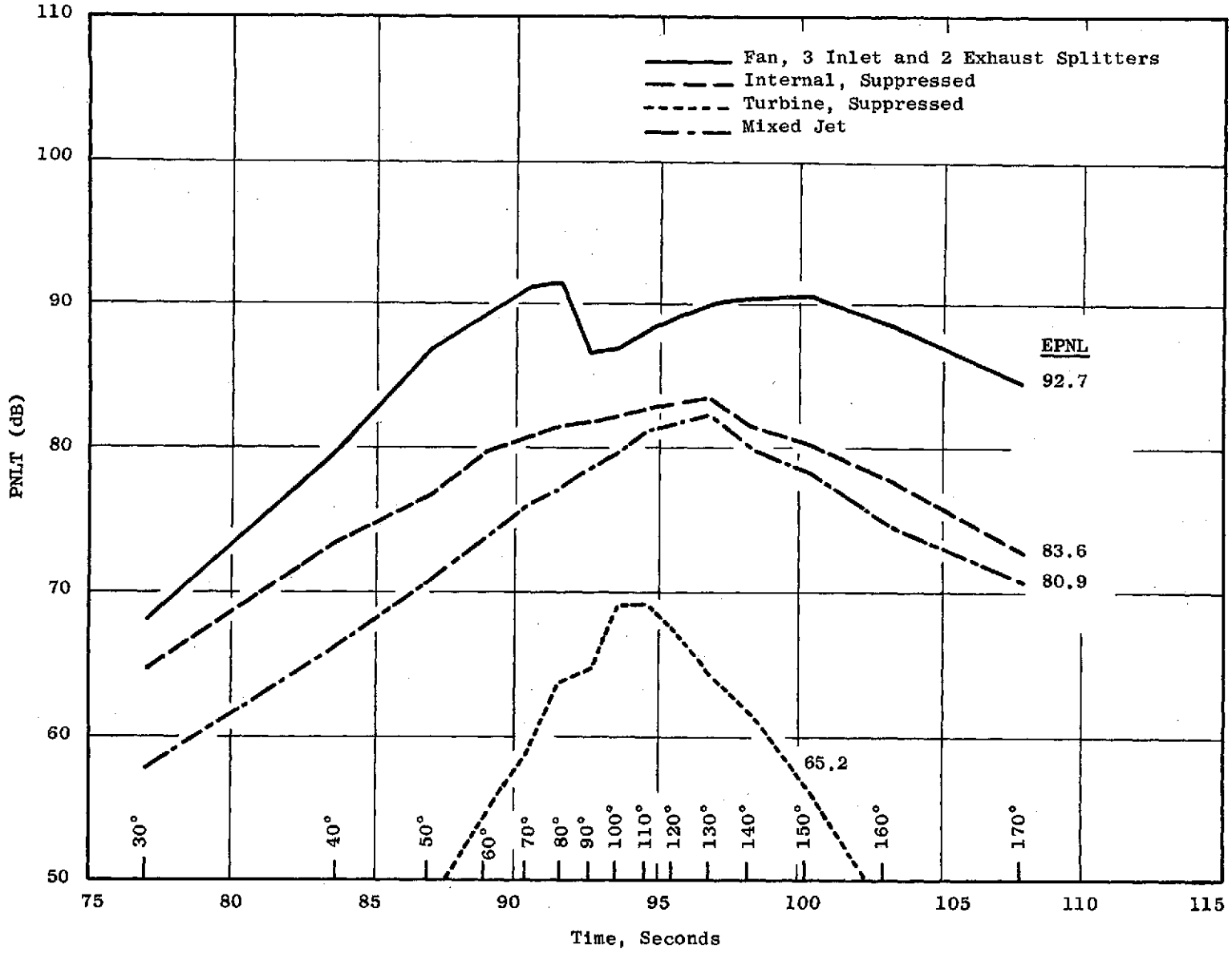

Figure 44. PNLT Vs. Time, Tri-Jet Takeoff, High Speed Engine.

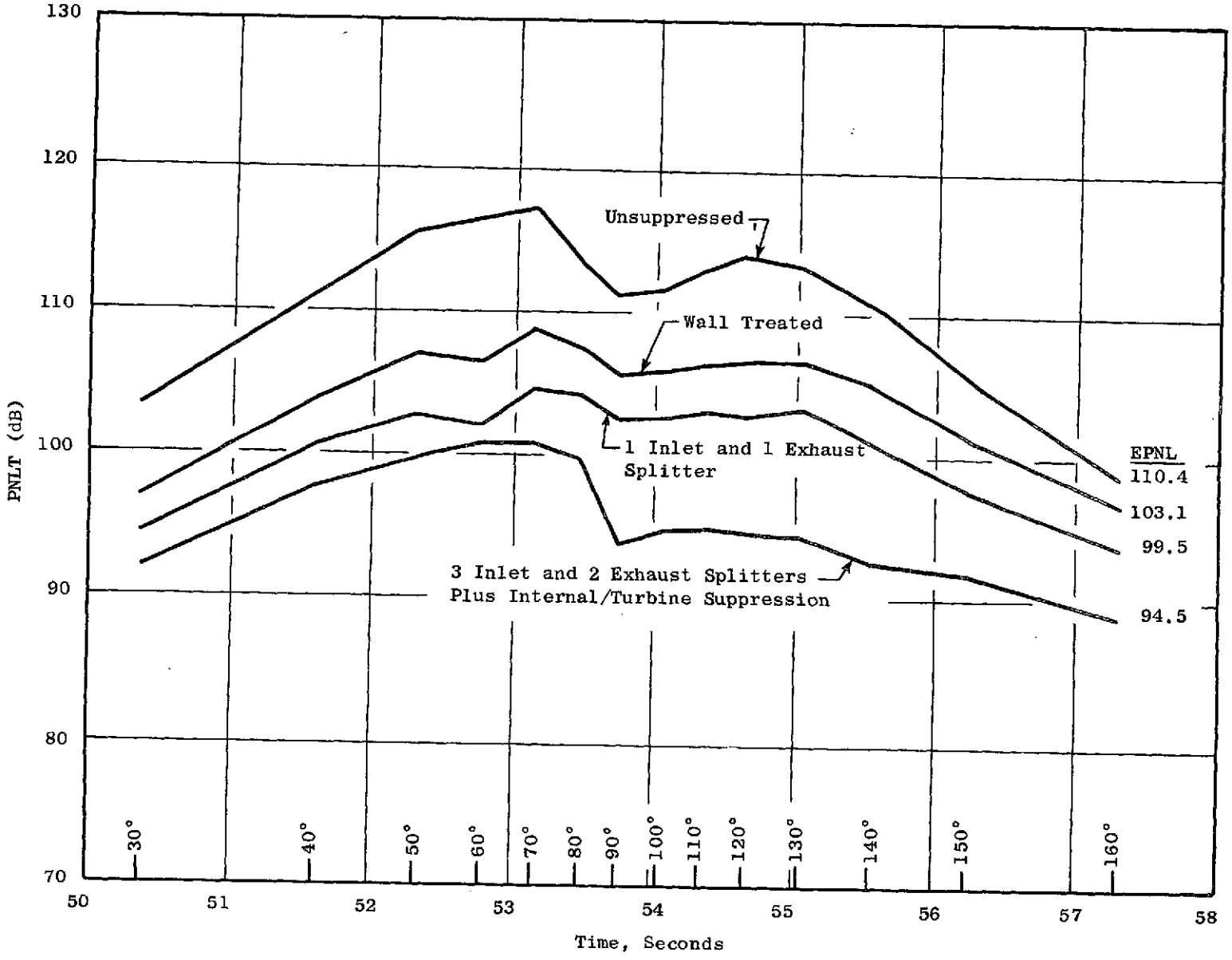

Figure 45. PNLT Vs. Time, Tri-Jet Approach, High Speed Engine Totals.

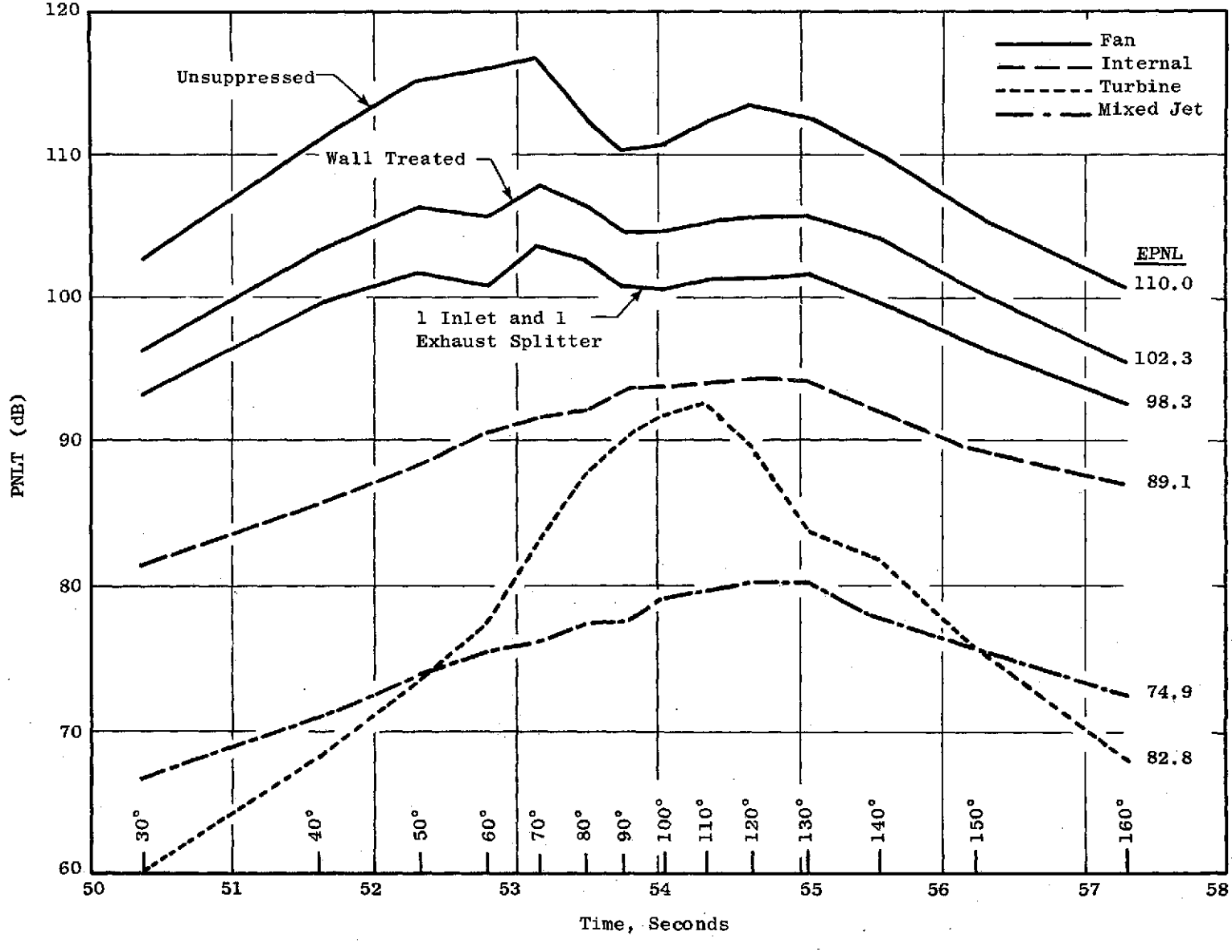

Figure 46. PNLT Vs. Time, Tri-Jet Approach, High Speed Engine Components.

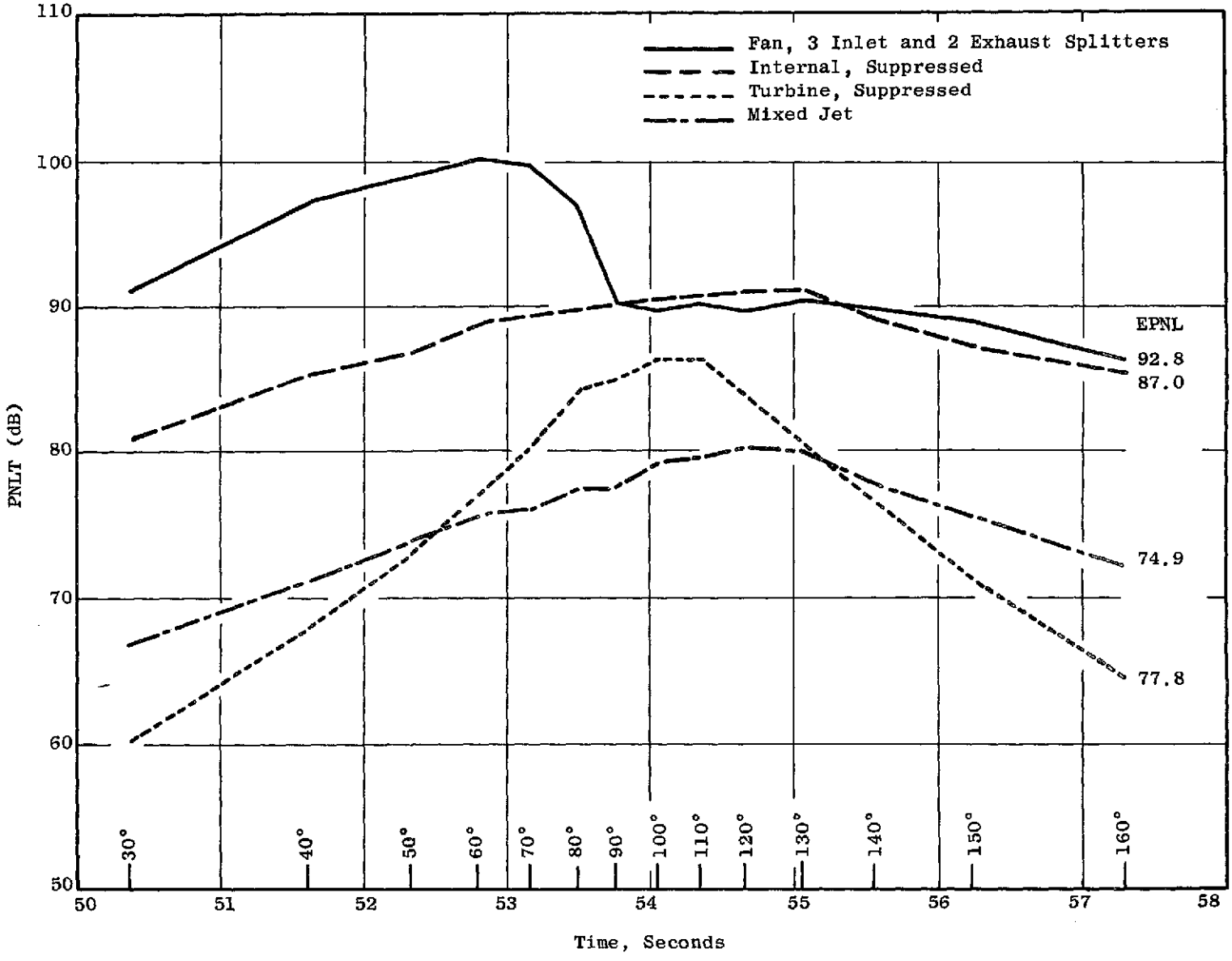

Figure 47. PNLT Vs. Time, Tri-Jet Approach, High Speed Engine.

Again, the above estimates (shown in the preceding figure) are obtained using component data taken over a hard surface without correction for ground nulls, etc. As a consequence, the anticipated noise levels corresponding to a normal certification measurement would also be the above estimates reduced by 2.0 EPNL. The final EPNL values (reflecting this 2 EPNL reduction) for the tri-jet aircraft at the FAR 36 takeoff and approach certification conditions are summarized in Table XXV.

Table XXV. Tri-Jet High Speed Engine EPNL Values. Nominal TOGW = 200,500 lb

Configuration	Takeoff	Approach
Hardwall Nacelle	103.1	106.9
Treated Wall	97.8	99.6
Treated Wall plus 1 inlet splitter plus 1 aft splitter	95.2	96.0
Treated Wall plus 3 inlet splitters plus 2 aft splitters	91.4	91.0
FAR 36	100	105

The results shown in Table XXV are considered representative of "status" levels, that is, expected levels based on demonstrated components, suppression effectiveness with current materials, etc.

7.4.5 Tri-Jet EPNL Contours

The following figures show the EPNL contours for a tri-jet CTOL transport equipped with the Quiet Engines defined in this Preliminary Flight Engine Design Study. Figures 48 through 51 present the contours for the High Speed Quiet Engine, and Figures 52 through 55 for the Low Speed Quiet Engine. Table XXVI summarizes the rating point EPNdB and 90 dB contour areas for the various Quiet Engine/nacelle configurations.

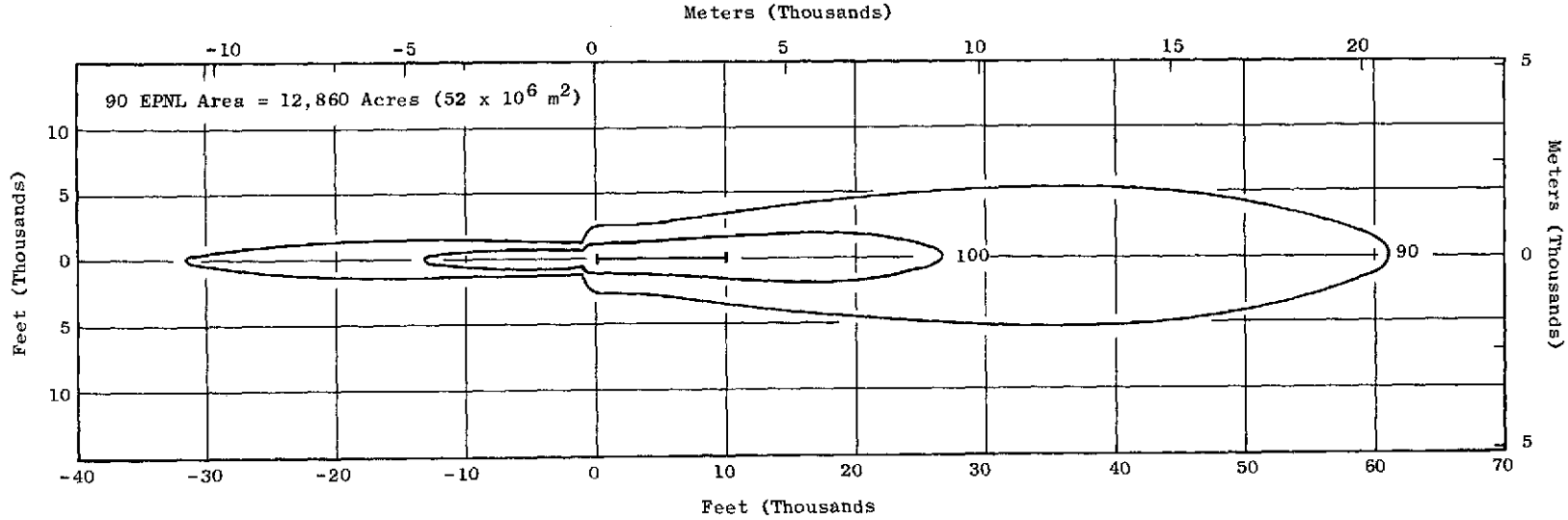

Figure 48. EPNL Contours, Tri-Jet CTOL Transport, High Speed Engine, Hardwall Nacelle.

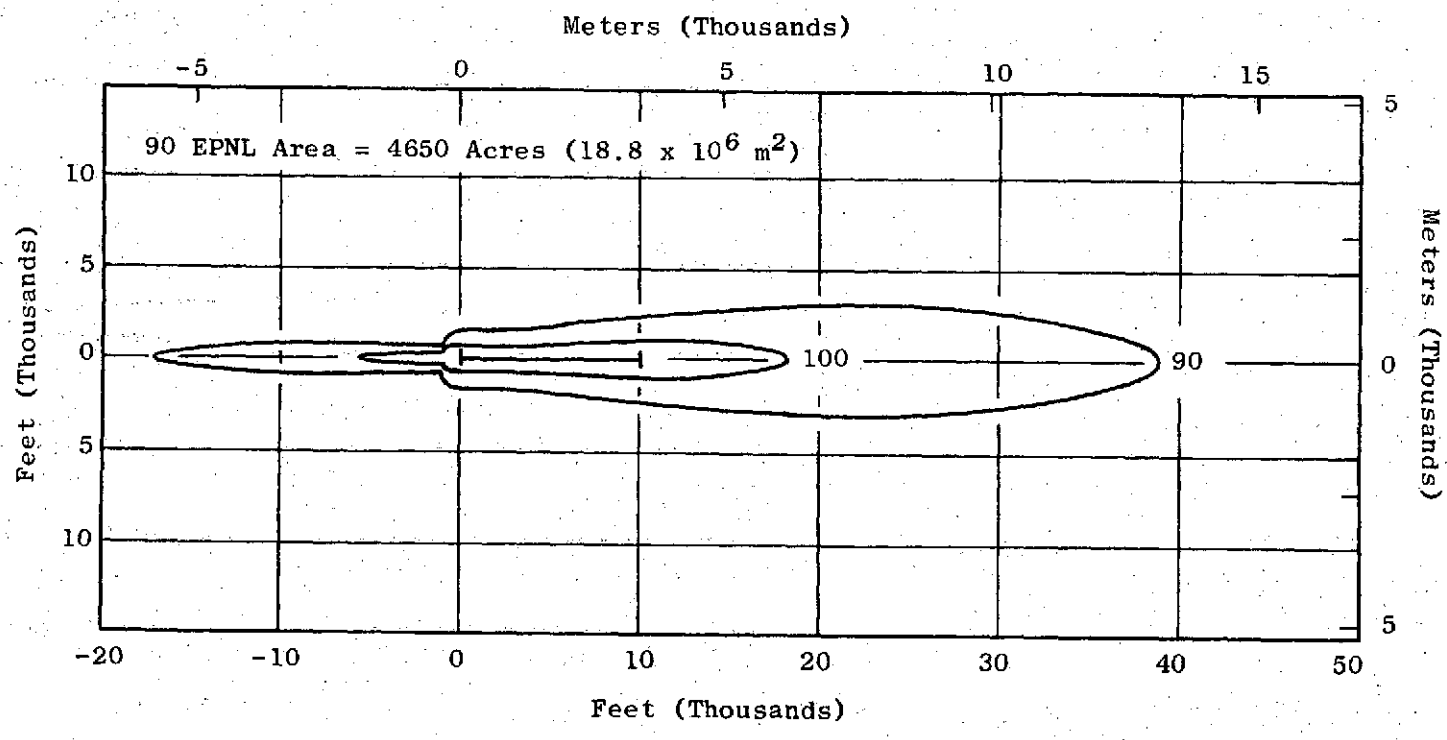

Figure 49. EPNL Contours, Tri-Jet CTOL Transport, High Speed Engine, Treated-Wall Nacelle.

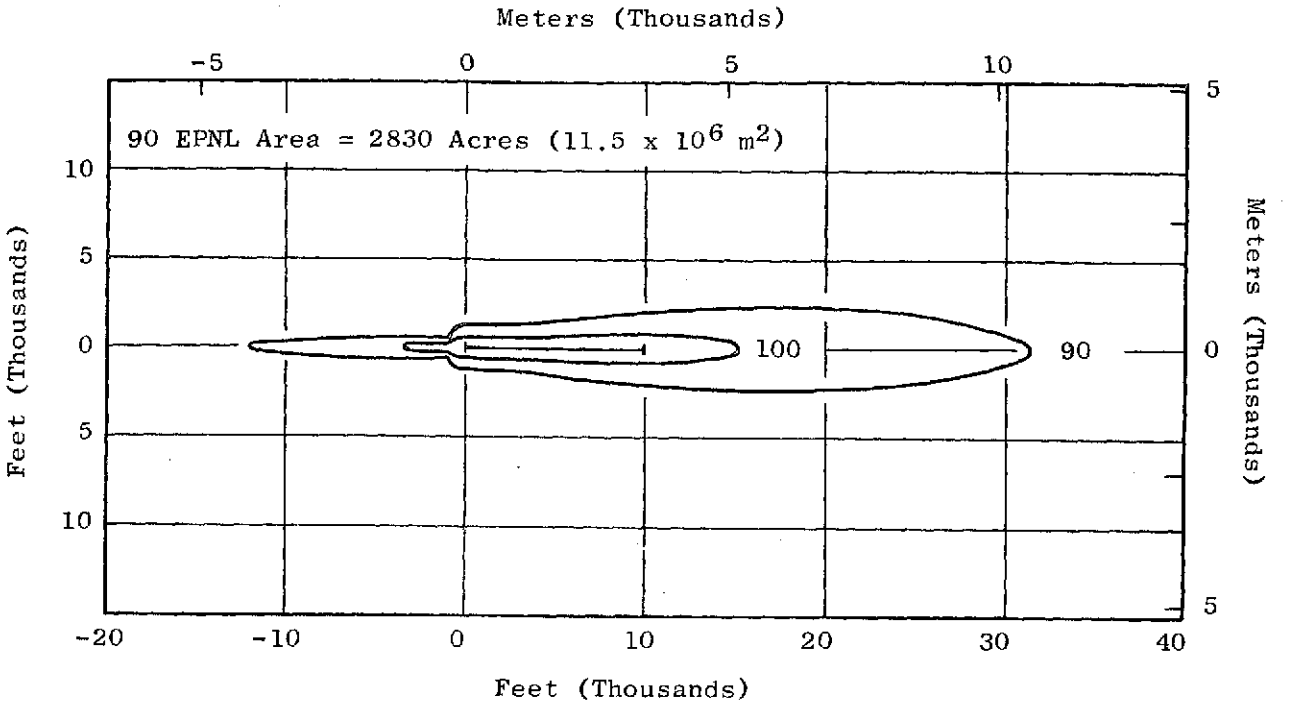

Figure 50. EPNL Contours, Tri-Jet CTOL Transport, High Speed Engine with One Inlet Splitter and One Exhaust Splitter.

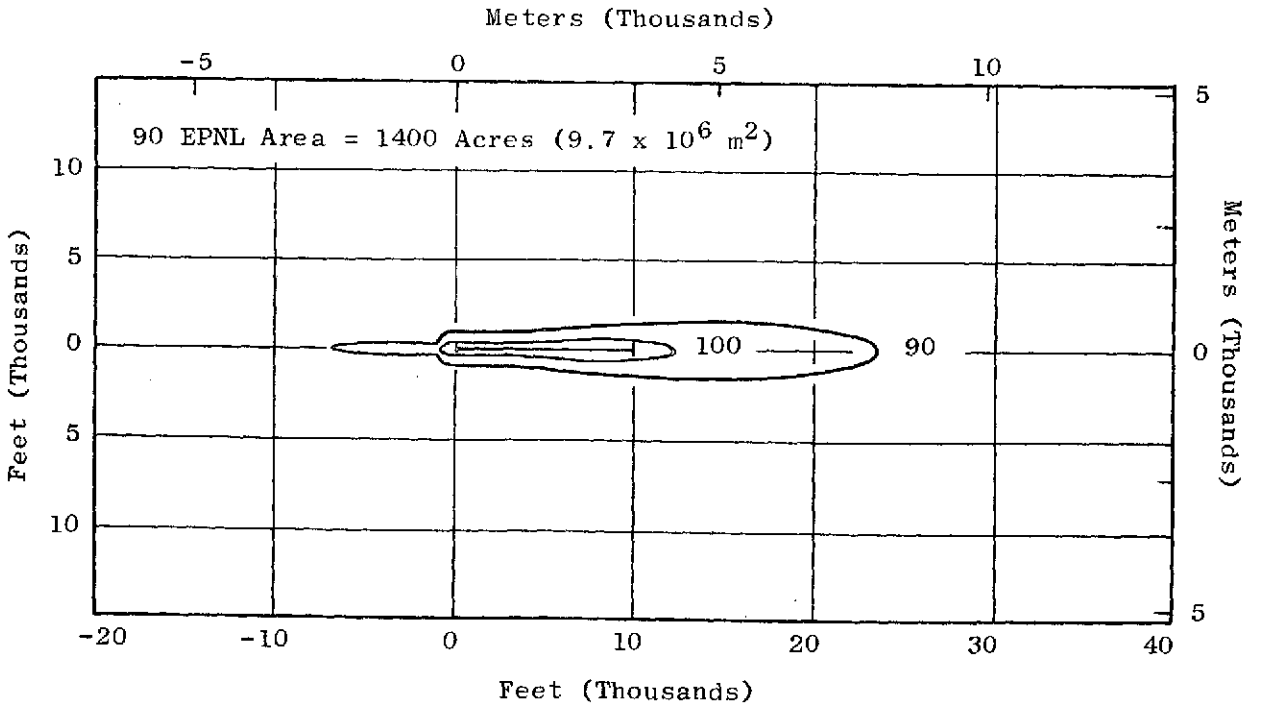

Figure 51. EPNL Contours, Tri-Jet CTOL Transport, High Speed Engine with Three Inlet Splitters and Two Exhaust Splitters.

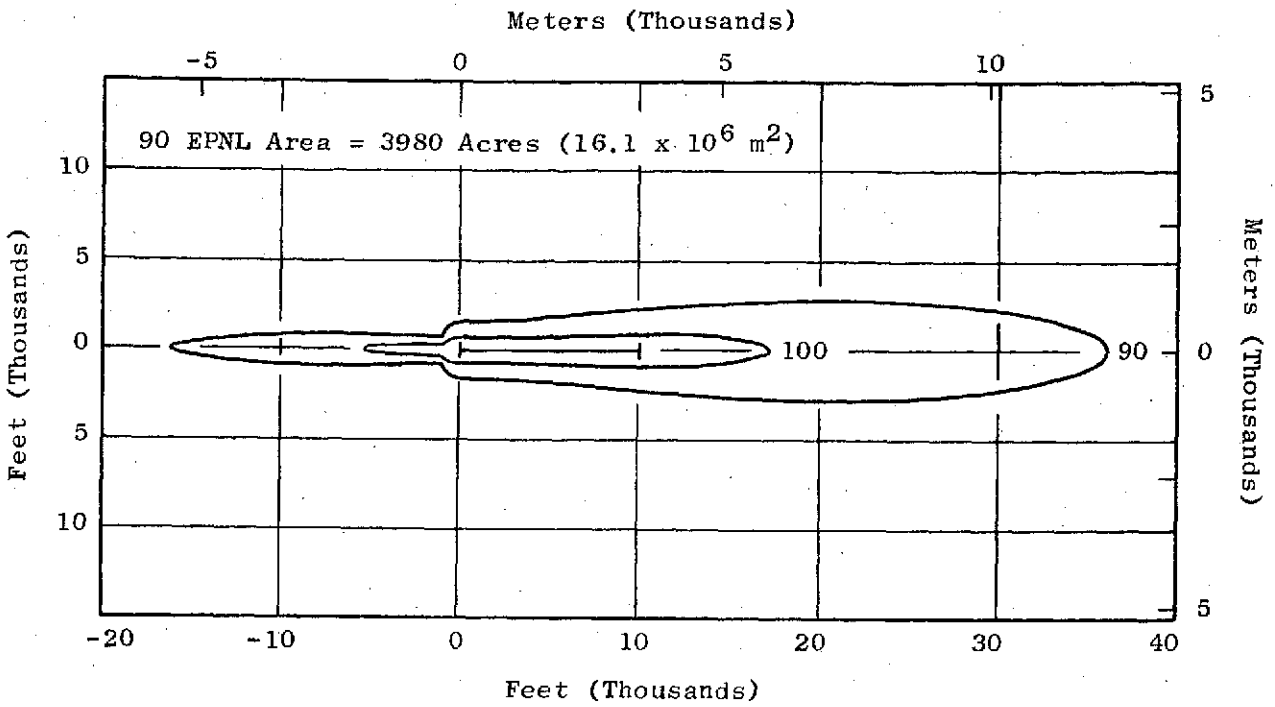

Figure 52. EPNL Contours, Tri-Jet CTOL Transport, Low Speed Engine, Hardwall Nacelle.

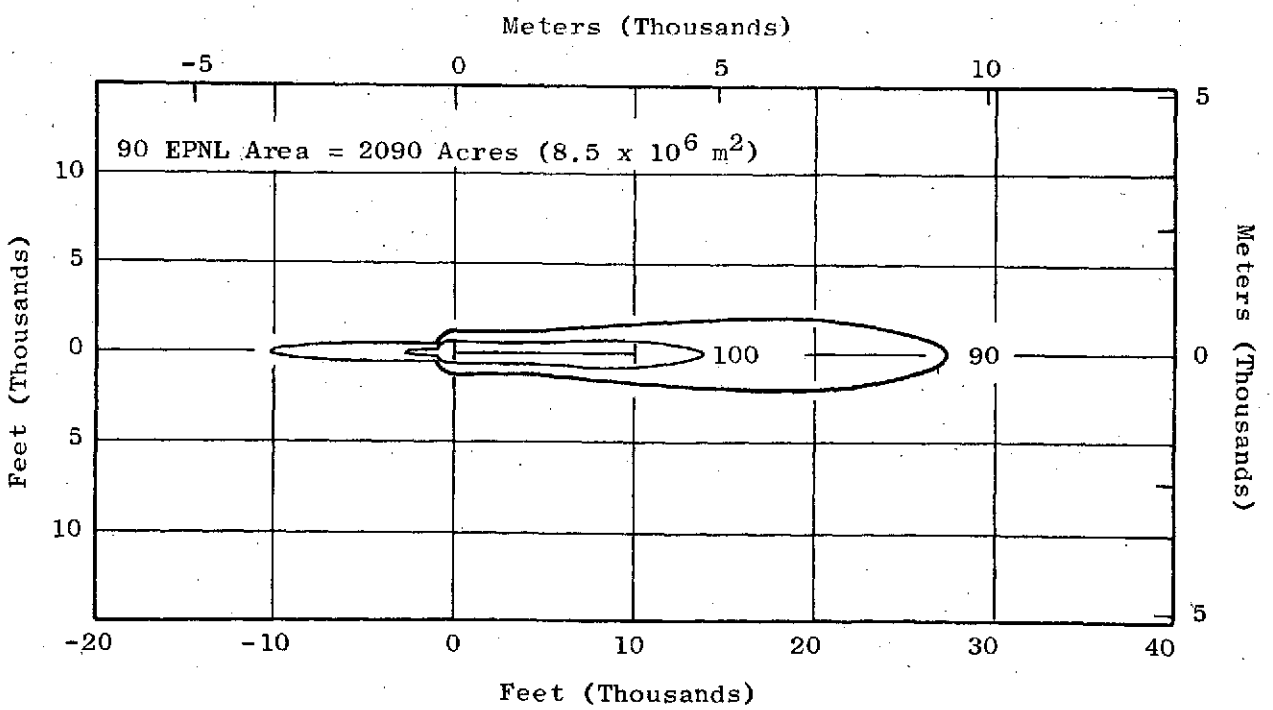

Figure 53. EPNL Contours, Tri-Jet CTOL Transport, Low Speed Engine, Treated-Wall Nacelle.

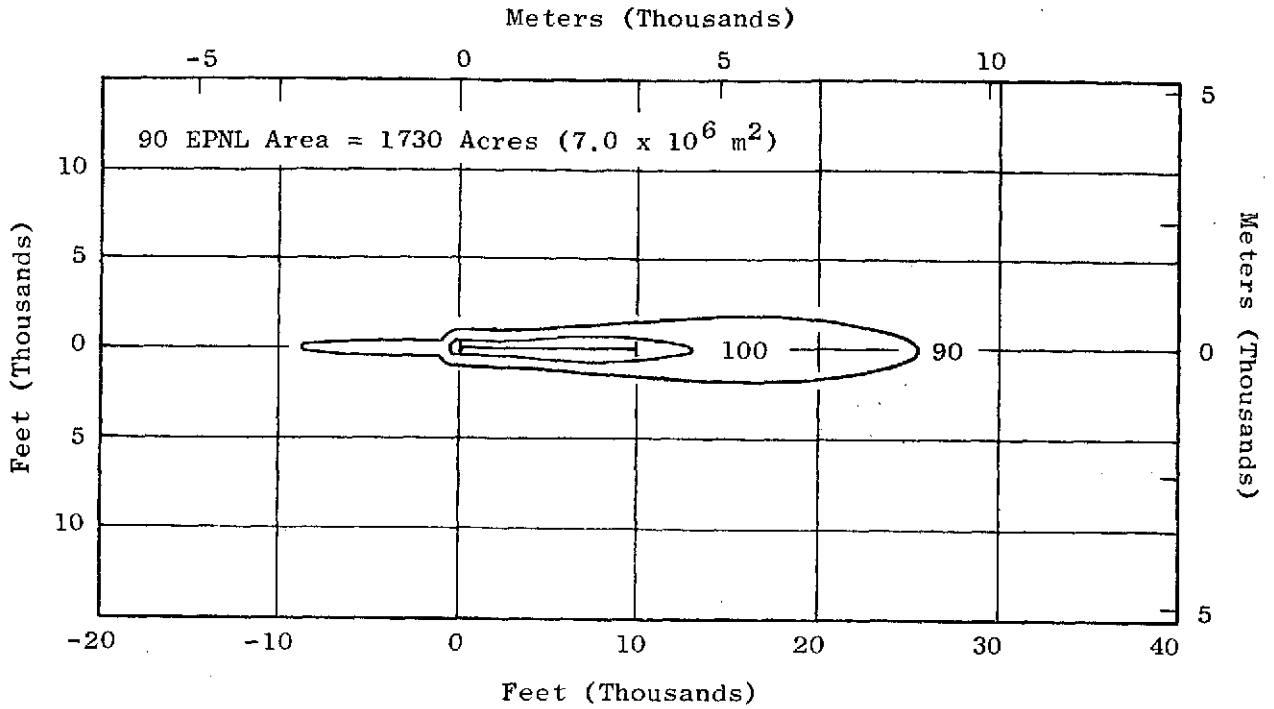

Figure 54. EPNL Contours, Tri-Jet CTOL Transport, Low Speed Engine with One Exhaust Splitter.

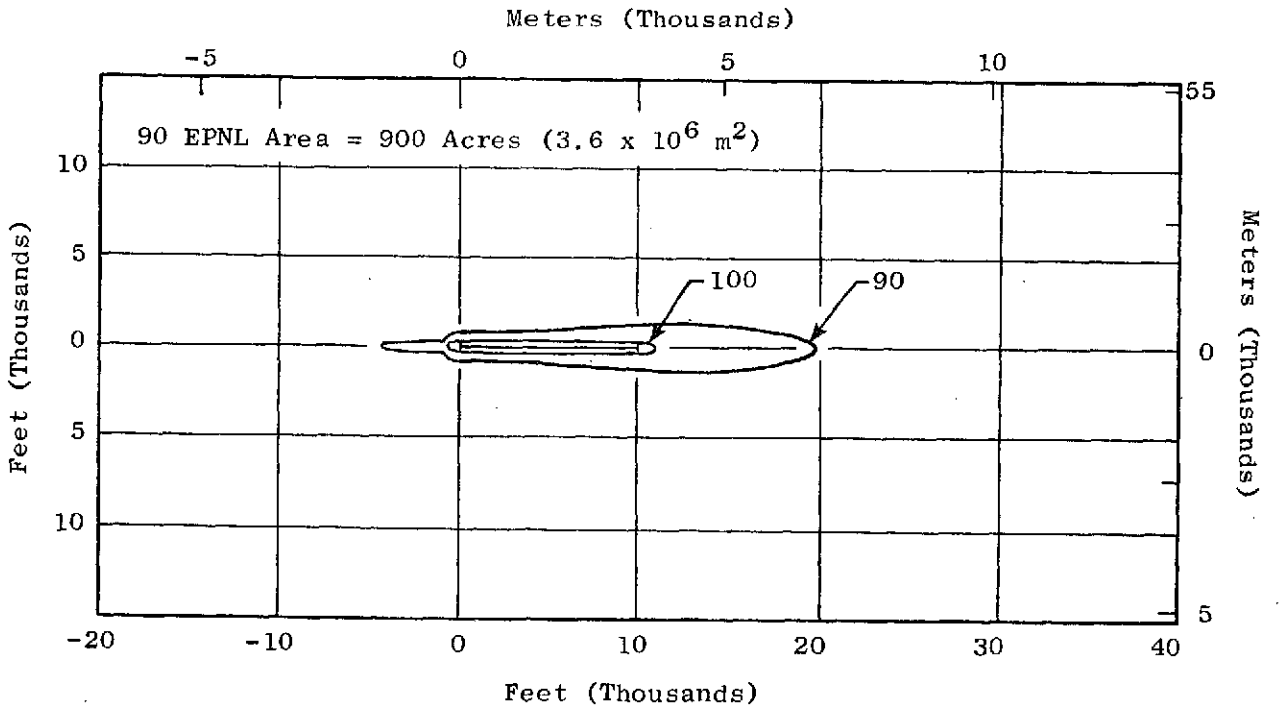

Figure 55. EPNL Contours, Tri-Jet CTOL Transport, Low Speed Engine with Three Inlet Splitters and Two Exhaust Splitters.

Table XXVI. Tri-Jet CTOL Transport Rating Point EPNL.

		Rating Point EPNdB	90 dB Contour Area, Acres ($m^2 \times 10^6$)
High Speed Engine			
Hardwall Nacelle	Takeoff	103.1	12,860 (52.0)
	Approach	106.9	
Treated Wall Nacelle	Takeoff	97.8	4,650 (18.8)
	Approach	99.6	
Treated Wall Plus 1 Inlet Splitter and 1 Aft Splitter	Takeoff	95.2	2,830 (11.5)
	Approach	96.0	
Treated Wall Plus 3 Inlet Splitters and 2 Aft Splitters	Takeoff	91.4	1,400 (5.7)
	Approach	91.0	
Low Speed Engine			
Hardwall Nacelle	Takeoff	97.0	3,980 (16.1)
	Approach	99.0	
Treated Wall Nacelle	Takeoff	93.5	2,090 (8.5)
	Approach	94.5	
Treated Wall Plus 1 Aft Splitter	Takeoff	92.5	1,730 (7.0)
	Approach	93.0	
Treated Wall Plus 3 Inlet Splitters and 2 Aft Splitters	Takeoff	89.0	900 (3.6)
	Approach	87.5	

C -2

8.0 CONCLUSIONS

Using the acoustic technology from the Quiet Engine Program in the preliminary flight engine designs and in the acoustically treated nacelles discussed in this report in a typical CTOL tri-jet transport results in projected noise levels well below FAR 36 requirements. Both high and low speed engines meet the FAR 36 requirements in a treated-wall nacelle configuration, and are significantly below the FAR 36 requirements in the fully suppressed nacelle. It has been determined that the economic penalty associated with the maximum feasible noise reduction (fully suppressed nacelle) is significant.

The EPNL/DOC relationship determined in the preliminary flight engine design study is shown in Figure 56. Considering both noise and DOC effects, at full power takeoff noise levels between FAR 36 and FAR 36 minus 5 EPNdB, with a typical tri-jet CTOL transport, a high speed engine in a treated wall nacelle appears to be the most economically attractive. As can be seen on Figure 56, the high speed engine yields a greater noise reduction for similar noise reduction features. For significant noise reductions below about FAR 36 minus 5 EPNdB, the cost increases for both low and high speed engines. For noise levels below approximately FAR 36 minus 5 EPNdB to FAR 36 minus 7 EPNdB the lower source noise of the low speed engine begins to dominate, and on a DOC basis, appears more economically attractive.

Technology developed since the conduct of the preliminary flight engine design study documented in this report indicates that the range of economic attractiveness of high speed fan engines may extend to lower noise levels.

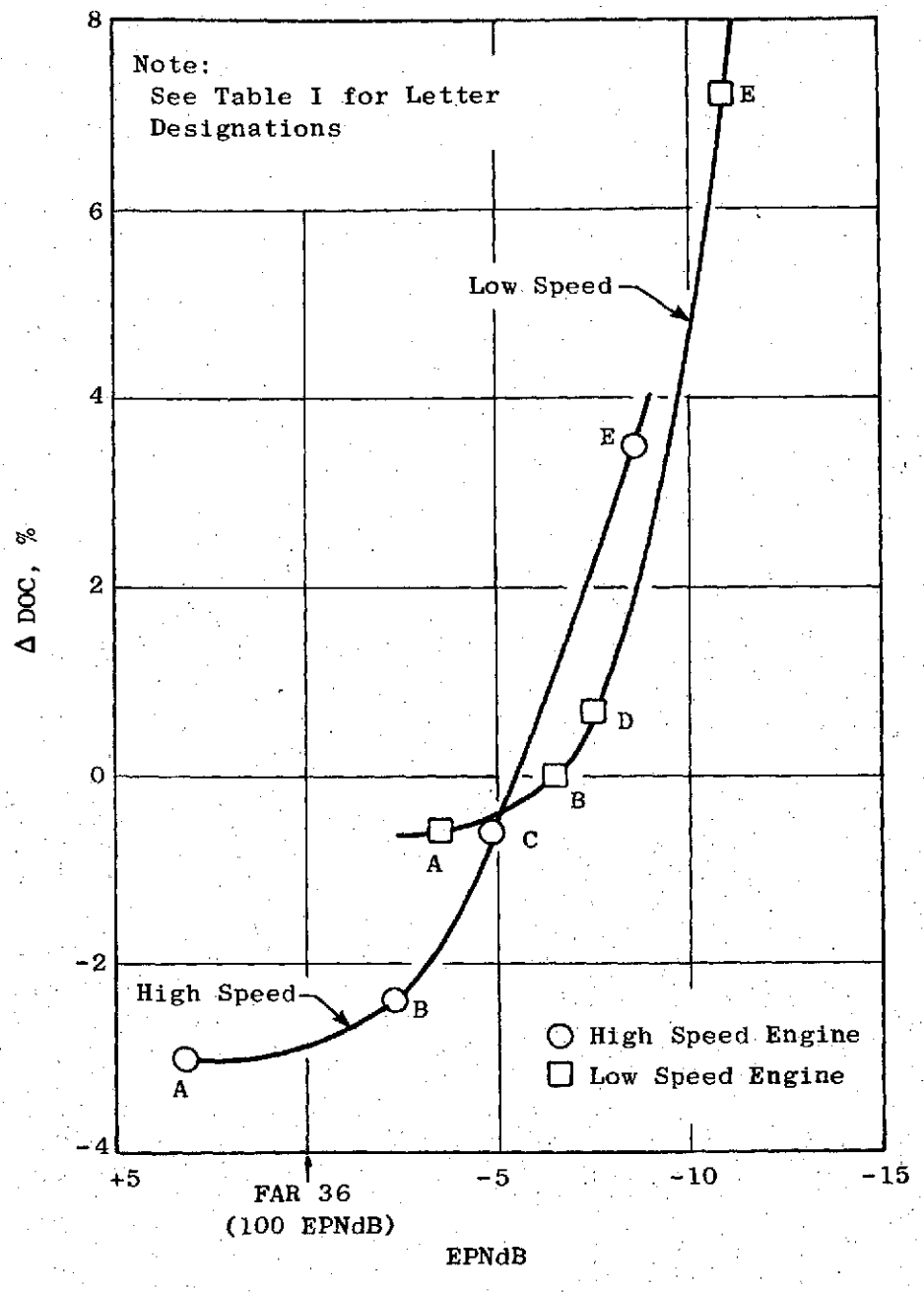

Figure 56. EPNL/DOC Relationship (Takeoff, No Cut-Back, Untraded).

APPENDIX A

NOISE PREDICTION PROCEDURES

I. SUMMARY

For high bypass fans typical of the Quiet Engine System, fan noise is the prominent component. Additional important engine noise sources include jet noise, turbine noise, and internal noise radiated rearward through the core exhaust duct. During an airplane flyover, noises from these engine sources peak at different instants and contribute to a complicated history of the flyover noise event. Since all engine noise sources are also present during static ground noise tests and information and verification of analytical techniques is available on this basis, static noise levels were obtained as the first step in providing airplane flyover noise levels.

II. FAN NOISE SCALING METHOD

The basic measured full-scale fan sound pressure levels were applied to a generalized spectrum scaling program in which the data are corrected for atmospheric absorption and for assumed scattering losses or EGA at the input arc distance prior to scaling. This produces an "ideal" arc spectrum. After frequency shifts attributable to speed and blade number changes and application of a weight flow adder, projection to the desired sideline is accomplished using square law distance effect, absorption , and standard EGA.

III. TURBINE NOISE PREDICTION METHOD

The noise spectra of the last two stages of the low pressure turbine for high speed and low speed engines were analytically predicted at both takeoff and approach power settings. GE computer program prediction routines were used in calculating these noise spectra. These computer programs require as inputs: basic geometry, aerodynamic, and cyclic parameters for each engine prediction. See Table X for some of the more important parameters used.

IV. INTERNAL NOISE PREDICTION METHOD

Two low frequency noise sources, formally classified as "jet" noise, are associated with the gas generator exhaust:

External jet noise - caused by interactions outside the engine.

Internal noise - similar in frequency to jet, but generated in the engine. The similarity between this noise and jet noise makes them inseparable on a farfield noise measurement basis and is usually pointed out as the reason for jet noise not decaying with a V^8 slope at low jet velocities [less than 800 ft/sec (244 m/sec)].

The specific sources (or source) of engine generated rumble are unknown. It most likely is caused by several sources in the combustor/turbine section. A prediction method is used which relates core noise to compressor discharge flow, temperature, and pressure and the combustor exit temperature. The method agrees well with noise data obtained on a TF34 engine with the fan highly suppressed and with noise data from turboshaft engines which have negligible jet noise.

V. MIXED JET NOISE PREDICTION METHOD

Mixed-flow jet noise was predicted based on test data from the Acoustic Aerodynamic Mixer Noise Tests performed by Fluidyne Engineering Corporation at their Medicine Lake Aerodynamic Laboratory (Reference 6). The configuration was an 18-lobe, area ratio 3.37, partial mixer with a bypass ratio (fan flow to core flow) of 6 to 1.

APPENDIX B

DOC CALCULATIONAL PROCEDURE

An outline of the DOC calculation procedure used in the current high speed and low speed engine study is compared to the corresponding economic elements used in previous NASA studies (Reference 5).

The economic factors are applied to variable-size airplanes on the basis of holding the payload and range constant as the two-fan engine in the various nacelles are installed on the aircraft.

DOC CALCULATION PROCEDURE

Price Base	Quiet Engine Trade Study (Consistent with ATT Studies) 1967	NASA Report DAC-68255A (NAS3-11151) Tables XI, XII 1967
Flying Operations	All Costs - $/Block Hour	
Crew Pay-Domestic Subsonic Jet ①	(2 man) $5x10^{-5}$ (Max. TOGW)+100 (3 man) $5x10^{-5}$ (Max. TOGW)+135 Add $35 for each additional crew member Add $20 for internation oper.	Same Same Same
Fuel ②	1.02 (Fuel Burned-lb/block hour) X (Fuel Cost - $/lb) Fuel Cost = $0.1/US Gallon Kerosene 1.02 = Nonrevenue Flying Factor	(Fuel Burned-lb/block hour) X (Fuel Cost $/lb)
Oil ③	(0.135 Ne)x(0.1 Cost $/lb) 0.1 Cost = $0.926/lb	0.125 Ne
Hull Insurance ④	(Insurance Rate) x C_t/U = Hull Ins. Insurance Rate = 0.02 U = f(Block Hour); ATA Equiv. Twinjet U = 3600 hours Trijet U = 4200 hours	Same U = 3800 hours
Depreciation Flight Equip. ⑤	$(C_t-R)/(DaxU)$ R = 0 Da = 15	Same, Except Da = 12

Aircraft Spares ⑥	(0.1 Ca)/(DaxU) Da = 15	Same, Except Da = 12
Engine Spares ⑦	(0.2 CeNe)/(DaxU) Da - 15 G.E. Experience	(0.4 CeNe)/(DaxU)
Direct Maintenance Aircraft		
Aircraft Labor (Excluding Engines) ⑧	$2.36K\left(1 - \frac{tgm}{blk.hr.}\right)$ + 4.0K/blk.hr. $K = 5x10^{-5}Wa+6-\left(\frac{630}{120+10^{-3}Wa}\right)$ K = Manhours/cycle Labor Rate = $4.00/hr.	Same Same
Aircraft Mat. (Excluding Engines) ⑨	$(3.08x10^{-6}Ca)\left(1- \frac{tgm}{blk.hr.}\right)$ + $(6.24x10^{-6}Ca)$/blk/hr.	Same
Direct Maintenance Engines		
Bare Eng. Labor ⑩	$(0.44+2x10^{-6}T)Ne\left(1 - \frac{tgm}{blk.hr.}\right)$ + $(0.45+2x10^{-6}T)$ Ne/blk.hr. GE Experience	$(2.4+1.08x10^{-4})Ne\left(1- \frac{tgm}{blk.hr.}\right)$ + 1.2 Ne$(1+10^{-4}T)$/blk/hr.
Bare Engine Mat. ⑪	$(25x10^{-6}CeNe)\left(1-\frac{tgm}{blk.hr.}\right)$ + $(10x10^{-6}$CeNe/blk.hr. GE Experience	$(25x10^{-6}NeCe)\left(1- \frac{tgm}{blk.\ hr.}\right)$ + $(20x10^{-6}$NeCe)blk.hr.
Reverser Labor ⑫	$0.24Ne\left(1- \frac{tgm}{blk.hr.}\right)$ + $5x10^{-6}C_rNe$/blk.hr.	None
Reverser Mat. ⑬	$5x10^{-6}C_rNe\left(1- \frac{tgm}{blk.hr.}\right)$ + $5x10^{-6}C_rNe$/blk.hr.	None

Burden (14)	1.8 x Total Labor	Same
DOC Total	Total of 1 through 14	Total of 1 through 14, except 12 and 13.

NOMENCLATURE

U	Utilization, Block Hours/Year
C_t	Total Aircraft Price
Ce	Engine Price Each
Ne	Number of Engines
Ca	C_t - CeNe, Aircraft Cost
R	Residual Value, $
Da	Depreciation Period, Years
K	Manhours/Flight Cycle
tgm	Ground Maneuver Time, Hours
Wa	Empty Weight Less Bare Engines
T	Engine Takeoff Thrust, lb
C_r	Reverser Selling Price

The following numerical example illustrates the DOC calculation procedure. Typical values for the 1650 nautical mile (3056 km) tri-jet are used for purposes of illustration.

The most significant differences are in aircraft depreciation and engine maintenance, but the values used in the DOC study are considered appropriate for the engine/aircraft system under study.

NUMERICAL INPUT

DOC SAMPLE CALCULATION

Maximum TOGW, lb (kg)	115,500 (52,500)
Block Hours	2.15
Ne	2
C_t, $	6,780,000
Ce, $	600,000
Ca = C_t-CeNe, $	5,580,000
Wa, lb (kg)	59,920 (27,200)
tgm, hours	0.25
T, lb (N)	22,000 (97,900)
C_r, $	175,000
Range, Nautical Miles (km)	800 (1310)
Payload, lb (kg)	28,800 (13,100)
Number Passengers	144
Fuel Burned/Mission, lb (kg)	11,320 (5,150)

DOC SAMPLE CALCULATION

	Item	Proposed Method QEP Trade Study $/BH	NASA Reports NAS3-11151 Tables XI, XII DAC-63256A $/BH
1.	Crew	140.78	140.78
2.	Fuel	80.18	78.70
3.	Oil	0.25	0.24
4.	Insurance	37.67	35.70
5.	Depreciation Flight Equip.	125.56	156.80
6.	Aircraft Spares	10.33	12.91
7.	Engine Spares	4.44	5.55
8.	Aircraft Maintenance, Labor	21.68	21.68
9.	Aircraft Maintenance, Material	31.38	31.38
10.	Bare Engine Labor	6.02	48.00
11.	Bare Engine Material	32.01	37.65
12.	Reverser Labor	0.64	---
13.	Reverser Material	2.36	---
14.	Burden	51.01	125.50
	TOTAL	544.31	694.90

APPENDIX C

QUIET ENGINES IN A DC-8-TYPE AIRCRAFT

I. SUMMARY

This appendix presents the results of a study to determine the effect on the Direct Operating Cost (DOC) of a DC-8-type aircraft on which the JT3D engines are replaced by the quiet engine and nacelle configurations defined during the preliminary flight engine study. Utilization of any of the quiet engine/nacelle combinations, both high speed and low speed fan engines, results in an approximately 40 to 50% DOC increase compared to the JT3D-powered DC-8-type aircraft. The primary reason for the sizable increase in DOC is the cost of the new engines and nacelles. A five year life (depreciation period) was assumed for this study. In fact, the DOC increase would undoubtedly be even greater than this study indicates since the current study had to assume no major airframe changes. A detailed examination of aircraft aerodynamics, including stability and control aspects, could potentially reveal the need for airframe changes resulting in even greater retrofit associated costs.

The maximum EPNL reduction resulting from the application of the Quiet Engine/nacelle configurations to the DC-8-type aircraft is approximately 20 EPNdB compared to the JT3D-powered version (takeoff).

II. INTRODUCTION

This study investigated the effects on DOC of replacing the JT3D on a DC-8-type aircraft with both high and low speed quiet engines. The quiet engines and nacelle characteristics used in this study were those defined in Section 3 (low speed engine) and Section 5 (high speed engine) of this report, and the pertinent aircraft charateristics were obtained from Reference 7. Factors considered in the study included engine and nacelle weight and cost, engine specific fuel consumption at cruise, and aircraft noise at the takeoff and approach noise rating points.

Based on an evaluation of these parameters the changes in Direct Operating Cost and in EPNL at the rating points were estimated for a DC-8-type aircraft with either high or low speed quiet engines with varying degrees of nacelle acoustic treatment. Estimates of the changes in DOC were obtained using the procedure applied in the ATT Studies (Reference 4) described in Appendix B.

III. DC-8-TYPE AIRCRAFT NOISE CHARACTERISTICS WITH QUIET ENGINES

The noise characteristics of the low speed and high speed quiet engines with varying amounts of nacelle acoustic treatment are described in detail in Sections 4 and 6, respectively, of this report. Using these engine and nacelle acoustic characteristics, the EPNL's were estimated for a DC-8-type aircraft equipped with the various engine/nacelle configurations. The resultant EPNL values, summarized in Table XXVII, were derived using the method defined in Section 7.4 of this report.

Table XXVII. DC-8-Type Aircraft EPNL.

	High Speed Quiet Engine		Low Speed Quiet Engine		JT3D		FAR36	
	T.O.	App.	T.O.	App.	T.O.	App.	T.O.	App.
Hardwall Nacelle	107.9	109.2	101.7	101.5	116	118	103	106
Treated Wall Nacelle	102.3	101.9	97.4	96.8				
Treated Wall Nacelle +1 Aft Splitter			96.1	95.1				
Treated Wall Nacelle +1 Inlet Splitter +1 Aft Splitter	100.7	98.3						
Treated Wall Nacelle +3 Inlet Splitters +2 Aft Splitters	95.5	93.3	92.6	89.6				

As can be seen from the tabulated EPNL values the application of low speed quiet engines with the basic nacelle without treatment results in a pronounced reduction from the JT3D-powered DC-8-type aircraft. Use of the high speed quiet engines in the basic nacelle without treatment configuration also results in a sizable noise reduction from the JT3D-powered version, although not as large a reduction as the low speed quiet engine provides. However, this is partially offset by the fact that the additional treatment configurations provide somewhat more reduction with the high speed quiet engine than they do with the low speed quiet engine. The addition of the maximum treatment considered, in both high and low speed quiet engines, results in approximately 3 EPNL more "baseline" to "maximum" suppression for the high speed quiet engine powered DC-8-type aircraft than for the low speed quiet engine powered version.

IV. DIRECT OPERATING COST COMPARISONS

The DOC of a DC-8-type aircraft utilizing both high and low speed quiet engines with various nacelle treatment configurations were compared to the DOC of a JT3D-powered version. The DOC estimates were calculated using the method described in Appendix B. The weight and performance characteristics of the high and low speed quiet engines with various nacelle acoustic treatment configurations were obtained from Sections 3 and 4, respectively, of this report and are summarized in Table XXVIII. The DC-8-type aircraft characteristics pertinent to the DOC estimation were obtained from Reference 7, and are summarized in Table XXIX.

The cost items included in the DOC calculation are shown in Table XXX, as well as what each of the cost items is a function of. Since the intent in this study was to determine the differential DOC effects for high and low speed

Table XXVIII. Quiet Engine Characteristics.

	High Speed Engine		Low Speed Engine	
Bare Engine Weight, lb (kg)	3500	(1592)	3940	(1791)
Takeoff Thrust, lb (N)	22,000	(97,900)	22,000	(97,900)
Cruise Thrust, lb (N)	4950	(22,000)	4950	(22,000)
Hardwall Nacelle - Weight, lb (kg)	6183	(2810)	6682	(3035)
- Cost, $-000's	849		874	
- Cruise, SFC	0.671		0.658	
Treated Wall Nacelle - Weight, lb (kg)	6237	(2835)	6831	(3105)
- Cost, $-000's	854		880	
- Cruise, SFC	0.671		0.660	
Treated Wall Nacelle - Weight, lb (kg)	---		6900	(3140)
+1 Aft Splitter - Cost, $-000's	---		884	
- Cruise, SFC	---		0.663	
Treated Wall Nacelle - Weight, lb (kg)	6468	(2940)	---	
+1 Inlet Splitter - Cost, $-000's	865		---	
+1 Aft Splitter - Cruise, SFC	0.679		---	
Treated Wall Nacelle - Weight, lb (kg)	7103	(3230)	7730	(3515)
+3 Inlet Splitters - Cost, $-000's	928		966	
+2 Aft Splitters - Cruise, SFC	0.689		0.679	

Table XXIX. DC-8 Aircraft and Utilization Characteristics.

Maximum TOGW, lb (kg)	325,000	(147,800)
Number Engines	4	
Airframe Cost, $-Millions	8.0	
Depreciation Period, years	5	
Ground Maneuver Time, hours	0.25	
Residual Value, $	0	
Payload (Space Limited), lb (kg)	56,845	(25,850)
Empty Weight, Less Engines, lb (kg)	132,300	(60,200)
Annual Utilization, hours	3800	

Table XXX. Direct Operating Cost Items.

	Cost Item	Function of	Included in Δ DOC Calcu.
1.	Crew Pay	Max. TOGW	No
2.	Fuel	SFC, Cruise F_N	Yes
3.	Oil	Number of Engines	Yes
4.	Hull Insurance	Total Aircraft Price, Utilization	Yes
5.	Flight Equipment	Total Aircraft Price, Depreciation Period, Utilization	Yes
6.	Aircraft Spares	Airframe Price, Depreciation Period, Utilization	No
7.	Engine Spares	Engine Price, Number of Engines Depreciation Period, Utilization	Yes
8.	Aircraft Labor (excluding engines)	Empty Weight Less Engines	No
9.	Aircraft Material (excluding engines)	Airframe Price	No
10.	Bare Engine Labor	Takeoff F_N	No
11.	Bare Engine Material	Engine Price, Number of Engines	Yes
12.	Reverse Labor	Number of Engines	No
13.	Reverser Material	Number of Engines, Reverser Selling Price	No
14.	Burden	Labor Total	Yes

engines with various amounts of nacelle acoustic treatment it was only necessary to include specific DOC cost items in the calculation as indicated in Table XXX. As can be seen in Table XXX the other cost items (e.g., crew pay and aircraft spares) are not a function of the engine/nacelle/aircraft configuration being studied.

As noted from Reference 7, a rigorous comparison of the DOC results of an engine substitution into an existing aircraft configuration would require a thorough and detailed design and analysis effort. Such an effort would need to consider detailed nacelle and pylon design, aircraft takeoff and cruise performance, stability characteristics, range, payload, and stage length. Evaluation of these factors would involve a design effort of major proportions including structural, stability and control, drag, and flutter investigations.

However, it was possible to make a number of logical simplifying assumptions and arrive at a consistent set of differential DOC values. The aicraft with quiet engines were assumed to continue to operate over the same stage lengths as the JT3D-powered version. Due to the improved SFC of the quiet engines and the assumption of the same stage length, the aircraft payload becomes space limited and payload variations need not be a consideration, even though the quiet engines and acoustically treated nacelles result in a higher operating weight empty than the JT3D-powered version. Table XXXI summarizes the weight changes due to application at the various quiet engine/nacelle configurations.

An additional assumption is required at this point, i.e., the aircraft basic structure need not be modified to accept the quiet engines and nacelles. The high and low speed quiet engines in this study were sized at 22,000 lb (97,900 N) thrust at takeoff, essentially the same size as used for the studies reported in Reference 7. Therefore, the DC-8-type aircraft performance and engine/airframe physical integration aspects could be considered essentially the same as reported in Reference 7. The specific high and low speed quiet engine and nacelle weights and costs were considered as described in this Appendix.

With these assumptions it becomes possible to calculate the differential DOC values for the quiet engines with various nacelle acoustic treatment configurations. The depreciation period used for the calculation of retrofit associated costs, 5 years, was the same as used in Reference 7. The results of these DOC calculations are summarized in Table XXXII.

The vast increase in DOC resulting from the application of either high or low speed quiet engines to a DC-8-type aircraft completely overshadows the DOC variations among the various high and low speed quiet engine and nacelle configurations. The single most significant factor causing the major increase in DOC when replacing the JT3D with quiet engines is the cost of the quiet engines and acoustically treated nacelles. The DOC is therefore, greatly affected by the depreciation period assumed, i.e., the assumed useful life of the retrofitted aircraft. Reference 7 assumed 5 years, as did the study reported in this Appendix. That depreciation period would need to be tripled to reduce the increase in DOC to a level where the differences in DOC for the high speed

Table XXXI. Weight Change Summary, Four Engines and Nacelles.

	Weight Removed, lb (kg)	Weight Added, lb (kg)	Δ Weight lb (kg)
JT3D Installation	36,858 (16,760)		
Low Speed QE			
Hardwall Nacelle		40,826 (18,560)	+ 3968 (1805)
Treated Wall Nacelle		41,422 (18,820)	+ 4564 (2075)
Treated Wall Nacelle and One Aft Splitter		41,698 (18,980)	+ 4840 (2200)
Treated Wall Nacelle with 3 Inlet and 2 Aft Splitters		45,018 (20,460)	+ 8160 (3710)
High Speed QE			
Hardwall Nacelle		38,830 (17,660)	+ 1972 (897)
Treated Wall Nacelle		39,046 (17,760)	+ 2188 (996)
Treated Wall Nacelle with Inlet Splitter and 1 Aft Splitter		39,970 (18,170)	+ 3112 (1414)
Treated Wall Nacelle with 3 Inlet and 2 Aft Splitters		42,510 (19,320)	+ 5652 (2570)

Table XXXII. DC-8-Type Aircraft, ΔDOC with Quiet Engines (JT3D Base).

Configuration	Δ DOC - % Low Speed Quiet Engine	Δ DOC - % High Speed Quiet Engine	JT3D
Basic Nacelle with Treatment	+48.2	+41.6	
Wall Treatment Only	+48.5	+41.9	
Wall Treatment and Single Aft Splitter	+48.8	+42.5	
Wall Treatment with 3 Inlet Splitters and 2 Aft Splitters	+52.5	+45.4	

quiet engines and low speed quiet engine and nacelle acoustic treatment configuration variations would become significant.

Figure 57 shows the change in DOC as a function of the noise reduction related to the JT3D-powered DC-8-type aircraft as a base. As can be seen, use of the high speed quiet engine results in the least increase in DOC required to attain a noise level equivalent to FAR36. However, for noise levels below approximately FAR36-10 the low speed quiet engine results in less DOC increase than the high speed quiet engine. It should be noted that use of either the high or low speed quiet engine results in a significant DOC increase, even in the hardwall (minimum suppression) version due to the retrofit costs discussed previously.

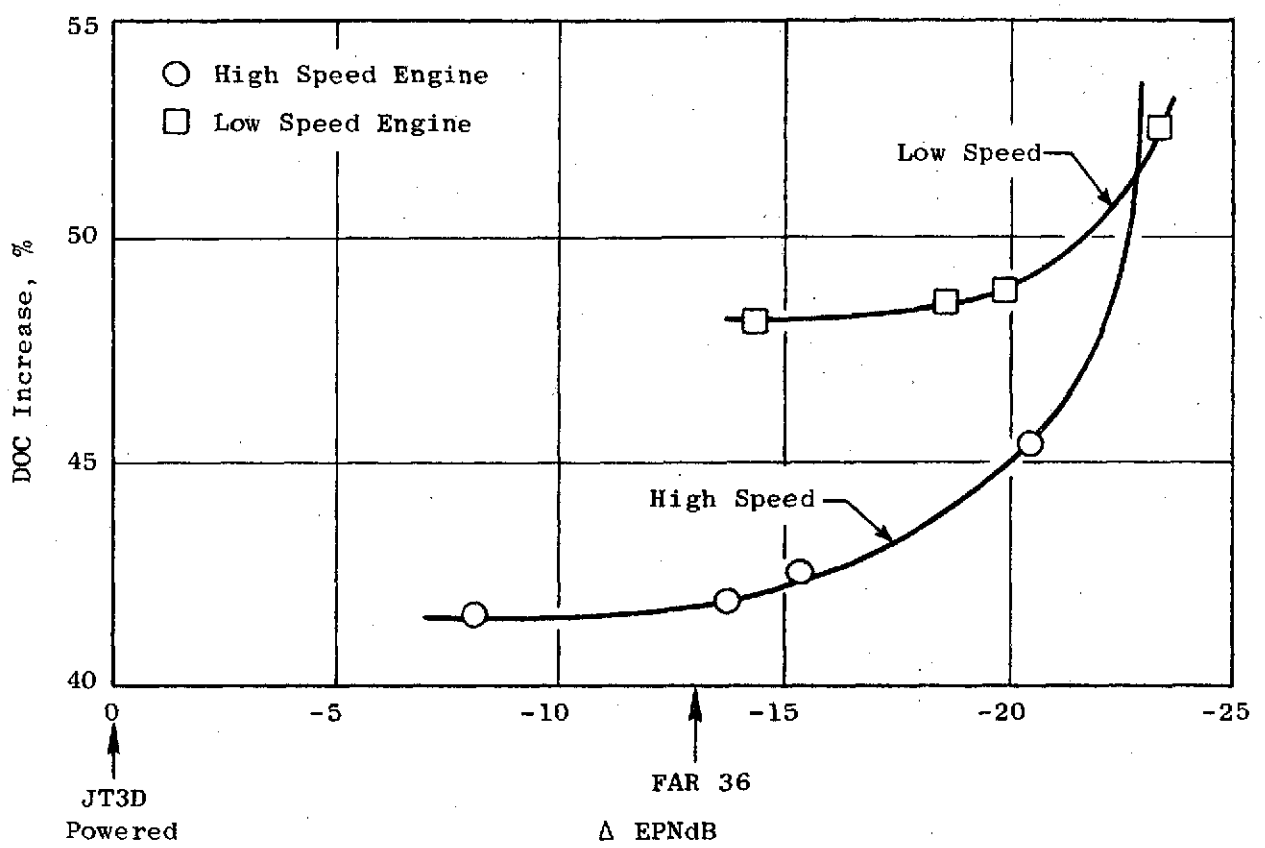

Figure 57. Quiet Engines in DC-8-Type Aircraft, Takeoff.

REFERENCES

1. Giffin, R.G., Parker, D.E., and Dunbar, L.W., "Experimental Quiet Engine Program Aerodynamic Performance of Fan A," NASA CR-120858, May 1971.

2. Giffin, R.G., Parker, D.E., and Dunbar, L.W., "Experimental Quiet Engine Program Aerodynamic Performance of Fan B," NASA CR-72993, August, 1972.

3. Giffin, R.G., Parker, D.E., and Dunbar, L.W., "Experimental Quiet Engine Program Aerodynamic Performance of Fan C," NASA CR-120981, August, 1972.

4. "Propulsion System Studies for an Advanced High Subsonic, Long Range Jet Commercial Transport Aircraft," NASA CR-121016, November, 1972.

5. Douglas Report DAC-68255A (NASA Contract NAS3-11151).

6. Holmberg, S.W., "Hot/Cold Flow Model Tests to Determine the Noise Characteristics of Two High Bypass Ratio Aerodynamic Mixer Exhaust Nozzles," Fluidyne Report 0787, May 1971.

7. McBride, J.F., "The Integration of Quiet Engines with Subsonic Tansport Aircraft," NASA CR-72548, August 1969.

REPORT DISTRIBUTION LIST

Addressee:			Number of Copies
1. NASA Lewis Research Center 21000 Brookpark Road Cleveland, Ohio 44135 Attention:			
	Report Control Office	MS: 5-5	1
	Technology Utilization Office	MS: 3-19	1
	Library	MS: 60-3	2
	Dr. S.C. Himmel	MS: 3-5	1
	Dr. A. Ginsburg	MS: 5-3	1
	M.J. Hartmann	MS: 5-9	1
	W.A. Benser	MS: 5-9	1
	T.F. Gelder	MS: 5-9	1
	S. Lieblein	MS: 100-1	1
	J.H. Povolny	MS: 60-4	1
	L.W. Schopen	MS: 77-3	2
	J.C. Williams	MS: 500-111	1
	E.W. Conrad	MS: 501-4	20
2. NASA Headquarters 600 Independence Avenue, S.W. Washington, D.C. 20546 Attention:			
	H.W. Johnson (RL)		1
	N.F. Rekos (RLC)		1
	Noise and Pollution Reduction Branch (RLN)		1
3. FAA Headquarters 800 Independence Avenue, S.W. Wahington, D.C. 20553 Attention:			
	John Powers		1
4. National Technical Information Service Department of Commerce Springfield, Virginia 22151			40
5. NASA Langley Research Center Hampton, Virginia 23366 Attention:			
	Donald Beals	MS: 403	1
	Harvey Hubbard	MS: 239	1
	Mark Nichols	MS: 403	1
	John Becker	MS: 186	1
	I.E. Garrick	MS: 115	1

REPORT DISTRIBUTION LIST (Continued)

Addressee:		Number of Copies
6. NASA Ames Research Center P.O. Box 273 Edwards, California 94035 Attention:		
David Hickey	MS: 221-2	1
7. NASA Flight Research Center P.O. Box 273 Edwards, California 93523 Attention:		
Norman McLeod	Room 2100	1
Don Bellman	Room 2106	1
8. Office of Secretary of Transportation 800 Independence Avenue, S.W. Washington, D.C. 20590 Attention:		
Charles Foster	TRT-30	1
9. Naval Air Propulsion Test Center Aeronautical Engine Department Philadelphia, Pennsylvania 19112 Attention:		
Robert Benham		1
10. Naval Air System Command Washington, D.C. 20360 Attention:		
Eugene Lichtman	Code Aero 330E	1
11. U.S. Army Aviation Material Laboratory Fort Eustes, Virginia Attention:		
John White		
12. Headquarters, USAF Wright Patterson AFB, Ohio 45433 Attention:		
Zeke Gershon	AFAPL/TBP	1
S. Kobelak	AFAPL/TBP	1
R.P. Carmichael	ASD/XRPH	1

REPORT DISTRIBUTION LIST (Continued)

Addressee:		Number of Copies
13. Department of Navy Bureau of Weapons Washington, D.C. 20525 Attention:		
Robert Brown	HAPPi4	1
14. The Boeing Company 3801 South Oliver Street Wichita, Kansas 67210 Attention:		
George Gregg	MS: 16-17	1
Steve Storch	MS: 16-12	1
Dean Nelson	MS: 16-31	1
15. The Boeing Company Commercial Airplane Division Renton, Washington 98055 Attention:		
J.F. McBride	MS: 47-35	1
J.V. O'Keefe	MS: 47-35	1
16. The Boeing Company P.O. Box 3707 Seattle, Washington 98124 Attention:		
G.J. Schott	MS: 73-24	1
17. Douglas Aircraft Company 8355 Lakewood Boulevard Long Beach, California 90801 Attention:		
J.E. Merriman	C1-250	1
18. Allison Division, GMC P.O. Box 894 Indianapolis, Indiana 46206 Attention:		
L. Corrigan	Dept. 8890	1
P. Tramm	Dept. 8894	1
Library		1

REPORT DISTRIBUTION LIST (Continued)

Addressee:		Number of Copies
19. Pratt and Whitney Aircraft Division, UAC East Hartford, Connecticut 06108 Attention:		
C.W. Bristol		1
J.D. Kester		1
A.A. Mikolajczak		1
Library (UARL)		1
20. Pratt and Whitney Aircraft Florida Research and Development Center West Palm Beach, Florida 33402 Attention:		
H.D. Stetson		1
B.A. Jones		1
21. Lockheed Aircraft Corporation P.O. Box 551 Burbank, California 91503 Attention:		
Harry Drell	Code 61-30	1
22. Lockheed Missile and Space Company P.O. Box 879 Mountain View, California 94040 Attention:		
Raymond Poppe	Dept. 80-91	1
23. Lockheed Georgia Company Marietta, Georgia 30060 Attention:		
H.S. Sweet	Dept. 72-71	1
24. Northern Research and Engineering 219 Vassar Street Cambridge, Massachusetts Attention:		
K. Ginwala		1
25. Curtiss-Wright Corporation Wright Aeronautical Woodridge, New Jersey Attention:		
S. Lomabardo		1

REPORT DISTRIBUTION LIST (Continued)

Addressee:	Number of Copies
26. Air Research Manufacturing Company 402 South 36th Street Phoenix, Arizona 85034 Attention:	
R.O. Bullock	1
27. Air Research Manufacturing Company 8951 Sepulveda Boulevard Los Angeles, California 90009 Attention:	
Technical Library	1
28. AVCO Corporation Lycoming Division 550 South Main Street Stratford, Connecticut 05497 Attention:	
David Knoblock	1
Clause Bolton	1
30. Teledyne Cae 1330 Laskey Road Toledo, Ohio 43601 Attention:	
Eli Bernstein	1
31. Solar San Diego, California 92112 Attention:	
P.A. Pitt	1
32. Williams Research Corporation P.O. Box 95 Walled Lake, Michigan Attention:	
J. Joy	1

REPORT DISTRIBUTION LIST (Continued)

Addressee:	Number of Copies
33. Caterpillar Tractor Company Peoria, Illinois 1601 Attention: J. Wiggins	1
34. Iowa State University Dept. of Mechanical Engineering Ames, Iowa 50010 Attention: George Serovy	1
35. Cornell University Aerospace Engineering Department Ithaca, New York 14850 Attention: W.R. Sears	1
36. California Institute of Technology Pasadena, California 91109 Attention: Duncan Rannie	1
37. Massachusetts Institute of Technology Cambridge, Massachusetts 92139 Attention: J.L. Kerrebrock	1
38. University of Toronto Institute of Aerospace Studies Toronto, Canada Attention: H.S. Ribner	1
39. Ministry of Technology National Gas Turbine Establishment Pystock, Farnborough, Hants. England Attention: Michael Neale	5

REPORT DISTRIBUTION LIST (Continued)

Addressee:	Number of Copies
40. Institute of Sound and Vibration Research The University, Southampton SO9 5NH England Attention: John Large	1
41. Rolls-Royce Limited Aero Engine Division P.O. Box 31 Derby, England Attention: L.G. Dawson	1
42. Rolls-Royce Limited Flight Test Establishment Hucknall, Nottingham, England Attention: J.S.B. Mather Dept. 428F	1
43. Rolls-Royce Limited Flight Test Establishment Hucknall, Nottingham, England Attention: M.E. House	1
44. Hawker-Siddeley Aviation Ltd. Hatfield, Hertz. England Attention: E.D.G. Kemp	1
45. Massport Aviation Technical Service Division 470 Atlantic Avenue Boston, Massachusetts 02210 Attention: George Bender, Jr.	1